Department of Electrical Engineering

The Hong Kong Polytechnic University

AVAILABLE TRANSFER CAPABILITY EVALUATION STUDY IN SYSTEM OPERATION UNDER ELECTRICITY MARKET AND ITS ENHANCEMENT BY FACTS DEVICES

CHENG YUN

A Thesis submitted in partial fulfillment of the requirements for the Degree of Doctor of Philosophy in Engineering

March 2005

CERTIFICATE OF ORIGINALITY

I hereby declare that this thesis is my own work and that, to the best of my knowledge and belief, it reproduces no material previously published or written, nor material that has been accepted for the award of any other degree or diploma, except where due acknowledgement has been made in the text.

_______________________________ (Signed)

CHENG Yun (Name of Student)

ABSTRACT

In this thesis, innovative studies are made on the Available Transfer Capability (ATC) evaluation methods in power systems with both dynamic and static constraints. The role of ATC as a market signal in addition to being a technical index in the power market environment and the interaction between the two roles are investigated. In addition, the ATC enhancement measures by Flexible AC Transmission Systems (FACTS) devices are also studied.

With the development of deregulated power markets, higher power transfer between interconnected systems and reduced reactive power reserves together with intensified competition, push the network authorities to determine ATC in short time with satisfactory accuracy. Thus system operation with both desirable economical benefit and sufficient security can be performed timely. Due to the increased transaction level associated with open access, the transmission systems are operating under more stressed conditions near the stability boundary. An optimized operation point of power system obtained with conventional static security constraints is possibly either transiently unstable or voltage unstable under certain credible contingencies. The calculation difficulties imposed by dynamic security considerations other than static limits lie in how to treat with the multi-dimensional Differential-Algebraic-Equations (DAEs) associated with them.

In this research, ATC evaluation methods with two different types of dynamic constraints are investigated. Firstly a variant Primal-Dual Predictor-Corrector Interior Point Method (PDPCIPM) is proposed to solve ATC calculation with transient angle stability constraints. It has the advantages of fast convergence and reasonable accuracy as well as that its iteration speed is insensitive to the system scale and number of control variables. A Quasi-Steady-State (QSS) approximation method is then proposed to evaluate dynamic voltage constrained ATC with acceptable accuracy while the calculation speed is accelerated considerably. Under the new power market environment, economic factors should be considered on the condition of stability operation. Hence ATC calculation with consideration on both stability and price bidding is investigated by a variant PDPCIPM method and their interactions are analyzed. Through an innovative risk-based optimal method, ATC determination with different contingences associated with the system transient instability risk is also developed. In this proposed method, both probabilities and costs of transient instability events are considered and the optimal ATC is compromised between economics and security. Besides the studies on algorithms of ATC evaluation with a variety of constraints as well multiple objectives, the participants of power market also pay attention on how to increase the ATC between areas. The application of various FACTS devices to enhance ATC is also studied in this research. Case studies and analysis results are presented to show the efficiency and validity of the above methods for ATC calculation and their improvement issues.

ACKNOWLEDGEMENTS

The work presented in this thesis was carried out under the supervision of Professor T. S. Chung, PhD, CEng, MHKIE, FIEE, SMIEEE, the leader of Power Systems Research Group, Dept. of Electrical Engineering, The Hong Kong Polytechnic University. It is with great pleasure and deep gratitude that the author acknowledges his invaluable guidance and continuous encouragement, which enabled the completion of this work.

The author would like to take this opportunity to acknowledge the co-supervisors Dr. C. Y. Chung and Dr. C.W. Yu of The Hong Kong Polytechnic University, for their academic advice and kind help. The author is also grateful to Dr. H. W. Ngan and Dr. C. T. Tse of The Hong Kong Polytechnic University for the useful discussions in their lectures.

The financial assistance of the Research Grants Council of Hong Kong by the award of research studentship is greatly appreciated. The author would like to thank the Research Office for much helpful assistance in the three years study in The Hong Kong Polytechnic University.

Last but not least, various forms of support provided by the Dept. of Electrical Engineering, The Hong Kong Polytechnic University are grateful acknowledged.

CONTENTS

CHAPTER 1

Introduction

1.1 Available Transfer Capability (ATC) of Power Networks Review

The earliest transfer capability calculation of transmission system could be traced back to 1970's (e.g. Landgren et al (1972) [37]), but the research did not receive researchers' interest until FERC (Federal Energy Regulatory Commission) mandated the order 888 and 889 in 1996. The mandate claimed that the public utility had to open its transmission grid for use by market participants and required that the ATC information of the transmission networks should be calculated and posted on OASIS (Open Access Same-time Information System). Shortly later in the same year, NERC (North American Electric Reliability Council) brought the industry together to establish a framework for ATC definition and evaluation. ATC was defined by NERC to be the transfer capability remaining in the physical transmission network for further commercial activity over and above already committed uses [50]. It is given by the relationship as:

$$ATC = TTC - TRM - CBM - existing\ transmission\ commitments \qquad \text{---- (1.1.1)}$$

Mathematically it means ATC is equal to the Total Transfer Capability (TTC) less the Transmission Reliability Margin (TRM), less the sum of existing transmission commitments and the Capacity Benefit Margin (CBM).

In particular, TTC is defined as the amount of electric power that can be transferred over an interface or a corridor of the interconnected transmission network in a reliable manner while meeting a specific set of defined pre- and post-contingency system conditions. TRM is defined as that amount of transmission transfer capability necessary to ensure that the interconnected network is secure under a reasonable range of uncertainties in system conditions. CBM is defined as that amount of transmission transfer capability reserved by load serving entities to ensure access to generation from interconnected systems to meet generation reliability requirements. Individual systems, power pools, sub-regions and regions should identify their TRM and CBM procedures used to establish such transmission transfer capability margins as necessary.

The definition of TTC between any two areas or across particular paths or interfaces is direction specific. TTC is the amount of electric power that can be transferred over the interconnected transmission network in a reliable manner based on all of the following conditions:

1) For the existing or planned system configuration, and with normal (pre-contingency) operating procedures in effect, all facility loadings are within normal ratings and all voltages are within normal limits.

2) The electric systems are capable of absorbing the dynamic power swings, and remaining stable, following a disturbance that results in the loss of any single electric system element, such as a transmission line, transformer, or generating unit.

3) After the dynamic power swings subside following a disturbance that results in the loss of any single electric system element as described in 2 , and after the operation of any automatic operating systems, but before any post-contingency operator-initiated system adjustment is implemented, all transmission facility loadings are within emergency ratings and all voltages are within emergency limits.

4) With reference to condition 1, when pre-contingency facility loadings reach normal thermal ratings at a transfer level below that at which any first contingency transfer limits are reached, the transfer capability is defined as that transfer level at which such normal ratings are reached.

5) In some cases, individual system, power pool, sub-regional, or regional planning criteria or guides may require consideration of specified multiple contingencies, such as the outage of transmission circuits using common towers or rights-of-way, in the determination of transfer capability limits. If the resulting transfer limits for these multiple contingencies are more restrictive than the single contingency considerations described above, the more restrictive reliability criteria or guides must be observed.

Issued on 20th December 1999, Order 2000 built upon the ISO concept by encouraging smaller transmission entities to join together into RTOs (Regional Transmission Organizations). In this order, FERC stipulated "to maintain OASIS and post the transmission capability (the TTC & ATC)" as one of the eight minimal functions that an RTO must perform. Order 888, 889 and 2000 have evolved with many major milestones that have resulted in the creation of different kinds of market structures and business practices in various regions of the USA.

The increase in power transfer among areas of interconnected systems and the reduction of reactive power reserves together with the competition in the power market, force the system operators and planners to look at the determination of the available transfer capability in a new perspective. Along with USA, European Transmission System Operators (ETSO) and some other countries also framed orders and regulations concerning issues about ATC.

Although there are definitions of ATC such as what NERC and ETSO established ([50] and [19]), the computational conditions or assessment procedures are not exactly clear. In the deregulated system, there has been an increase in interchange transactions among utilities, and the behavior of electricity trading and the resulting generation and load patterns are becoming more difficult to predict and analyze. Since the power system conditions are constantly evolving, ATC is a quantity that fluctuates with the time lapse. In addition, the differences between contract path and actual power flow path introduce additional complexity to the quantification of ATC. At this stage, many researchers throughout the whole world address on issues around the evaluation of ATC, and the key problem is on how to get the best compromise between the accuracy and calculation speed.

Although ATC research nowadays is focused mainly on its evaluation, ATC is not only a technical index for the safe operation of power grid, but also a market signal that reflects the capability of more commercial activities between interconnected transmission networks in the power market. It should be viewed from a unified perspective of both technology and economics.

1.2 Literature Reviews

1.2.1 Methods Used for the Evaluation of ATC

Since the need for ATC appears only after the electrical industry started deregulation and open access, not many fast ATC calculation algorithms are available nowadays. From the investigations which have been performed on the ATC evaluation, the adopted algorithms may be mainly classified into two categories as probabilistic or deterministic methods. From an engineering perspective, the former can give comprehensive information during the operational planning stage which is off-line executed shortly before the real-time operation, while the latter may provide timely pertinent information to on-line operational performance.

Table 1. 1 Comparison of the Pros and Cons among
Four Probabilistic Modeled Approaches for ATC Evaluation

Approach	Pros	Cons
Stochastic Approach [78]	It can settle both discrete and continuous variables and account for most of the key uncertainties.	The calculation speed is not quite favourable for large system.
Enumeration Method [76]	It combines the system state enumeration and optimal algorithm.	It is unsuitable for the ATC evaluation of large system.
Monte-Carlo Simulation [44]	It is easy to deal with a large number of uncertainties of power system and is suitable for large systems.	It can not settle the relativity among the system components and the accuracy of this method is questionable under certain circumstances.
Bootstrap Algorithm [65]	It can utilize the latest market information sufficiently.	It cannot favourably settle the uncertainty of some grid parameter (e.g. the stochastic fault of the transmission line).

For off-line calculation, substantive uncertainty factors which may influence the resultant accuracy of ATC should be involved, and the power systems' behaviour arising from random equipment outages and load variations are of stochastic nature. The challenges of ATC computation lie in the need to consider all likely base cases, all likely contingencies, and systematically compute the maximum transfer capability. To make the ATC useful in an acceptable scope and at the same time reduce the calculation burden and save evaluating time, probabilistic-based method is generally utilized for the determination of ATC. At this stage, the probabilistic model is mainly settled by four approaches, the comparison of their advantages and disadvantages is listed in Table 1.1.

Since various uncertainties of contingency may be involved in the probabilistic approaches, these methods may evidently yield much full-scale information as forecasted. From their result, the most harmful uncertainties may be detected during the operational planning stage, and certain pertinent countermeasures may be raised in early time to prevent more serious or wide-spread faults. What's more, the off-line calculation results may assist the selection of most critical contingencies for on-line evaluation. Although they have the above merits, compared with on-line calculations, besides the calculation speed is comparatively slow, results by off-line calculations are mostly approximate values. As far as the operational planning stage is concerned, they can meet the requirement, for the error produced by the approximation can be neglected in comparison with system uncertainties effect on ATC.

For on-line calculation, i.e. in an operations environment where ATC values are posted on a shot-term (usually one to several hours or even shorter) basis, calculation of ATC may be performed for most limiting constraints. One reason is that the time for calculation is limited and ATC value must be updated rapidly. The other reason is that the calculation is based on relatively more certain operation condition. For a given system, under certain operation conditions, base system conditions are identified and represented for the period being analyzed, including forecasted customer demands, generation dispatch, system configuration, specific transaction and base scheduled transfers. It is not difficult to find the most critical contingencies by contingency filter scheme. In this case, there may be no need to consider constraints which will never be enforced. It is also assumed that critical paths or interfaces and where to calculate ATC, are also preconditions known from off-line studies.

The methods of on-line ATC calculation are based on deterministic model, and they may be solved by several methods, such as Direct Method, Extended Distribution Factor Methods (e.g. Load Open Distribution Factor (LODF), Power Transfer Distribution Factor (PTDF), Generation Shifting Factor (GSF)), Sensitivity Method, CPF (Continuation Power Flow) and OPF (Optimal Power Flow). The comparison of their performance is listed in Table 1.2.

Table 1.2 Comparison of the Pros and Cons among

Five Deterministic Modeled Approaches for ATC Evaluation

Approach	Pros	Cons
Direct Method [25]	Evaluation is fast and easy.	1. If the starting point is very far from the result, no convergence may be encountered. 2. It cannot include nonlinear

		constraints such as VAR limits and transient stability constraints.
Extended Distribution Factor Methods (LODF, PTDF, GSF, etc) [18, 27, 58]	1. There is no need for any iteration and calculation speed is fast. 2. It may include 'N-1' static security constraints and branch overflow limits conveniently.	The voltage constraints and reactive power factors cannot be directly taken into account; thus calculation error may be considerable for untight systems with insufficient reactive power support.
Sensitivity Method [26]	Based on certain ATC data under certain system conditions, fast calculation of the new ATC after some parameters are changed can be performed.	1. This is not an independent method which must be combined with other ATC calculation methods. 2. When large change occurs in system operation, calculation speed may be slowed and accuracy cannot be guaranteed
CPF [17, 21, 28]	1. It is able to incorporate the effects of reactive power flows, static voltage limitations, voltage collapse as well as the traditional thermal loading effects. 2. Divergency can be avoided around the voltage limit point.	1. Calculation speed is not very satisfied. 2. Since it adopts a common factor, a conservative result may be conduced when calculating a special transfer limitation without the optimization of generation and load distribution.

OPF [12, 15, 38, 59]	1. It can incorporate various complex constraints and different objectives in the mathematical model. 2. It can adopt the new optimization methodology easily.	The optimization methods for different objectives and constraints are still in deep research.

In theory, both the system steady-state and dynamic constraints should be considered in the ATC calculation. However, few methodologies are available to evaluate this quantity with full representation of the power system dynamic behavior at this stage. Since the dynamic constraints involve differential equations, they are often ignored or simplified in most research. Such simplification may render the result accuracy to calculation speed. Under certain conditions, the system which satisfies the steady-state constraints is restricted by undesirable dynamic behavior after large disturbance. An iterative approach for calculating ATC with dynamic constraints was first proposed by Hiskens et al (1998) [30]. The method uses the concept of trajectory sensitivities and is prone to full representation of the power system modeled as a set of differential-algebraic-discrete equations. The application of the method is limited, however, to the evaluation of a single free parameter that can be used to yield marginally stable trajectories. The computational complexity for applications to large system has not been fully assessed.

Later a pilot literature including dynamic constraints in the ATC calculation was published by De Tuglie et al (2000) [14]. The main feature of the approach is the capability to treat static and dynamic security constraints in a unique integrated piece of software. The software structure is simple and compatible with existing EMS. However, the authors experienced some difficulties of oscillatory convergence around the solution.

In the recent years, more work has been performed in the ATC evaluation with transient angle stability considerations. Among them, several DAE (Differential Algebraic Equation) optimization methodologies have been applied to treat problem efficiently, e.g. Zhang et al (2004) [83] has used Dot Product as a criterion for rotor angle stability, and an algorithm based on Control Variable Parameterization (CVP) is implemented to solve the formulated transient angle stability constrained optimization problem.

1.2.2 OPF Technique Relative with ATC Evaluation

The application of optimization techniques to power system planning and operation problems has been an area of active research recently. Optimal Power Flow (OPF) is a generic term that describes a broad class of problems, in which a specific objective function is optimized with satisfying certain constraints. Generally, OPF can reliably find a steady-state operating point (e.g. generation dispatch, voltage profile, and transformer tap settings), which minimizes certain criteria while enforcing a variety of operational constraints dictated by operational and physical particulars of the electric network. Its general mathematical description is as follows:

Objective function: min f = f(x) ---- (1.2.1)

Subject To: g(x) = 0 ---- (1.2.2)

$$\underline{h} \le h(x) \le \overline{h} \quad \text{---- (1.2.3)}$$

$$\underline{x} \leq x \leq \overline{x} \qquad \text{---- (1.2.4)}$$

Conventional OPF formulations usually aim to minimize the system real power losses or the operating cost with subjecting to satisfy constraints represented by bus active and reactive power balances in term of voltages magnitudes and phase angles [32].

After 1990s, great changes have occurred in many countries on the administrative mechanism and market structure of electrical industry. The relationship of the reliability, economic property and power quality in the system operation correspondingly transferred from the traditional “safety stands the unconditional first priority” to a harmonious and accordant balance. Thus tremendous development of OPF in the power system under electricity market has been observed on the complication of objective function together with constraints and enlargement of application field. Understanding on the economic merit of OPF is improved gradually. For certain objective function and/or constraints of voltage, current, power, etc., OPF can be utilized to integrate them under the same valuation standard and on the basic requirement of the system operation (on both economics and safety). It can also depress the discrepancy between the operation cost and electricity price, settle the conflict among IPPs, power grids and customers. Under the electricity market, OPF foots the pivotal status in EMS and can be broadly applied in many aspects of power system under market environment, such as optimal dispatch, optimal ancillary control, bidding strategy and demand side management.

The development of research on OPF is mainly in two parts. The first is on perfecting the algorithm model, i.e., expressing the actual constraints rigorously by appropriate mathematical formulae. The second is on upgrading the calculation method, i.e., finding optimal technologies to get the result of OPF problem rapidly and efficiently.

A wide variety of optimization technologies has been applied to solve the OPF problems. The techniques can be classified into two categories, the traditional algorithm and the modern ones. The former includes linear programming (LP), quadratic programming (QP), nonlinear programming (NLP), Newton-based method, hybrid versions of linear programming and integer programming and Interior Point Methods. The latter is investigated enthusiastically in recent years, such as tabu search, simulated annealing, genetic algorithms, artificial neural networks, stochastic optimization, fuzzy sets, Lagrange relaxation algorithm, etc. Each of them has its particular advantages and is appropriate to solve certain special problems. In recent years, some traditional algorithm has also experienced gradual development with the changes and new requirements of electrical industry.

As an off-line analysis tool, OPF has been utilized widely and achieved good results. However, as an on-line optimal control instrument, deep research on the algorithm is still in progress.

In the following, a brief review will be made on several optimal technologies which are appropriate to be used in power system.

I. Linear Programming (LP)

In 1968, Wells [73] developed a linear programming approach to determine an economical schedule that is consistent with network security requirements for loading plants in a power system. The cost objective and its constraints were linearized and solved using the simplex method.

In 1970, Shen and Laughton [60] presented a dual linear programming technique. Both primal and dual problems were obtained using the revised simplex method.

Later，Stott and Hobson (1978) [63], Irving and Sterling (1983) [35], Housos and Irisarri (1983) [31], Mota-Palomino and Quintana (1984) [47] presented a series of papers applying modified linear programming to solve active power systems problems, among them, some exploration on economic dispatch has also been executed.

Some researchers also tried to use this method to solve reactive power optimization problems. In 1986, Mota-Palomino and Quintana [48] presented a penalty-function linear-programming-based algorithm to solve reactive power dispatch problems. In 1987, Santos-Nieto and Quintana [56] presented a linear programming technique used for solving linear reactive power flow problems. A penalty function linear programming algorithm was implemented along with a scheme for handling infeasibility. However, the calculation speed and result accuracy of LP in solving optimization problems with reactive power constraints are not very satisfied.

In summary, Linear Programming treats problems with constraints and objective function formulated in linear forms with non-negative variables. The objective functions (voltage, loss, economic dispatch and VAR) are linearized to enable LP solution. When dealing with the optimal calculation on the active power problems of large systems, LP appears rapid on speed, reliable on iteration and it is convenient to manage bulk constraints. However, it is unsuitable for optimization problems with high requirement on reactive power, which has strong non-linear characteristics.

II. Newton-based Method and Quadratic Programming (QP)

In the Newton-based method, the necessary conditions of optimality commonly referred to as the Kuhn-Tucker conditions are obtained. In general, these are nonlinear equations requiring iterative methods of solution. The Newton method is favored for its quadratic convergence properties and it can employ the sparsity of power system. However, the diagnostic factors corresponding to the control variables are prone to be very minimal value even zero, thus cause the matrix singularity; and initial value of the induced Lagrange multiplier may influence the stability of the iteration evidently. Further, since the second order partial derivative of Lagrange function should be calculated in the iteration progress, the speed of this method is not very satisfactory for real-time use.

Quadratic Programming is a special form of nonlinear programming whose objective function is quadratic with linear constraints. It has been widely used in settling the OPF problems with reactive constraints.

Newton-based method and Quadratic Programming are all second order method, and they are all good at convergence accuracy. But since the latter may be transferred to linear problem via Taylor expansion, it may simplify the calculation and demonstrate advantages of run time and the robustness.

III. Mixture of Linear Programming and Quadratic Programming Category

In 1973, Nabona and Ferris [49] presented a method which involved quadratic and linear programming for optimizing the economic dispatch objective. The on-line operation of this approach seems feasible and avoids the difficulties associated with the gradient optimization approach.

In 1986, Contaxis et al [11] presented a method to solve the optimal power problem by decomposing it into two sub-problems: the real and reactive sub-problems. This method employed both linear and quadratic programming. A quadratic programming approach was used to solve the two sub-problems at each iteration, and a linear programming approach was used if the valve point loading was to be considered.

With the increasing urge of planning and operation to consider active and reactive control simultaneously and try to get the result rapidly, more researchers have contributed much on this problem. PQ decomposition is used as the basic principle in most research, because of the weak physical coupling characteristic of the power system, i.e., P is more relative with θ (the angle of V), Q is more relative with the magnitude of V, P & Q can be optimized separately by decomposition, thus the disadvantages of long calculation duration, vast calculation burden can be overcome. In the sub-problems of reactive power, Quadratic Programming is usually employed.

However, with the development of electrical engineering, more new and complex devices appear. In the systems equipped with FACTS devices, the power flow of certain lines is relative to both P and Q, and they cannot be separated thoroughly. Modification must be made on the mathematical formula and calculation method. Ge and Chung (1998) [23] have proposed an innovative hybrid decoupled OPF method to include the effects of four typical FACTS devices and the specified needs for power flow controls. In this method, the variables related with both active and reactive power can be optimized in both APOPF (active power OPF) and RPOPF (reactive power OPF) by introducing the active and reactive power flow equations of FACTS branches into RPOPF and APOPF respectively.

IV. Interior Point Methods (IPM)

Interior Point Method is an optimal method that starts the process from an interior point of feasible space and constructs a path that reaches the optimal solution after a few iterations, and every interim point gained after each iteration step is always within the feasible space [3].

It was presented in previous research that IPM enables fast speed and reasonable accuracy, suitable for optimal problems in large system. Its iteration times are not influenced by the system scale and/or the number of control variables. Interior point features good starting point and fast convergence. Besides its robustness, it also demonstrates well on settling the inequality constraints. It can be used in both linear and nonlinear problems. Numerical experiences of IPM to power system optimization reported that this method are very effective and has great potential for such a large scale system with more and more complex nonlinear characteristics.

Even though the Interior Point Method was devised as early as 1947 and sparked by

Karmarkar's breakthrough in 1984, its application to power system optimization problems just began in the last two decades [53]. In 1991, Clements et al [10] presented one of the first interior point technique for solving power system state estimation problems, which facilitates detection and identification of bad data. Ponnambalam et al (1992) [52] presented a newly developed dual affine (DA) algorithm implemented to solve the hydro-scheduling problem. Momoh et al (1994) [45] presented an implementation of a Quadratic Interior Point (QIP) method for optimal power flow problems. This method is an extension of the dual affine algorithm and solves power system optimization problems such as economic dispatch and VAR planning problems. The method is capable of accommodating the nonlinearity in objectives and constraints. Granville (1994) [24] presented an IPM for solving the VAR planning objective function of installation cost and losses. The primal-dual logarithmic barrier method employed in this paper has shown superior computational performance when applied to linear and quadratic programming problems. However, proper weights must be specified in order for the algorithm to reach a solution satisfactory for both loss minimization and reactive injection costs.

In recent years, IPM is further developed and employed on solving various OPF problems in the power system. Some newly modified algorithm appears, and now there are mainly three kinds of IPM in this field:

1) Karmarkar's projective scaling method. Since standard form need to be obtained via complex transformation in the real calculation, it is rarely used in practice case;

2) Affine scaling method. As a mature method, Primal-Dual Affine Scaling method is widely used for linear programming (LP), quadratic programming (QP) and nonlinear programming (NLP) in State Estimation (Wei et al (1998) [72]), Reactive Power

Optimization (Granville (1994) [24]), Economic Dispatching (Yan and Quintana (1997) [81], Irisarri et al (1998) [33]), Optimal Power Flow (Wu et al (1994) [75], Wei et al (1998) [72]), Power Flow Insolvability (Granville (1996) [24]), Maximum Loadability (Irisarri et al (1997) [34], Wang et al (1998) [71]), Simultaneous Transfer Capacity (Mello et al (1996) [44]), Hydro-Thermal Co-ordination (Medina et al (1998) [42]) and Spot Pricing (Xie et al in 1998), etc. Among them, the method of predictor-corrector extension has performed impressively in the recent years.

3) Path following method. With the characteristics of rapid convergence, strong robustness and not sensitive to the initial value, it is the most potential IPM.

From the above investigation addressed by forerunners, OPF-based algorithms in evaluating power system problems are conceptually rather nice. Implementation on some test systems or networks have been reported and the performance was found satisfactory. Its deeper and wider application in the real-time scope is desired. Different optimal methods have specific characteristics and are suitable for certain problems, researchers are continuously devoting to find better methods to solve various optimal problems in the power system.

1.2.3 The Application of FACTS on Improving the System Performance

Since the early 1980's, advances in Flexible AC Transmission Systems (FACTS) controllers in power systems have led to their application in improving stability of power networks [29, 61]. Several studies analyzing the application of FACTS controllers for voltage and angle stability have been reported in the literatures (e.g. [4, 6]). In such research, the effect of the FACTS controller on the economic operation and voltage stability of the network is the principle motivation behind incorporating the FACTS into various OPF formulations. The main idea behind FACTS is to use network parameters as controls to direct flow, thus eliminating problems caused by unwanted loop or parallel flows.

Since FACTS controllers provide reactive-power compensation and benefit to increase the active power transfer between areas, their applications for various purposes are developed under the electricity market. In the research field of ATC, FACTS may be applied to enhance the ATC value. Exploration has been carried on this topic, e.g. Xiao et al (2003) [79] proposed a methodology for improving ATC by UPFC via stochastic approach.

1.2.4 Research on Transient Angle Stability by OPF

Since its first proposal, OPF has been an area of active research. Many successful techniques have been developed in the past decades for power system applications. In the conventional OPF formulation, static security constraints are considered and transient stability constraints are usually excluded. However, the systems operated at the point suggested by the OPF may fail to maintain transient stability when subject to a credible contingency. It should be noted that, as the power industry moves into a competitive environment, increasingly more transmission systems have been pushed to the stability limitation bounder. For these systems, transient angle stability should be one of the main concerns in the operation [7, 54]. As it is pointed out at the IEEE 1995

Winter Power Meeting by Panel Session on Challenges to OPF, ‘How will the future OPF provide local or global control measures to support the impact of critical contingencies, which threaten system voltage and angle stability’ has become one of the main challenges in OPF and is under deep research during the recent years.

Mathematically, Transient Stability Constrained OPF (TSCOPF) is nonlinear semi-infinite extended OPF problem with additional equality and inequality constraints. The additional equality constraints are a set of differential-algebraic equations (DAEs), in which, the ordinary differential equations are defined by the dynamics of the generators and the loads as well as their controllers, while algebraic equalities are described by the current balance equations of the transmission network (corresponding to the Kirchoff’s laws at each bus or node) and internal static behaviors of passive devices (e.g., shunt capacitors and static loads). The additional inequality constraints consist of angle stability constraints, and also some practical requirements of system dynamic behavior, such as limits on the transient voltage sag/rise etc. There are two major difficulties in TSCOPF. The first one is how to deal with multi-dimensional variables constrained by multi algebraic inequalities and equalities. The second one is how to satisfy the differential equations, which control the trajectories of all event disturbances.

In the past, several different approaches have been developed for this challenging problem. In some investigations, the problem is formulated as a static optimization problem by certain discretizing scheme, and any standard nonlinear programming technique can be applied to the problem. However, converting differential equations into algebraic equations by discretizing scheme may not only produce inaccuracy of computation because of the approximation but also cause convergence difficulties due to the introduction of a large number of variables and equations at each time step to the original OPF. In particular this is true for large scale power systems with a large number of the credible contingencies. At the same time, various different research methods have also under development to overcome this problem. For example, in 2004, Zhang et al [83] proposes a method which adopts equilibrium equations to describe steady-state constraints of pre- and post-disturbance conditions and uses dot product as a criterion for rotor angle stability. An algorithm based on control variable parameterization (CVP) is implemented to solve the formulated problem. Also in 2004, Xia [77] et al introduced a concept of 'most effective section of transient stability constraints' to reduce the massive calculation of the Jacobian and Hessian matrices of the stability constraints.

1.2.5 Research on Voltage Stability

Power transmission has traditionally been limited by either rotor angle (synchronous) stability or by thermal loading capabilities. Voltage stability, however, is now a new major concern in both planning and real-time operating power systems [8]. With the open access of power systems, more and more electric utilities are facing voltage stability limits. Voltage instability and collapse have resulted in several major system blackouts such as what occurred in Japan, France, USA etc. in recent years.

Compared with transient angle stability, voltage stability is still a fresh subject. It will remain a challenge for the foreseeable future and, indeed, is likely to increase in importance. In the last two decades, and especially in the recent years, with the evolution of open-access that prevails in an increasing number of power systems, more utility engineers, consultants, and university researchers have been addressing in the intense study of voltage stability.

At this stage, bifurcation theory is the primary tool to tackle voltage stability or voltage collapse issues [64, 68]. It can interpret the mechanism of voltage collapse evolution clearly, and many investigations have shown that generally voltage collapse is related with either Saddle Node Bifurcation (SNB) or Limit Induced Bifurcation (LIB). However, since OPF methods perform well for problems with various constraints and thus are suitable for disposing collapse by limits, OPF theories have been applied in the analysis of voltage stability limits. Including voltage stability in the OPF means adding such items to the constraints of the mathematical model. Similar to transient stability, these stability constraints themselves are algebraic or differential equations [62]. To obtain the results of the objective problem with these constraints, massive calculation is needed and methods to accelerate the evaluation process are required.

Several publications have dealt with optimization techniques for preventive control of voltage stability. The various formulations aim at either maximizing a load power margin (e.g. Dobson et al (1998) [16], Canizares (1998) [5], Wang and Lasseter (2000) [70] and Rosehart et al (1999) [55])or minimizing an objective function with voltage security constraints (e.g. Rosehart et al (1999) [55], Wang et al (1998) [71], Feng et al (2000) [20] and Vaahedi et al (2001) [66]). In the latter, margins can be determined through more accurate, dynamic simulations, and many researchers are quite interested in it.

1.3 Research Scope

The main contributions of this research work are summarized in the following, which show the highlights of this thesis.

1) Some previous investigations have proposed efficient methods of evaluating ATC with static constraints and some special considerations. However, since dynamic system operation conditions were usually simplified or omitted in these methods, an optimization point obtained by them may be transiently unstable or voltage unstable under credible contingencies.

In this research, the ATC calculation is considered with both static and dynamic constraints during the real-time stage, which may provide more helpful information for the operators during on-line dispatching in a stable and reliable way. In the dynamic constrained ATC evaluation, not only transient angle stability but also voltage stability influences are investigated. A variant PDPCIPM is proposed in the former and a QSS method is presented in the latter problem. Case studies show the validity of the proposed methods. The correspondingly different operation conditions and contingency types for these two kinds of dynamic constrained ATC are also analyzed and compared.

2) ATC is originally established to be both a technical indicator for secure operation and a commercial signal in power market. Following the research of ATC evaluation as a security index, its role as a commercial signal in the power market is also investigated. An innovative multi-purpose objective function with consideration of both stability control and economical dispatch is proposed and solved by a variant OPF method, where the first purpose is to maximize the ATC value, and the second one is to minimize

the investment and operation costs on enhancing ATC and solving congestion. In this way, the market influence on ATC can be reflected together with the stability constraints.

3) In this thesis, a new risk-based approach for assessment of optimal ATC with transient stability constraints is also attempted and proposed. In this approach, probabilities and costs of contingencies are simultaneously considered in building up the ATC model, expectation rule is adopted for the TTC decision-making process, and the ATC solution is optimized between the economics and security of system operation.

4) To meet the requirement of higher power transaction between interconnected areas, measures should be taken to improve the transfer performance. In this research, application of FACTS devices to enhance the available transfer capability is investigated. The objective problem is established in an OPF formulation with security and control constraints, which includes those of FACTS control parameters. A variant PDPCIPM method is employed as the solution methodology. Test is implemented to show the effect of FACTS devices on the enhancement of ATC.

1.4 Publications

Arising from this research work, one paper has already been published in journal, one paper is submitted and is under review, eight international conference papers have been presented or accepted. These papers are listed below:

Refereed Journal Papers Published:

Cheng Y., Chung T.S., Chung C.Y., Yu C.W., "ATC Evaluation of Inter-Connected Power System with the Incorporation of Dynamic Voltage Stability Constraints," Automation of Electric Power Systems, vol. 28, No. 6, pp. 30 - 34, 2004

Paper under review:

Cheng Y., Chung T.S., Chung C.Y., Yu C.W., "The ATC Determination of Power System with Incorporation of Dynamic Voltage Stability Constraints," submitted to International Journal of Electrical Power & Energy Systems

International conference papers:

1. Cheng Y., Chung T.S., Chung C.Y., Yu C.W., "Incorporation of Dynamic Voltage Stability Constraints in the ATC Determination of Power System," Proceedings, IEE APSCOM 2003 Conference, Hong Kong, vol. 2, pp. 619 - 623, Nov. 2003
2. Sun X., Zhang Q.P., Zeng M., Cheng Y., Chung T.S., Gu X., "Analysis on the Competition of Generating Market in the Ongoing Power Market of China," Proceedings, IEE APSCOM 2003 Conference, Hong Kong, vol. 2, pp. 846 - 849, Nov. 2003
3. Tong M.G., Zhao Q.B., Zeng M., Cheng Y., Chung T.S., Jing X., "The Application of Expanded Queuing Method on the Price Bidding Algorithm in the Power Market," Proceedings, IEE APSCOM 2003 Conference, Hong Kong, vol. 1, pp. 333 - 337, Nov. 2003
4. Cheng Y., Chung T.S., Zeng M., "Development Of Reliability-Based Conditional Maintenance In Electric Power Plants," Proceedings, RIUPEEEC 2003 Conference, Hong Kong, Paper no. A5-2 , Aug. 2003

5. Cheng Y., Chung T.S., Chung C.Y., Yu C.W., "Available Transfer Capacity Evaluation of Inter-Connected Power System with the Incorporation of Dynamic Voltage Stability Constraint," <u>Proceedings, 28th China Electric Power Control and Operation Conference</u>, Beijing, China, pp. 570 - 575, Oct. 2003
6. Cheng Y., Chung T.S., Yu C.W., Chung C.Y., Zeng M., Sun X., "Application of Reliability-Centered Stochastic Approach and FMECA to Conditional Maintenance of Electric Power Plants in China," <u>Proceedings, IEEE DRPT Conference</u>, Hong Kong, vol. 2, pp. 463 – 467, Apr. 2004
7. Cui K., Fang D.Z., Chung T.S., Cheng Y., "Risk-Based Optimal TTC Evaluation With Transient Stability Constraints," accepted by <u>IEEE IAS 2005 Conference</u>, Hong Kong, Oct. 2005
8. CHENG Y., CHUNG T.S., YU C.W., CHUNG C.Y., "ATC Evaluation with Multi-objective Optimization of System Stability and Economic Benefit in Power Market and Its Enhancement by FACTS Devices," accepted by <u>29th China Electric Power Control and Operation Conference</u>, Shang Hai, Oct. 2005

CHAPTER 2

ATC Calculation with Transient Angle Stability Constraints by a Variant Interior Point Method

2.1 Introduction

The evaluation of Available Transfer Capability (ATC) should take into consideration all the system security constraints, such as the thermal limits, steady-state stability limits (e.g. generator output active and reactive power limit, bus voltage upper and lower limit, etc.), transient angle stability limits as well as dynamic voltage stability limits [1, 74]. In the early years after this research topic was launched, a wide variety of mathematical and computational techniques, either conventional or new, were adopted to obtain the result with static system operation optimization (mainly "N-1" criteria) and some special considerations, such as multi-contingency constraints, reactive consideration, market based limits, etc. Among them, some methods can obtain satisfactory results with considerably fast calculation speed. However, since dynamic system operation conditions were not included, few of them can deal with dynamic constraints effectively, and an optimization operation point obtained by them may be transiently unstable or voltage unstable under certain credible contingencies. In recent years, under the competitive market environment, more and more bulk power systems are pushed to operate near the stability boundary [9, 13]. Hence to provide more helpful information for on-line power system operation at this stressed operating condition, more investigations of ATC evaluation with dynamic constraints are raised.

In this research context, the ATC evaluation with two major types of dynamic constraints is investigated separately; one is transient angle stability, and the other is dynamic voltage stability. This chapter is focused on the former, and the following chapter is on the latter type.

Among the diverse schemes for improving system representation and reducing computational time, Optimal Power Flow (OPF) has shown potentially outstanding ability on solving power system problems with various security constraints. In this research, OPF is thus chosen as the mathematical method and the ATC evaluation with dynamic considerations are described in the context of OPF problems. A variant Primal-Dual Predictor-Corrector Interior Point Method (PDPCIPM) with quadratic convergence and reasonable accuracy, which is insensitive to the system scale and the number of control variables, is proposed in this chapter for the ATC evaluation with transient angle stability constraints. The proposed method is presented, followed by case study illustration and result analysis.

2.2 Assessment on the Margins of ATC Calculation

Mathematically, ATC is defined as the Total Transfer Capability (TTC) less the Transmission Reliability Margin (TRM), less the sum of existing transmission commitments and the Capacity Benefit Margin (CBM), i.e.

$$ATC = TTC - TRM - CBM - existing\ transmission\ commitments \quad \text{---- (2.2.1)}$$

While in ATC evaluation the key component is the determination of TTC, attention should also be paid on both TRM and CBM, which account for the system reliability (Ou and Singh (2002) [51]). TRM is defined as that amount of transmission transfer capability necessary to ensure that the interconnected network is secure under a reasonable range of uncertainties in system conditions. CBM is defined as that amount of transmission transfer capability reserved by load serving entities to ensure access to generation from interconnected systems to meet generation reliability requirements.

As TRM accounts for the inherent uncertainty in system conditions and the need for operating flexibility to ensure reliable system operation when system conditions change, several uncertain operation factors are involved in the determination of TRM, such as branch outage, generation control, load forecasting, parallel power flow etc. All of them should be included and assembled reasonably instead of being simply summed up in the TRM assessment. In general, the longer the time span, the more serious is their uncertainty.

At this stage, there are several approaches of TRM assessment proposed. e.g. repeated computation of TTC using variations in the base case data (the difference between the largest and the smallest TTC is TRM), a single repeat computation of TTC using limitations reduced by a fixed percentage (i.e., 4%), TTC reduced by a fixed percentage (i.e., 5%), first order sensitivity method to take the effect of changes in load and simultaneous transfer on ATC, and probabilistic approach using statistical or other systematic reliability concepts etc. For individual systems with special construction characteristics and market regulations, the rules to determine their TRMs are different. Hence the specific methodologies for determining and identifying necessary TRMs may vary among regions, sub-regions, power pools, individual systems and load serving entities and they are very system dependent.

As for the on-line requirement, since the time span is very short between the base case and the desired operating point, it is not necessary to account for TRM on-line. In most conditions, TRM can be assessed as a fixed percentage of TTC and this simplification is feasible. In a power system with tight construction and abundant reactive power support, this percentage is allowed to be comparatively small.

The situation on CBM assessment is similar. In general, it can also be accounted for as a fixed percentage of TTC.

In this study, TRM and CBM are both regarded as a fixed percentage of TTC. ATC can be obtained as

$$ATC = \alpha\% * TTC - existing\ transmission\ commitments \qquad \text{---- (2.2.2)}$$

here α is a fixed number (α value is different among individual system, and it is usually between 90 and 98). To simplify the illustration, in the following sections, the calculation of ATC is actually that of TTC.

2.3 Problem Formulation

The ATC calculation with transient angle stability constraints problem can be formulated as:

2.3.1 Objective Function

$$\text{Min - P}_{ATC} = Min - \sum_{mn \in L_t} P_{mn} \qquad \text{---- (2.3.1)}$$

where

P_{ATC} is the ATC (Available Transfer Capability) between source area and sink area;

L_t is the set of tie lines between the source area and sink area;

mn is one of the tie lines, where m and n are respectively the start bus in source area and the ending bus in sink area;

P_{mn} is the active power transferred along tie line of mn.

This objective function expresses the power transfer between the source area and sink area. It is subjected to the following constraints:

2.3.2 Power Flow Equations

$$P_{Gi} - P_{Li} - \sum_{j=1}^{n} |U_i||U_j| \left(G_{ij} \cos\theta_{ij} + B_{ij} \sin\theta_{ij} \right) = 0 \qquad \text{---- (2.3.2)}$$

$$Q_{Gi} - Q_{Li} - \sum_{j=1}^{n} |U_i||U_j| \left(G_{ij} \sin\theta_{ij} - B_{ij} \cos\theta_{ij} \right) = 0 \qquad \text{---- (2.3.3)}$$

where

P_{Gi} is the active power output of i-th bus;

Q_{Gi} is the reactive power output of i-th bus;

P_{Li} is the active power consumption of i-th bus;

Q_{Li} is the reactive power consumption of i-th bus;

U_i and U_j are the voltage magnitude of i-th and j-th bus;

θ_{ij} is the phase angle difference between buses i and bus j;

$Y_{ij} = G_{ij} + jB_{ij}$ is the admittance matrix for the network.

Parameter i and j denote a set of buses with either generator or load or both.

Mathematically, the above are algebraic equation constraints.

2.3.3 Transient Angle Stability Constraints

Transient angle stability for various credible contingencies is expressed by the non-violation of a suitable criterion. In this study, maximum relative rotor angle criterion is used as the rule, in which rotor angles with respect to Center of Inertia (COI) are restricted to change in an allowed range. Under this definition, transient angle stability constraints are formulated as:

$$\delta_{\min} \le \delta_i - \delta_{COI} \le \delta_{\max} \qquad \text{---- (2.3.4)}$$

where $$\delta_{COI} = \sum_{i=1}^{ng} M_i \delta_i \Big/ \sum_{i=1}^{ng} M_i \qquad \text{---- (2.3.5)}$$

In this research, the adopted power system model for transient stability analysis is the classical model based on the following simplifying assumptions:

1) The synchronous machine is represented by a voltage source of constant magnitude E_i determined from the pre-fault steady-state conditions, in series with a reactance $X_{di}^{'}$ which is commonly called the direct axis transient reactance. The phase angle of the voltage behind transient reactance coincides with the rotor angle δ_i .

2) Loads are represented as constant impedances based on the pre-fault voltage

conditions.

3) The mechanical input power P_{mi} is assumed to be constant and equal to the pre-fault value during the time interval of interest which is of the order of 1-2 seconds.

In this case, the swing equation set is :

$$\dot{\delta} = \omega_i - \omega_0 \quad \text{---- (2.3.6)}$$

$$M_i \dot{\omega}_i = \omega_0 \left(-D_i \omega_i + P_{mi} - P_{ei} \right) \quad \text{---- (2.3.7)}$$

$i = 1,2,\cdots,ng$

where

δ_i is rotor angle of i-th generator

ω_i is rotor speed of i-th generator

M_i is inertia constant of i-th generator

D_i is damping constant of i-th generator

P_{mi} is mechanical input power of i-th generator

P_{ei} is electrical output power of i-th generator,

$$P_{ei} = \sum_{j=1}^{ng} E_i E_j \left(B_{ij} \sin \delta_{ij} + G_{ij} \cos \delta_{ij} \right)$$

ω_i is synchronous speed

ng is number of generators

Mathematically, the above are differential equations and extended inequality constraints.

2.3.4 Operation Boundary Limits

$$U_{i\min} \le |U_i| \le U_{i\max} \quad \text{---- (2.3.8)}$$

$$P_{Gi\min} \le |P_{Gi}| \le P_{Gi\max} \quad \text{---- (2.3.9)}$$

$$Q_{Gi\min} \le |Q_{Gi}| \le Q_{Gi\max} \quad \text{---- (2.3.10)}$$

$$|I_{ij}| \le I_{ij\max} \quad \text{---- (2.3.11)}$$

$$0 \le |P_{Li}| \le P_{Li\max} \quad \text{---- (2.3.12)}$$

$$0 \le |Q_{Li}| \le Q_{Li\max} \quad \text{---- (2.3.13)}$$

The above are inequality constraints dictated by operation boundary.

(2.3.8) expresses the bus voltage limits, where U_i is the voltage magnitude of i-th bus, $U_{i\min}$ and $U_{i\max}$ are the lower and upper limits of i-th bus voltage respectively; In the similar format with (2.3.8), (2.3.9) to (2.3.13) respectively describe generator active and reactive power output limits, thermal limit of transmission line, load active and reactive power limits of i-th bus.

2.3.5 General Formulation of the Presented Problem

For brevity, the above expressions may be represented as follow:

Min f(x, y, u) ---- (2.3.14)

s.t. $h_1(y,u) = 0$ ---- (2.3.15)

$g_{1\min} \le g_1(y,u) \le g_{1\max}$ ---- (2.3.16)

$\dot{x}(t) = h_2(x(t), y)$ ---- (2.3.17)

$g_{2\min} \le g_2(x(t)) \le g_{2\max}$ ---- (2.3.18)

where, y is the set of state variables, u is the set of control variables, x(t) is the set of transient angle stability variables.

Thus, the ATC calculation with transient angle stability constraints problem is formulated as a general OPF problem with differential-algebraic equations (DAEs) and inequality constraints.

2.4 A Variant Interior Point Method (IPM)

2.4.1 Why and How to Adopt IPM

From the above mathematical formulation, it can be observed that there are two major difficulties in Transient Security Constrained OPF (TSCOPF). The first one is how to deal with multi-dimensional variables constrained by multi algebraic inequalities and equalities. The second one is how to satisfy the differential equations which controls the trajectories of all event disturbances.

To tackle the multi-dimensional problem, Interior Point Method (IPM) is a suitable choice. In the last two decades, IPM has been employed on solving various optimization problems. It was reported that IPM has fast speed and reasonable accuracy, suitable for optimal problems in large systems. Its iteration times are not influenced by the system scale and/or the number of control variables, and it features fast convergence which is not quite sensitive to the selection of initial point. Hence for the optimization problem of ATC determination with transient angle stability constraints, IPM will be suitable with potential efficiency.

To deal with the differential and algebraic equations together, equation (2.3.17) can be discretized at n_T time steps. In this research, trapezoidal rule is adopted, i.e. the swing equation set (2.3.6) and (2.3.7) can be equivalent with the following algebraic equations:

$$\delta_i^{t+1} - \delta_i^t - \frac{\Delta t}{2}\left[\left(\omega_i^t - \omega_0\right) + \left(\omega_i^{t+1} - \omega_0\right)\right] = 0 \qquad \text{---- (2.4.1)}$$

$$\omega_i^{t+1} - \omega_i^t - \frac{\Delta t}{2}\frac{\omega_0}{M_i}\left[\left(-D_i\omega_i^t + P_{mi} - P_{ei}^t\right) + \left(-D_i\omega_i^{t+1} + P_{mi} - P_{ei}^{t+1}\right)\right] = 0 \qquad \text{---- (2.4.2)}$$

$i = 1,2,\cdots,ng$; $t = 0,1,\cdots,n_T$

where

$$P_{ei}^t = \sum_{j=1}^{ng} E_i^t E_j^t \left(B_{ij}^t \sin\delta_{ij}^t + G_{ij}^t \cos\delta_{ij}^t\right) \qquad \text{---- (2.4.3)}$$

Prior to the disturbance, the power system is operated at a steady state with δ_i^0, E_i^0 and $\dot{\delta}_i = 0$, where δ_i^0 and E_i^0 are determined by the power flow of pre-disturbance.

Thus, equations (2.3.14) to (2.3.18) can be represented as the following compact notation:

Min f(x, y, u) ---- (2.4.4)

s.t. $h(x, y, u) = 0$ ---- (2.4.5)

$g_{\min} \le g(x, y, u) \le g_{\max}$ ---- (2.4.6)

Obviously the dimension of problem is enlarged substantially after discretization. However, since IPM has the merit of fast convergence, at the same time, the power system has the characteristic of sparsity, the calculation burden of ATC with transient angle stability can be reduced by employing these two advantages. In addition, the variant Primal-Dual Predictor-Corrector Interior Point Method proposed in this research can effectively eliminate some constraints in the process, thus the problem size may be reduced substantially.

2.4.2 Variant Primal-Dual Predictor-Corrector Interior Point Method (PDPCIPM)

2.4.2.1 Formulation of Algorithm

Interior Point Method is an optimization method that starts the process from an interior point and constructs a path that reaches the optimal solution after a few iterations, and the interim point gained after each iteration step is always within the feasible space [3].

Based on the IPM method presented by Wei et al (1998) [72] and Yuan et al (2003) [82], the proposed variant Primal-Dual Predictor-Corrector Interior Point Method (PDPCIPM) actually combines the merits of Lagrange function, logarithmic barrier function and Newton method. Thus it is able to transfer the constrained problem to unconstrained problem, transfer the inequality constraints to quality constraints and find the optimal search direction.

For an optimization problem with the general formulation as follows:

Min f(x)

s.t. $h(x) = 0$ ---- (2.4.7)

$\underline{g} \le g(x) \le \overline{g}$ ---- (2.4.8)

$x \in R^n, h(x) \in R^m, g(x) \in R^r$

1) Construction of Lagrangian function

Firstly, two slack variables l and u are introduced to transform inequality constraints into equality constraints and adding barrier penalties to the original objective function.

$$f_\mu(x,l,u,\mu)= f(x)-\mu\left(\sum_i \ln l_i + \sum_i \ln u_i\right) \qquad \text{---- (2.4.9)}$$

where $g_i(x)+u_i = \overline{g}_i$ ---- (2.4.10)

$$g_i(x)-l_i = \underline{g_i} \qquad \text{---- (2.4.11)}$$

$$(l,u)\geq 0$$

μ is the barrier parameter.

A Lagrangian function associated with the above can be constructed as:

$$L = f(x)- yh(x)- z^T\left(g(x)-\underline{g}-l\right)- w^T\left(g(x)-\overline{g}+u\right)-\mu\left(\sum_i \ln l_i + \sum_i \ln u_i\right)$$

---- (2.4.12)

where x, l, u are primal variables, and y, z, w are dual variables.

2) Solve the Search Direction

To find the optimal solution of function (2.4.12), based on the perturbed Karush-Kuhn-Tucker (KKT) optimality conditions, i.e.

$$\frac{\partial L}{\partial x}=\frac{\partial L}{\partial l}=\frac{\partial L}{\partial u}=\frac{\partial L}{\partial y}=\frac{\partial L}{\partial z}=\frac{\partial L}{\partial w}=0$$

the following equations are obtained:

$$\nabla_x L = \nabla f(x)-\nabla h(x)y-\nabla g(x)(z+w)=0$$

$$\nabla_l L = LZe-\mu e = 0$$

$$\nabla_u L = UWe+\mu e = 0$$

$$\nabla_y L = h(x)=0$$

$$\nabla_z L = g(x) - \underline{g} - l = 0$$

$$\nabla_w L = g(x) - \overline{g} + u = 0 \qquad \text{---- (2.4.13)}$$

where L, U, Z, W $\in R^{r \times r}$ are diagonal matrices with the element l_i, u_i, z_i, w_i, $e = [1, \cdots, 1]^T \in R^r$

Then, by applying Newton's method to (2.4.13), the search direction of primal and dual variables between iteration steps, i.e. $\Delta x, \Delta l, \Delta u, \Delta y, \Delta z, \Delta w$, can be obtained by:

$$\left(\nabla^2 h(x) y + \nabla^2 g(x)(z + w) - \nabla^2 f(x)\right)\Delta x + \nabla h(x)\Delta y + \nabla g(x)(\Delta z + \Delta w) = L_{x0}$$

---- (2.4.14)

$$Z\Delta l + L\Delta z = -L_{l0}^{\mu} \qquad \text{---- (2.4.15)}$$

$$W\Delta u + U\Delta w = -L_{u0}^{\mu} \qquad \text{---- (2.4.16)}$$

$$\nabla h(x)^T \Delta x = -L_{y0} \qquad \text{---- (2.4.17)}$$

$$\nabla g(x)^T \Delta x - \Delta l = -L_{z0} \qquad \text{---- (2.4.18)}$$

$$\nabla g(x)^T \Delta x + \Delta u = -L_{w0} \qquad \text{---- (2.4.19)}$$

where $L_{x0}, L_{l0}^{\mu}, L_{u0}^{\mu}, L_{y0}, L_{z0}, L_{w0}$ are the values at an expansion point and they denote the residuals of the perturbed KKT equations. $\nabla^2 f(x)$, $\nabla^2 h(x)$ and $\nabla^2 g(x)$ are Hessian matrices of $f(x)$, $h(x)$ and $g(x)$.

By substituting $\Delta l, \Delta u, \Delta z, \Delta w$ obtained from the relationship of (2.4.15), (2.4.16), (2.4.18) and (2.4.19) into (2.4.14), the following reduced correction equation is derived:

$$\begin{bmatrix} H(\cdot) & J(x)^T \\ J(x) & 0 \end{bmatrix} \begin{bmatrix} \Delta x \\ \Delta y \end{bmatrix} = -\begin{bmatrix} \varphi(\bullet, \mu) \\ h(x) \end{bmatrix} \qquad \text{---- (2.4.20)}$$

where

$$H(\cdot) \equiv H_h + H_g = \left(\nabla^2 h(x) y + \nabla^2 g(x)(z + w) - \nabla^2 f(x)\right) + \nabla g(x)\left(U^{-1}W - L^{-1}Z\right)\nabla g(x)^T$$

$$J(x) \equiv \nabla h(x)^T$$

$$\varphi(\bullet,\mu) \equiv \nabla h(x)y - \nabla f(x) + \nabla g(x)\left(U^{-1}WL_{w0} - L^{-1}ZL_{z0} - \mu\left(U^{-1} - L^{-1}\right)e\right)$$

---- (2.4.21)

Thus Δx and Δy are obtained.

The major computational effort in this method lies in solving the symmetric system of equation (2.4.20). However, since its elements are with sparse constructions, the sparse techniques may be used to save memory space and improve speed.

From (2.4.20) and (2.4.21), H_g prevents inequality constraints $g(x)$ from violating their two-sided limits, the reduced equation has eliminated both variable inequality constraints and functional inequality constraints; hence the size of (2.4.20) is only determined by the number of variables and equality constraints, and is much smaller than that of (2.4.14) to (2.4.19).

3) Determine the Maximum Iteration Step Length

Since units and physical meanings of primal variables and the dual variables are different, their actions and moving trajectories in the optimal process are distinct from each other. To gain better convergence, individual iteration step lengths for primal and dual variables are adopted separately.

For the primal variables,

$$\alpha_P = 0.9995\min\left\{\min_i\left(-\frac{l_i}{\Delta l_i};\Delta l_i < 0; -\frac{u_i}{\Delta u_i};\Delta u_i < 0;\right),1\right\} \qquad \text{---- (2.4.22)}$$

For the dual variables,

$$\alpha_D = 0.9995\min\left\{\min_i\left(-\frac{z_i}{\Delta z_i};\Delta z_i < 0; -\frac{w_i}{\Delta w_i};\Delta w_i > 0;\right),1\right\} \qquad \text{---- (2.4.23)}$$

$i = 1,2,\cdots r$

4) Iteration Stop Criteria

Set an initial small tolerance ε , $0 < \varepsilon << 1$,

Define the complementary gap $C_{Gap} \equiv \sum_{i=1}^{r} \left(l_i z_i - u_i w_i \right)$ ---- (2.4.24)

If $C_{Gap} < \varepsilon$, the optimal problem is convergent and iteration can be stopped; otherwise, after acceptable steps of iteration, if it is still true that $C_{Gap} > \varepsilon$, the computation does not converge.

2.4.2.2 Proposed Variant PDPCIPM

1) Computation Steps:

Initialization: set k=0, K_{max}=30, centering parameter $\sigma \in (0,1]$, and tolerance $\varepsilon = 10^{-6}$. Choose a starting point for primal and dual variables which satisfy the condition that the state variables of x are the corresponding parameters at base case, the unknown control variables are set as the average of their upper and lower limits, and $l_0 = g(x_0) - \underline{g}, u_0 = \overline{g} - g(x_0)$, $y_0 = 10^{-8}, z_0 = 1, w_0 = -1$.

While k< K_{max},

Step 1: Test of convergence: compute the complementary gap C_{Gap} by equation (2.4.24), if $C_{Gap} < \varepsilon$, then output the optimal solution and stop; otherwise, go to step 2.

Step 2: Predictor-corrector process. To explain it clearly, it will be described in the following.

Step 3: Update the barrier parameter: $\mu = \sigma \frac{C_{Gap}}{2r}$ ---- (2.4.25)

Step 4: Update the primal and dual variables: compute the maximum iteration step length α_P , α_D by equation (2.4.22) and (2.4.23), as well search direction $\Delta x, \Delta l, \Delta u, \Delta y, \Delta z, \Delta w$ by equation set (2.4.20) and (2.4.21), then update the variables as:

$$\begin{bmatrix} x \\ l \\ u \end{bmatrix} = \begin{bmatrix} x \\ l \\ u \end{bmatrix} + \alpha_P \begin{bmatrix} \Delta x \\ \Delta l \\ \Delta u \end{bmatrix}, \begin{bmatrix} y \\ z \\ w \end{bmatrix} = \begin{bmatrix} y \\ z \\ w \end{bmatrix} + \alpha_D \begin{bmatrix} \Delta y \\ \Delta z \\ \Delta w \end{bmatrix} \quad \text{---- (2.4.26)}$$

Step 5: k=k+1, go to step 1

Step 6: When k= K_{max}, but the convergence criteria still cannot be satisfied, stop the computation and output “Computation does not converge”.

2) Predictor-Corrector Process

The Predictor-Corrector method of IPM is first proposed by Mehrotra in 1992 [43]. The main difference between the Predictor-Corrector IPM and the pure IPM is that the former introduces nonlinear terms to make the convergence better.

From the above, the barrier parameter μ changes during the iteration with the variety of the complementary gap C_{Gap} and centering parameter σ, and it strongly influences the convergence through correction equation (2.4.20). Hence if the centering parameter σ can be dynamically and optimally evaluated between iteration steps, convergence of the problem may be improved.

In section 2.4.2.1, Newton’s method is applied to search the direction of primal and dual variables. In equation (2.4.15) and (2.4.16) high order terms are ignored and only the first order ones are included in the computation. If expressed more exactly by second order Taylor series expansion, they can be represented as:

$$Z\Delta l + L\Delta z + \Delta Z\Delta l = -L_{l0}^{\mu} \quad \text{---- (2.4.27)}$$

$$W\Delta u + U\Delta w + \Delta W\Delta u = -L_{u0}^{\mu} \quad \text{---- (2.4.28)}$$

Based on the affine-scaling concept suggested by Mehrotra [43], the predictor-corrector process is as follows:

Step 2.1: set the centering parameter $\sigma = 0$ and $\varphi(\bullet,\mu) = \varphi(\bullet,0)$, solve (2.4.15), (2.4.16), (2.4.18), (2.4.19) and (2.4.20), get the affine-scaling direction $\left[\Delta x^{aff}, \Delta y^{aff}, \Delta l^{aff}, \Delta u^{aff}, \Delta z^{aff}, \Delta w^{aff}\right]$, and substitute them into (2.4.26) to get $\left[l^{aff}, u^{aff}, z^{aff}, w^{aff}\right]$.

Step 2.2: Determine the corresponding step length $\left(\alpha_{P,}{}^{aff} \alpha_D{}^{aff}\right)$by (2.4.22) and (2.4.23), then $C_{Gap}{}^{aff}$ by (2.4.24).

Step 2.3: Dynamically estimate the centering parameter σ by $\sigma = \left(C_{Gap}{}^{aff} \big/ C_{Gap} \right)^2$.

By dynamical evaluation of σ, the convergence may be improved as follows. If $C_{Gap}{}^{aff} << C_{Gap}$, $\delta \approx \mu \approx 0$, the correction equation gives a standard Newton direction, known as affine-scaling direction. Along this profitable direction, the algorithm can reduce the complementary gap C_{Gap} in a more optimal way. While if $C_{Gap}{}^{aff} \approx C_{Gap}$, $\delta \approx 1$, under this condition, δ influences little on the convergence. However this can improve the algorithm feasibility and is likely to reduce the complementary gap at the next iteration. It should be noted that the Hessian matrix stay unchanged and the previously factored matrix is used again in this process. Thus this process helps the algorithm converge faster with little additional computation burden.

2.5 Case Study and Discussions

The proposed variant PDPCIPM has been tested on two test systems: 6-bus and IEEE 30-bus test systems.

2.5.1 6-bus System

The 6-bus test system shown as Fig. 2.1 is selected as a test system for validating the proposed variant PDPCIPM algorithm. This system consists of 3 generators, 6 buses, 3 load centers and 11 transmission lines, detail data of its parameters are listed in Appendix A. For the evaluation of this investigation, the 6-bus system is divided into two parts of A and B as shown in Fig. 2.1. The tie lines between subsystems A and B include 5 branches of line 2-4, 2-1, 2-5, 6-5 and 3-5. The system power base is 100MVA, and it is operated at the frequency of 60 Hz. Its base case operation data are shown in Table 2.1, and the base-case power transfer across the interface is 0.613p.u. The upper and lower limit of generator reactive power output is 1.5p.u. and -1.5p.u. respectively, and voltage magnitude is allowed to change within the boundary of 1.1p.u. to 0.9p.u., δ_{max} is set as 120^0. The transient process is set as 5s long.

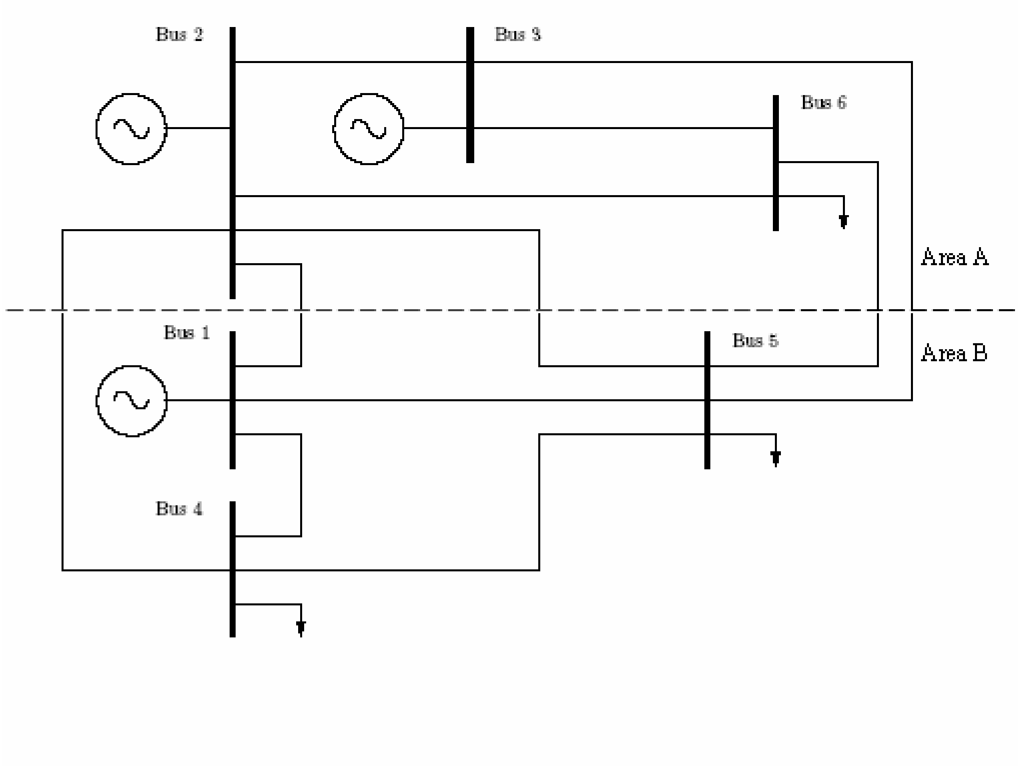

Fig. 2.1 One-line Diagram of 6-bus Test System

Table 2.1 Base Case Data of 6-bus Test System

Bus	1	2	3	4	5	6
P (p.u.)	0.9	1.396	0.6	-0.9	-1	-0.9
Q (p.u.)	0.315	0.651	0.733	-0.51	-0.66	-0.51

At t=1s, a three-phase fault occurs near bus 5 at the end of line 4-5. The fault is subsequently cleared at t=1.25s by opening line 4-5. Fig. 2.2 shows the variation of Barrier Parameter and maximum power flow mismatch along with iteration steps, and Fig. 2.3 shows the optimization process and result of objective function (ATC) with respect to iteration steps.

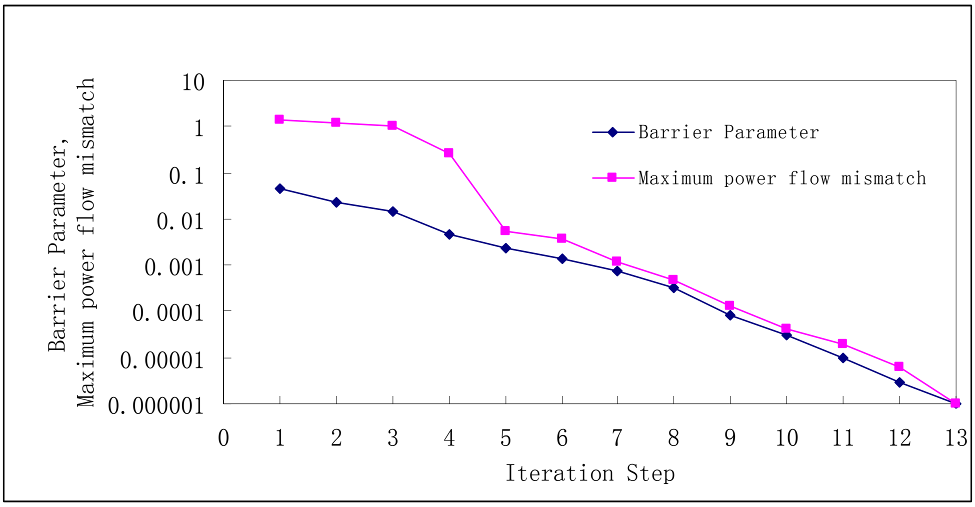

Fig. 2.2 Variation of Barrier Parameter and Maximum Power Flow Mismatch with Iteration

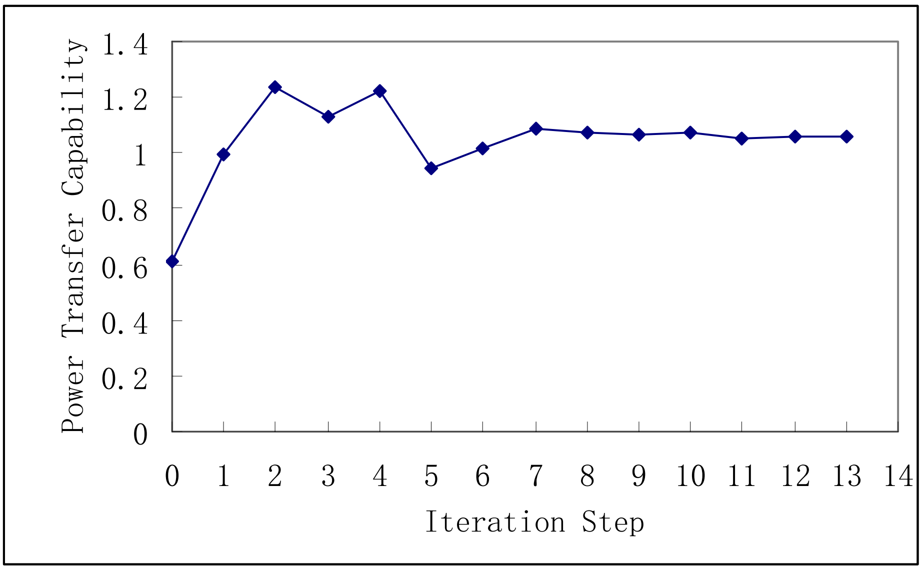

Fig. 2.3 Optimization of ATC with Respect to Iteration

2.5.2 IEEE 30-bus Reliability Test System

The IEEE 30-bus Reliability Test System is a standard test system with 6 generators, 30 buses, 21 load centers and 41 transmission lines. Its one-line diagram is shown in Fig. 2.4, detail data of its parameters are listed in Appendix B. In this research, it is divided into three parts of A, B and C, and the objective function is selected as the ATC of interface A-C. The power transfer between area A and C is 0.205p.u. at the base case.

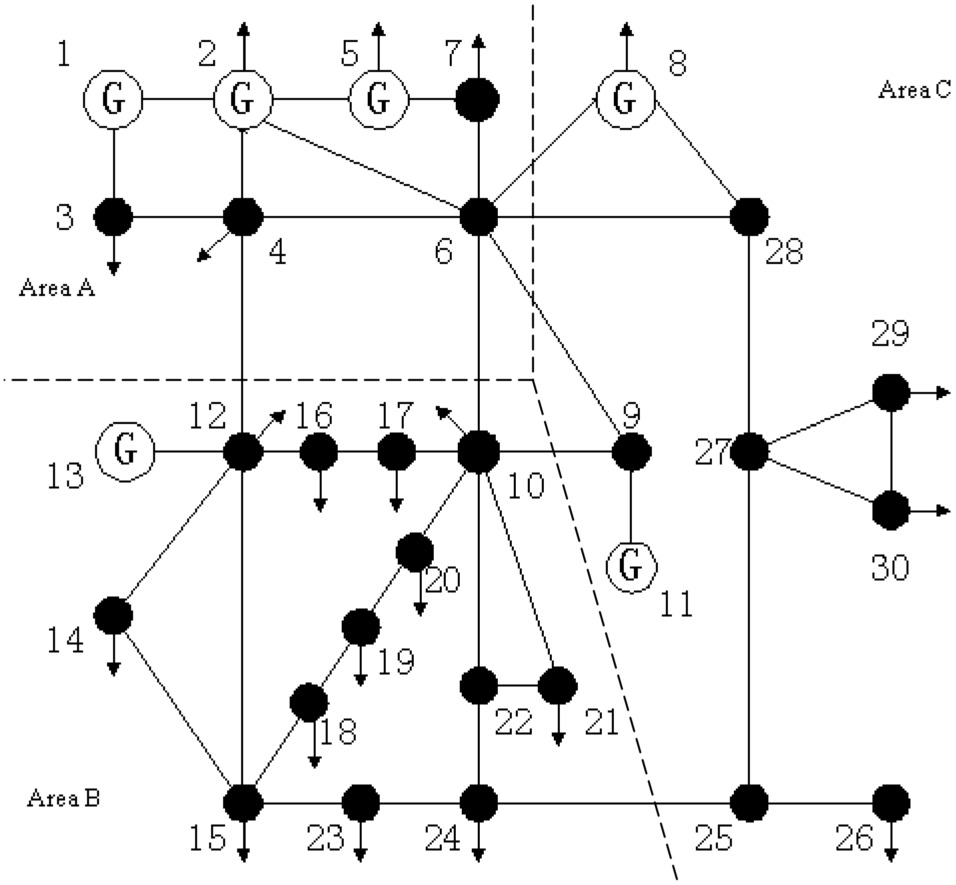

Fig. 2.4 One-line Diagram of IEEE 30-bus Reliability Test System

Similar with the above system, the optimization results is obtained by the proposed Variant PCPDIPM after 20 iteration steps. Table 2.2 shows the brief information about the validation on two test systems, where the CPU time is based on a computer of 1.6GHz processor/256M RAM/80G hard disk.

Table 2.2 Optimization of PCPDIPM on 6-bus and IEEE 30-bus Test System

	Number of Iterations	ATC (p.u.)	CPU time
6-bus Test System	13	1.062	33s
30-bus RTS	20	0.731	68s

2.5.3 Discussions on the Case Study

After applying the proposed variant PCPDIPM algorithm on the two test systems, it is found that the method can obtain ATC with transient angle stability constraints in acceptable number of iterations. Comparison of the simulation on two different size systems also shows that number of iteration does not enhance much with the increment of system scale.

In Fig. 2.3, during the first several iteration steps, the value of objective function varies in a comparatively wide range, and after the seventh step, it converges to the optimal value within a narrow range quickly. This is because in the beginning steps of PCPDIPM, the algorithm is seeking for the binding set. After this binding set is determined, its calculation burden is decreased much from one step to the next in the following iterations.

2.6 Summary

In this chapter, a variant PCPDIPM algorithm is proposed to solve one kind of dynamic ATC problems, the ATC evaluation with transient angle stability constraints. In the optimal formulation model, maximum relative rotor angle criterion is used as the rule of transient angle stability. With the variant PCPDIPM algorithm, system ATC can be obtained without violating the transient angle stability with fast convergence and reasonable accuracy while the algorithm is insensitive to the system scale and the number of control variables. Case studies demonstrate the effectiveness of the proposed method.

CHAPTER 3

ATC Evaluation with Dynamic Voltage Stability Constraints by Quasi-Steady-State Method

3.1 Introduction

Market oriented restructuring of electricity industry has been proceeding worldwide. Stimulated by the economic benefits, many power systems are often operating near the stability boundary and modern system operating conditions change more frequently than the traditional ones. Hence in addition to static stability limits, dynamic stability constraints are becoming more and more crucial in the system security considerations [36, 39, 57]. In the last chapter, ATC calculation with transient angle stability constraints has been investigated. In this chapter, the other type of dynamic constraint which concerns voltage stability will be incorporated in the research on ATC evaluation.

With the interconnection of bulk power systems spreading over several countries and regions, mass power transmission via long distance makes it possible that the area with sufficient power supply and little demand can provide support to a remote area where the power consumption requires much more than local generation capability. This is one of the advantages brought about by power market, and it benefits both sides of source area and sink area in economics and society. However, under this condition, transmission systems are operating under more stressed conditions due to the increased transaction level associated with open access, and voltage instability has become a major threat to maintain system security as well as being a dominant factor to limit power transmission. In recent years, widespread abnormal voltage instability and voltage collapse have occurred in several countries, including France, Japan, U.S.A. etc. Hence in the determination of ATC, how to keep the voltage profile and hold the voltage stability under control should be one of the major considerations.

In order to ensure system security operation, the ATC computation must be accurately and quickly updated as system conditions change. To satisfy the need of updating ATC at regular intervals, on-line voltage stability assessment with acceptable accuracy is required. However, it remains a demanding and time-consuming task, even though significant improvement has been made in the computer technology and efficient variable step size algorithms.

Different from the transient angle stability, voltage stability is a multi-time-scale dynamic category [67]. Classified along the time-scale, voltage stability of a system may be split into two categories: the short-term and the long-term dynamics. The former is rapid, while the latter is relatively slow. In practice, by fast protective devices and advanced auto-control technology, the voltage profiles of most systems respond in a stable way during the short-term following a disturbance. Hence when considering the determination of ATC, to simplify the calculation, the short-term dynamics may be filtered out by appropriate method and only the long-term dynamics are taken into account.

In this research, Quasi-Steady-State (QSS) approximation of long-term dynamics is proposed to evaluate ATC with dynamic voltage stability constraints. ATC determination scheme using QSS approximation is presented and implemented on test system. Performance of the QSS approximation is also compared with the full-time-scale simulation, and the results show that QSS can simplify the analysis and accelerate the calculation speed with acceptable accuracy.

3.2 QSS Concept

The idea of Quasi-Steady-State (QSS) is not new, but its application in power system analysis has just been tested in recent years [67]. It is adopted either as one operation mode of dynamic simulation or as a separate time-domain simulation program.

QSS is an approximation method for dynamic problems with multi-time-scales, which usually consists of a short-term and a long-term part. This method acts in the following ways of decomposition and approximation. If the dynamic mechanisms are different in the short and long terms, and the short-term dynamic ends with a stable point therefore has no effect on the stability of following long-term dynamic, it may be filtered out in the analysis and replaced with a quasi steady model. Thus the complicated computation and simulation in this short phase can be avoided. In the analysis of long term, by modifying the step sizes adaptively to the process or reconstructing the dynamic model of components in this phase or other appropriate measures, pivotal temporary balance points are obtained instead of the whole series of dynamic trajectory. The curve which consists of these pivotal temporary balance points has a serrated profile, and it can approximate the dominating characters of the original smooth dynamic trajectory. In this way the calculation in the long-term is sped up.

3.3 Problem Formulation

To evaluate ATC with long-term dynamic voltage stability constraints in this research, the following assumptions are made:

1. The system has survived the short-term period following a disturbance. From then on it is driven by the long-term dynamics. During the short-term fast transients, the slow state parameters keep unchanged.
2. The load in the test system is heavy and the transmission line is very long, so that the voltage stability limit emerges above other limits.
3. Considering the focus of this research, loads included in the model are designated to be with constant power characteristics.
4. Ignore the dead-band of the Under-Load-Tap-Changer (ULTC) transformer.

3.3.1 Objective Function

$$\text{Min - P}_{ATC} = Min - \sum_{mn \in L_t} P_{mn} \qquad \text{---- (3.3.1)}$$

This is same with the objective function in section 2.3.1, and the physical meaning of factors in the function is also the same.

3.3.2 Equation Constraints

In the following analysis, the power flow equations (2.3.2) and (2.3.3) are simply represented as algebraic equation (3.3.2), and the short-term dynamics are described by the differential equation (3.3.3).

In the deregulated environment, many power grids of large size are required to transfer electric power over long distance. From the power supply side to the demand side, there are various voltage levels, and ULTCs are commonly employed to hold the voltage profile of the load area. Although it is designed to restore load after disturbance, with the increasing complexity of load, the dynamic characteristics of ULTC may complicate the long-term dynamics and thus cause long-term voltage instability. In this research, the influence of ULTC on load restoration in the long-term dynamics is included.

The long-term dynamics are described by both continuous and discrete equations as (3.3.4) and (3.3.5).

$$\mathbf{0} = \boldsymbol{t}(\boldsymbol{x}, \boldsymbol{y}, \boldsymbol{Z}_c, \boldsymbol{Z}_d) \qquad \text{---- (3.3.2)}$$

$$\mathring{\boldsymbol{x}} = \boldsymbol{f}(\boldsymbol{x}, \boldsymbol{y}, \boldsymbol{Z}_c, \boldsymbol{Z}_d) \qquad \text{---- (3.3.3)}$$

$$\mathring{\boldsymbol{Z}}_c = \boldsymbol{h}_c(\boldsymbol{x}, \boldsymbol{y}, \boldsymbol{Z}_c, \boldsymbol{Z}_d) \qquad \text{---- (3.3.4)}$$

$$Z_d(k+1) = h_d(x, y, Z_c, Z_d(k)) \quad \text{---- (3.3.5)}$$

In the above equations,

t and **f** are smooth functions of time, i.e. **P**, **Q**, etc;

x are the state vectors during the short-term dynamics, i.e. rotor angle $\boldsymbol{\delta}$, rotor speed $\boldsymbol{\omega}$, internal transient voltage $\mathbf{E_q}'$, $\mathbf{X_{oxl}}$ of OXL (OvereXitation Limiter), etc;

y are the magnitudes and angles of bus voltages, i.e. **V**, $\boldsymbol{\theta}$;

$\mathbf{Z_c}$ and $\mathbf{Z_d}$ are the continuous and discrete state vectors during the long-term dynamic respectively, for example, $\mathbf{X_t}$ of OXL is considered as $\mathbf{Z_c}$, and transformer ratio of the ULTC is treated as $\mathbf{Z_d}$. In this research, we concentrated on the influence of ULTC on the load restoration in the long-term dynamics.

According to the QSS concept and the voltage dynamic process along multi-time-scale, when considering the voltage dynamics during long-term phases, it is acceptable to neglect the short-term dynamics and assume it may keep equilibrium after infinitely fast instantaneous time. Hence the detailed differential equation of it (equation (3.3.3)) may be replaced by the corresponding equilibrium equation $\mathbf{0} = f(x, y, Z_c, Z_d)$ (3.3.6). By this filtering, some parameters may be represented by simpler steady-state models. A reduced set of the equations involving reduced state vectors is obtained and analysis with less computational efforts may be carried out.

Since the dynamic behavior of some components in equation (3.3.4) mainly occurs during the short-term period, their mathematical model can be reconstructed in a simpler way to represent just their characteristics during the long-term phase. Only those components which influence the long-term voltage dynamics are reserved. In the search of the optimal objective, to speed up the process, binary search is used to find the boundary between the stable and unstable operation section.

Thus in the multi-time-scale simulation, the short-term dynamics are passed over while the long-term evolution is reproduced and QSS approximation is yielded in the long-term dynamics.

3.3.3 Inequality Constraints

Same as section 2.3.4, the operation boundary limits are listed in the inequality constraints as follows:

$$U_{i\min} \le |U_i| \le U_{i\max} \quad \text{---- (3.3.7)}$$

$$P_{Gi\min} \le |P_{Gi}| \le P_{Gi\max} \quad \text{---- (3.3.8)}$$

$$Q_{Gi\min} \le |Q_{Gi}| \le Q_{Gi\max} \quad \text{---- (3.3.9)}$$

$$|I_{ij}| \le I_{ij\max} \quad \text{---- (3.3.10)}$$

$$0 \le |P_{Li}| \le P_{Li\max} \quad \text{---- (3.3.11)}$$

$$0 \le |Q_{Li}| \le Q_{Li\max} \quad \text{---- (3.3.12)}$$

Since in the dynamic voltage variation, the behavior of ULTC influences the stability process much, its tap ratio limit should also be included. It is shown as below:

$$r_{\min} \le r \le r_{\max} \quad \text{---- (3.3.13)}$$

where, r is the tap ratio of ULTC, $r_{\min}$ and $r_{\max}$ is respectively the lower and upper limit of the tap ratio adjustment.

3.3.4 Voltage Dynamic Mechanism of System with ULTC after Disturbance

From the above formulations, when considering the long-term voltage dynamics, the dynamic characteristic of ULTC together with the complexity of load influences the process much. Hence, an analysis on the dynamic long-term voltage mechanism of a system with ULTC is presented in this section.

Under the power market environment, interconnected bulk power networks are required to deliver electric power over long distance. In many power networks, ULTC is commonly equipped between buses with different voltage levels to hold the voltage profile of the load area and restore the load power on the secondary side after a disturbance. Fig. 3.1 shows the trajectory of the operation point after a disturbance that shows the mechanism of the dynamic process of how the ULTC helps the network to restore at a new stable operation point. The P-V curves are those on the primary side of the ULTC, and the ULTC is assumed to be an ideal transformer. In other words, it absorbs no power and there is no power loss from the primary side to the secondary side. The system originally operates at point A as the base case. After a disturbance, the fast transient soon dies out, in other words, the short-term dynamics are passed in a stable way; and the P-V curve shrinks from pre-disturbance curve 1 to post-disturbance curve 2. Since ULTC is a slowly acting device and it usually moves its tap after a time delay of 30 seconds or so, the primary voltage will firstly decline along the original ULTC load characteristic with the tap ratio of $r=r_1$ and it falls to point B on curve 2. The voltage at this point is V_B, which is lower than the original voltage $V_{A.}$ This causes the voltage on the secondary side synchronously drops to a lower value than the reference. Then the ULTC is triggered to react and it decreases the tap ratio to r_2 to boost the voltage of the secondary side. The operation point shifts along curve 2 from B (which is with the original ULTC tap ratio r_1) to C, which is with the new tap ratio r_2. C is the intersection of the post-disturbance curve and the steady-state load characteristic. If V_C is still unsatisfactory, the operation point will continue to move similarly to the above until finally the system operates at a new stable point. However, the system may become unstable or even collapse if the power to be restored is beyond the capability of the ULTC; for example at point E which is on a P-V curve that has no intersection with the load characteristic. The illustration also shows the reduction of Voltage Stability Margin (VSM). With the first movement of the ULTC, it shrinks from VSM_1 before the disturbance to VSM_2 after the disturbance.

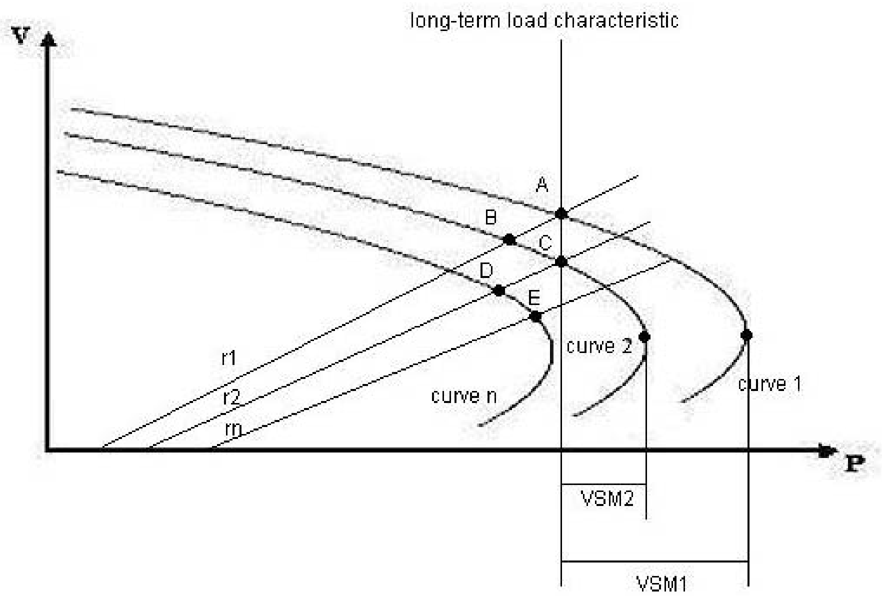

Fig 3.1 Trajectory of Operation Point Triggered by a Disturbance

3.4 Solution Strategy

The calculation procedures of ATC with voltage stability constraints by QSS approximation is illustrated in Fig. 3.2. In this research, the convergence tolerance for the simulation is 5 MW.

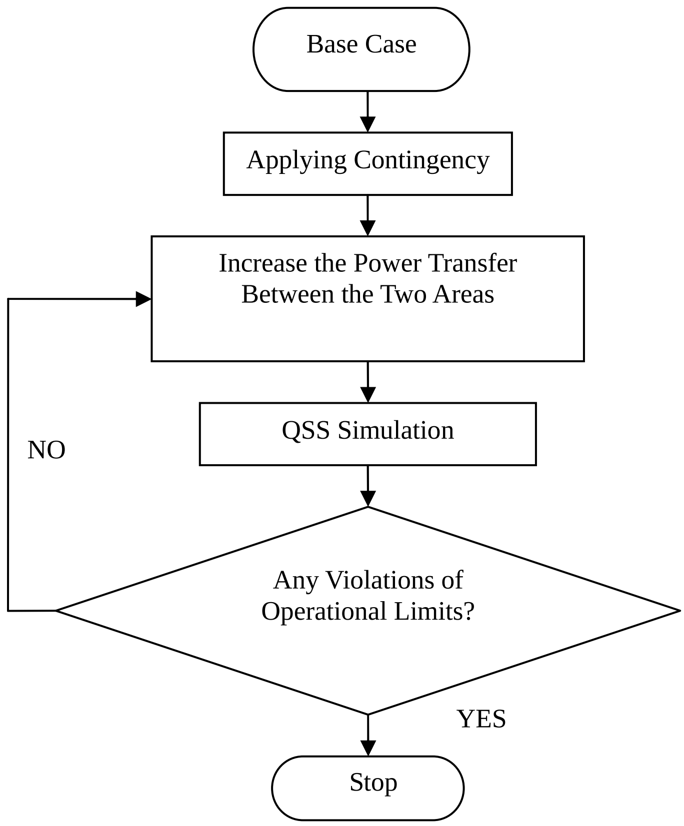

Fig. 3.2 Calculation Procedure of ATC with Voltage Stability Constraints by QSS Approximation

3.5 Case Study and Discussions

The proposed QSS approximation simulations are tested on an 11-bus, 4-generator test system equipped with ULTC as shown in Fig. 3.3. The full system parameters are available in [36]. The system has two areas. The system initially operates stably at the base case with the generation outputs and load data as shown in Table 3.1. Then the load in area 2 increases synchronously with the generation in area 1 to meet its demand. The total generation increment is shared by G1 and G2 equally. After a contingency has occurred (e.g. an outage on one of the 5 tie-lines between bus 6 and bus 7), the ULTC moves its tap after a time delay of 30 seconds, and moves subsequently after every 5 seconds delay to restore the system. At the same time, the power transfer between the two areas is kept increasing until finally the interface transmission lines cannot transfer more power and the system becomes unstable. The increment of total load in the sink area at the critical point of instability above the base case is taken as ATC between the two areas.

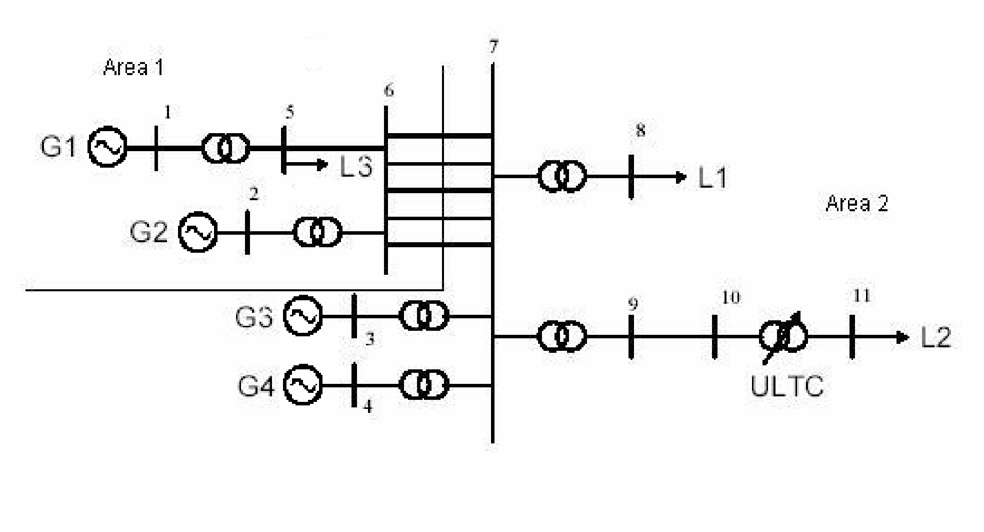

Fig. 3.3 The 11-bus, 4-generator Test System

Table 3.1 Generation Outputs and Load Data of the Test System in Base Case

Bus	P (MW)	Q (MVar)
1	4176.77	934.70
2	1536.00	374.30
3	475.00	198.38
4	478.00	198.54
5	-500.00	0
8	-2671.00	-980.00
11	-3284.00	0

Considering the result accuracy, Full-Time-Scale (FTS) simulation is the most favourite choice. Nevertheless, its computational efficiency is not high enough and in most circumstances, it can just satisfy the off-line instead of real-time requirement. In this research, FTS simulation is also carried out on the same system and compared with the QSS method to check the result accuracy of the latter as well as to compare the calculation speed of the two methods.

Fig. 3.4 and Fig. 3.5 show the evolution of the bus voltages magnitude before the collapse in the QSS and FTS simulations respectively. It is found that in this heavily stressed system, under a contingency of line outage, the voltage instability occurs before the system reaches the angle stability limits and thermal limits. The figures also show that the short-term dynamics, which is damped with a stable end in this case, is clearly displayed in the FTS. This is filtered out in the QSS simulation. The highlighted black curve is the voltage magnitude of the most critical bus: bus 10. From these two figures, we can observe that the simulation process of long-term dynamics and the results of the two methods are quite similar which manifest that the veracity of QSS is creditable. Furthermore, the difference of ATC value by the two methods is 640-637.5=2.5MW, which is within the tolerance of 5MW. Hence the accuracy of QSS is quite acceptable. However, the calculation speed of the former is more than 10 times faster than the latter. Table 3.2 shows the comparison of the two simulation methods.

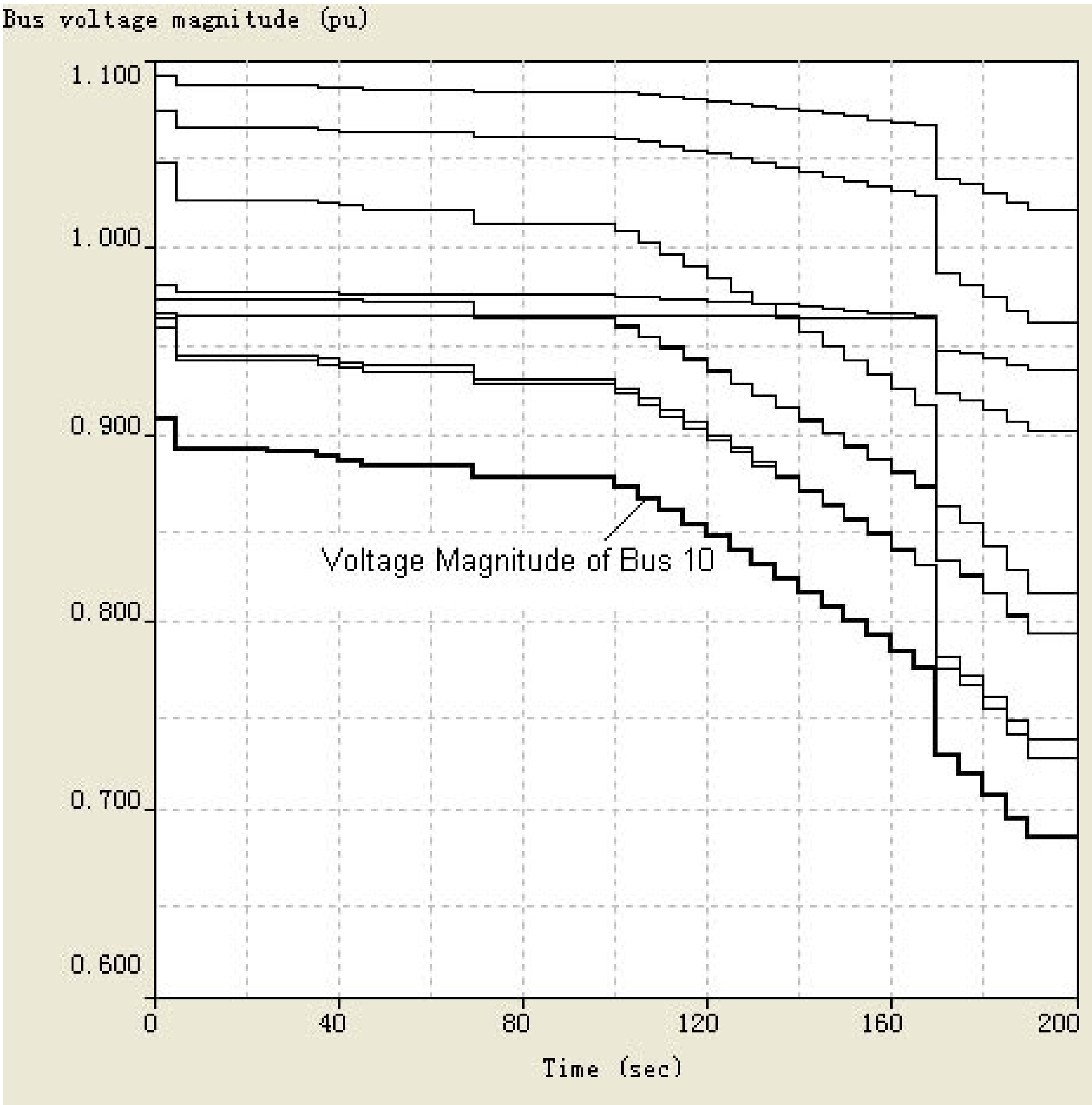

Fig. 3.4 Bus Voltage Magnitude Diagram by QSS Approximation Simulation

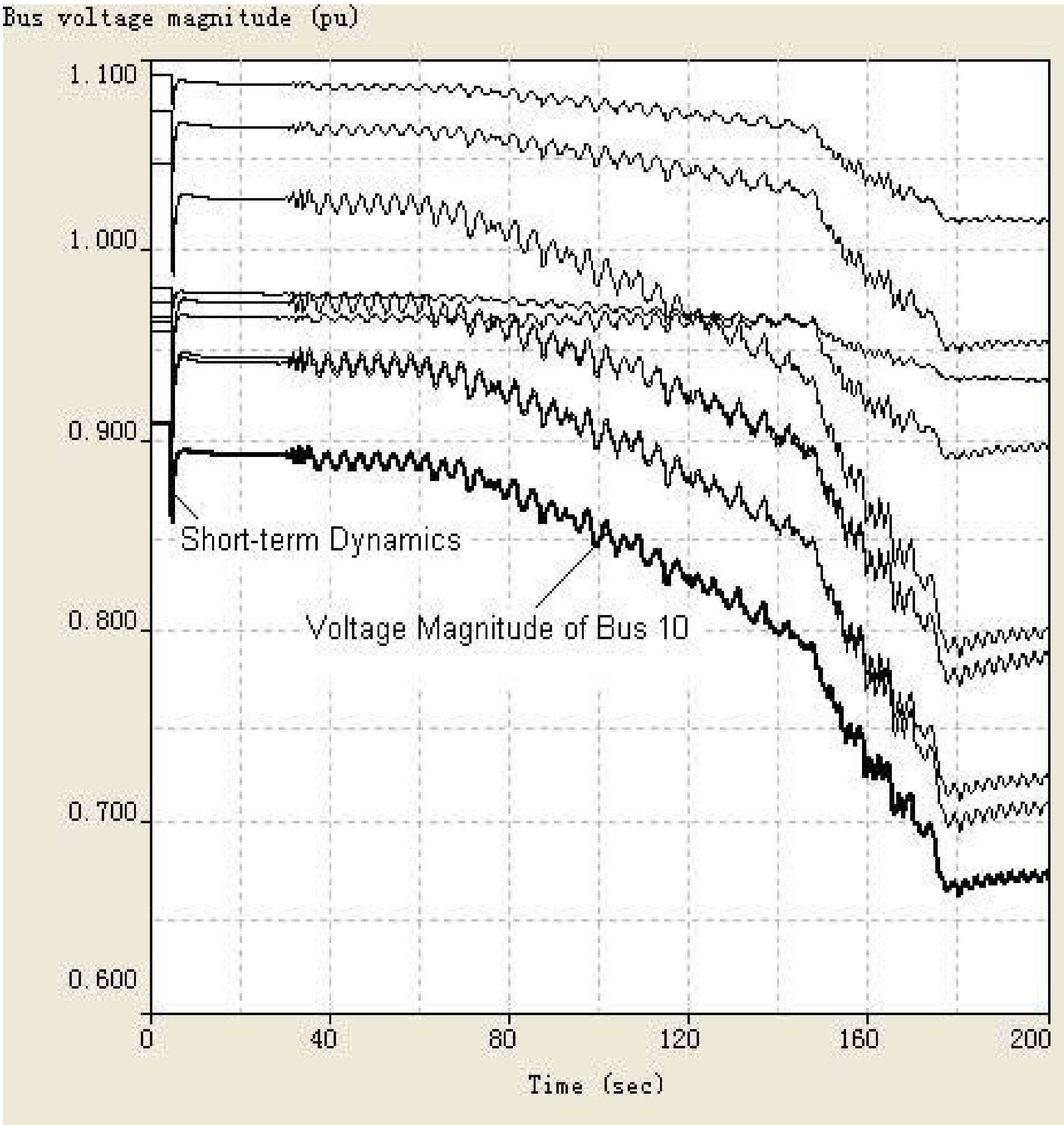

Fig. 3.5 Bus Voltage Magnitude Diagram by Full-Time-Scale Simulation

Table 3.2 Summary of Test Results

	ATC value above base case (MW)	Evaluation Time Duration (Sec)
QSS Simulation	637.5	4.8
Full-Time-Scale Simulation	640	65.3

In this case it is found that the changing of ULTC tap impacts the voltage stability and is one of the reasons that result in voltage collapse. This is because the action of ULTC tap changing leads the increment of load reactive consumption and worsens the imbalance of reactive power in the system. Hence in a system which is in shortage of reactive power, ULTC can merely maintain the voltage profile of local bus. Its action is insufficient to increase the voltage condition of the whole network and sometimes it is harmful to the system voltage stability.

3.6 Summary

With the development of deregulated power market, the power networks are more exposed to the risk of voltage instability than ever. In an increasing number of systems, in particular those which transmit large power flow over long distance, voltage instability is recognized as a major threat for system operation which is at least as important as thermal overload and angle instability. This makes it essential for the voltage stability to be a prominent consideration when declaring on-line information on the OASIS. Hence, under the deregulation environment, the ATC value that is required to be published on the OASIS on-line should consider the dynamic voltage stability constraints.

In this chapter, the dynamic voltage stability evolution mechanism of a power system is illustrated, and QSS approximation is applied in the determination of ATC with consideration of dynamic voltage stability constraints. Simulation by QSS approximation method is implemented on an 11-bus, 4-generator heavily loaded test system equipped with ULTC. Full-Time-Scale simulation is also performed on the same system. It is found that in this heavily stressed system, under a contingency of line outage, the tendency of voltage instability is more serious than the angle stability limits. The simulation results show that the proposed QSS approximation method can evaluate ATC with dynamic voltage stability constraints with acceptable accuracy while the calculation speed is accelerated considerably.

CHAPTER 4

ATC Calculation with Multi-Objective Optimization of Economical and Secure Operation in Power Market

4.1 Introduction

Different from the traditional load capacity or transmission capacity in a vertical integrated electrical power industry, ATC in power market is not just a technical indicator for secure operation. As one of the crucial information that is required to be provided on OASIS in a power market, it is also a commercial signal for the power supplier and consumer. Following the research of ATC evaluation as a security index in the former two chapters, its role as a commercial signal in the power market is also investigated in this research.

In this chapter, an innovative multi-purpose objective function with consideration of both stability control and economical benefit of ATC is proposed and solved by a variant Primal-Dual Predictor-Corrector Interior Point Method (PDPCIPM). In this context, the first purpose is to maximize the ATC value with certain security operation considerations and the second one is to minimize the investment and operation costs on enhancing ATC and solving congestion. The latter is based on the former and is also constrained by the operation security limits which confine the former; meanwhile the former is optimized with the economic factors included in the latter. In individual power systems, since the power system physical structure and market commercial degree is different from one another, interactions between the two objectives are not always the same. Therefore a weighting factor is introduced to reflect the concerning rate. For system with a structure which is robust enough to undergo steep and complicated perturbations, economic consideration is the main purpose for optimization; while for a system which is not very robust or the security operation is required to be maintained at special preference, the proportion on the stability part should be enhanced. In this way, the market role of ATC can be represented together with the stability constraints.

4.2 Problem Formulation

4.2.1 Objective Function

For the sake of providing operators and market participants with a series of solutions to allow them to analyze the effect of power bids based on certain security level, thus proper operating and bidding decisions can be practiced, a multi-objective model is proposed as follows:

$$\mathrm{Min}R = Min\left\{\tau\left(-\sum_{mn\in L_t} P_{mn}\right) + (1-\tau)\left(\sum_{i\in I} B_{Si}P_{Gi} - \sum_{j\in J} B_{Dj}P_{Lj}\right)\right\} \qquad \text{---- (4.2.1)}$$

The above function is a decomposition formula which allows both power pricing and operation security. The first half part refers to the maximization of ATC values, while the latter half part means maximizing social benefit, which is the economic consideration when determining the ATC value.

To include the economic factors in the objective function, there are different choices. Here the maximization of social benefit is employed rather than minimizing the total generation costs or other objective. This is because in the evaluation of ATC, the economical benefit of both the power suppliers and consumers are considered together. The social benefit is represented by the difference between total active power demand biddings and total supply biddings. Since reactive power generating costs are much less than those of active power and it is usually not included in the biddings under current utility operation, the operating costs of providing a generator's reactive power is assumed to be negligible.

Denote $\tau \in (0,1)$, where τ is the weighting factor that may be chosen as different value for individual power system or different operation conditions in the same system. When τ is close to 0, it means that social benefit is the main concern in the objective function. On the other hand, when τ is close to 1, maintaining the security is the dominating priority. It is observed that the two parts of the objective function is usually counted in different units, i.e., typically, the former term is in p.u., and the latter term is in $/h. To combine these two terms in the same function, proper scale should be included in the choice of τ .

In function (4.2.1),

L_t is the set of tie lines between the source area and sink area;

mn is one of the tie lines where m and n are respectively the start bus of the source area and the ending bus of the sink area;

P_{mn} is the active power transferred along tie line of mn;

B_{Si} is the active power supply bidding of generator at bus i;

B_{Dj} is the active power demand bidding of load at bus j;

P_{Gi} is the active power output at bus i;

P_{Lj} is the active power consumption at bus j;

I is the set of buses with active power supply;

J is the set of buses with active power demand.

In this chapter, the main research interest is in combining the technical and economic role of ATC as a whole. For the sake of simplification, in this chapter, the dynamic constraints will not be included in the computation as detailed in the former two chapters. A new parameter ρ_c is introduced to express the power supply and demand condition at critical point. This critical point could be corresponding to the operation condition which is limited by any concerned constraints, such as transient angle stability limit, dynamic voltage stability limit, bus voltage limit, generator active or reactive power output limit, system singularity, thermal limit, etc. At the critical point, the active power of generator and load is as follows:

$$P_{Gc} = (1 + \rho_c + \lambda_{Loss})P_{G0} \qquad \text{---- (4.2.2)}$$

$$P_{Lc} = (1 + \rho_c)P_{L0} \qquad \text{---- (4.2.3)}$$

where, λ_{Loss} is the coefficient that represents the system active power loss;

P_{G0} and P_{L0} is respectively the power supply and demand at base case.

The upper and lower limits of ρ_c are obtained by previous studies with special concerned constraints. For example, investigations such as what have been implemented in the former two chapters can provide useful information for these limits. When ATC reaches the optimal value with constraints, it means the critical point is found, and ρ_c

is obtained.

Thus the objective function can be reconstructed in a more direct appearance as:

$$\mathrm{Min}R = Min\left\{\tau(-\rho_c)+(1-\tau)\left(\sum_{i\in I} B_{Si}P_{Gi} - \sum_{j\in J} B_{Dj}P_{Lj}\right)\right\} \quad \text{---- (4.2.4)}$$

4.2.2 Equality Constraints

Two groups of equality constraints should be satisfied. One is the same with former chapters; the other is the power flow equations at the critical point.

$$P_{Gi} - P_{Li} - \sum_{j=1}^{n} |U_i||U_j|(G_{ij}\cos\theta_{ij} + B_{ij}\sin\theta_{ij}) = 0 \quad \text{---- (4.2.5)}$$

$$Q_{Gi} - Q_{Li} - \sum_{j=1}^{n} |U_i||U_j|(G_{ij}\sin\theta_{ij} - B_{ij}\cos\theta_{ij}) = 0 \quad \text{---- (4.2.6)}$$

$$P_{Gic} - P_{Lic} - \sum_{j=1}^{n} |U_{ic}||U_{jc}|(G_{ij}\cos\theta_{ijc} + B_{ij}\sin\theta_{ijc}) = 0 \quad \text{---- (4.2.7)}$$

$$Q_{Gic} - Q_{Lic} - \sum_{j=1}^{n} |U_{ic}||U_{jc}|(G_{ij}\sin\theta_{ijc} - B_{ij}\cos\theta_{ijc}) = 0 \quad \text{---- (4.2.8)}$$

4.2.3 Inequality Constraints

In addition to the inequality constraints associated by operation limits, such as the bus voltage limits, generator active and reactive power output upper and lower limits, load active and reactive power limits, thermal limits, tap ratio limit of ULTC, etc., a new constraints related with ρ_c is set in this study.

$$\rho_{c\min} \le \rho_c \le \rho_{c\max} \quad \text{---- (4.2.9)}$$

$$U_{i\min} \le |U_i| \le U_{i\max} \quad \text{---- (4.2.10)}$$

$$P_{Gi\min} \le |P_{Gi}| \le P_{Gi\max} \quad \text{---- (4.2.11)}$$

$$Q_{Gi\min} \le |Q_{Gi}| \le Q_{Gi\max} \quad \text{---- (4.2.12)}$$

$$|I_{ij}| \le I_{ij\max} \quad \text{---- (4.2.13)}$$

$$0 \le |P_{Li}| \le P_{Li\max} \quad \text{---- (4.2.14)}$$

$$0 \le |Q_{Li}| \le Q_{Li\max} \quad \text{---- (4.2.15)}$$

$$r_{\min} \le r \le r_{\max} \quad \text{---- (4.2.16)}$$

$\rho_{c\min}$ and $\rho_{c\max}$ are obtained by previous studies with special concerned constraints. The physical meanings of parameters in inequality (4.2.10) to (4.2.16) are the same as those in section 2.3.4 and section 3.3.3.

4.3 Solution Strategy

For the multi-objective OPF problem as formulated in section 4.2, the variant Primal-Dual Predictor-Corrector Interior Point Method (PDPCIPM) proposed in section 2.4.2 is employed to be the solution method with the aim of both robustness and reliability. Details about this method can be found in section 2.4.2 and would not be repeated in this chapter.

It should be pointed out that for this problem with economic factors in the objective function, some new indicators for power market and electricity pricing can be obtained as by-product of the proposed PDPCIPM. The solution of the multi-objective OPF problem produces not only the optimal operating point, but also some sensitivity variables through the Lagrangian multipliers. For example, Locational Marginal Price (LMP) at each node is found. The LMP of active power supply is the sensitivity of generation production cost with respect to active power supply at bidding, and it is actually the Lagrangian multipliers of power flow equations associated with P_{Gi}. From the Lagrangian function (4.2.17) which is established in the solution process of PDPCIPM, LMPs can be gained from the KKT optimality conditions, i.e., by the partial difference of the Lagrangian function to active power.

$$L = f(x) - yh(x) - z^T\left(g(x) - \underline{g} - l\right) - w^T\left(g(x) - \overline{g} + u\right) - \mu\left(\sum_i \ln l_i + \sum_i \ln u_i\right)$$

---- (4.2.17)

When substituting the detailed parameters in equations (4.2.4) to (4.2.16) for the general variables in the above equation, from the KKT optimality conditions, the partial difference of the Lagrangian function to generating active power is:

$$\partial L / \partial P_{Gi} = B_{Si} - LMP_{P_{Gi}} + w_{P_{Gi}} P_{Gi\max} - z_{P_{Gi}} P_{Gi\min} = 0 \qquad \text{---- (4.2.18)}$$

Hence, the LMP for power supply at bus i can be obtained by:

$$LMP_{P_{Gi}} = B_{Si} + w_{P_{Gi}} P_{Gi\max} - z_{P_{Gi}} P_{Gi\min} \qquad \text{---- (4.2.19)}$$

Similarly, LMP of power demand at bus i can be obtained.

4.4 Case Study and Discussions

To manifest the proposed multi-objective ATC problem with variant PDPCIPM method, numerical implementation is performed on the 6-bus test system as shown below.

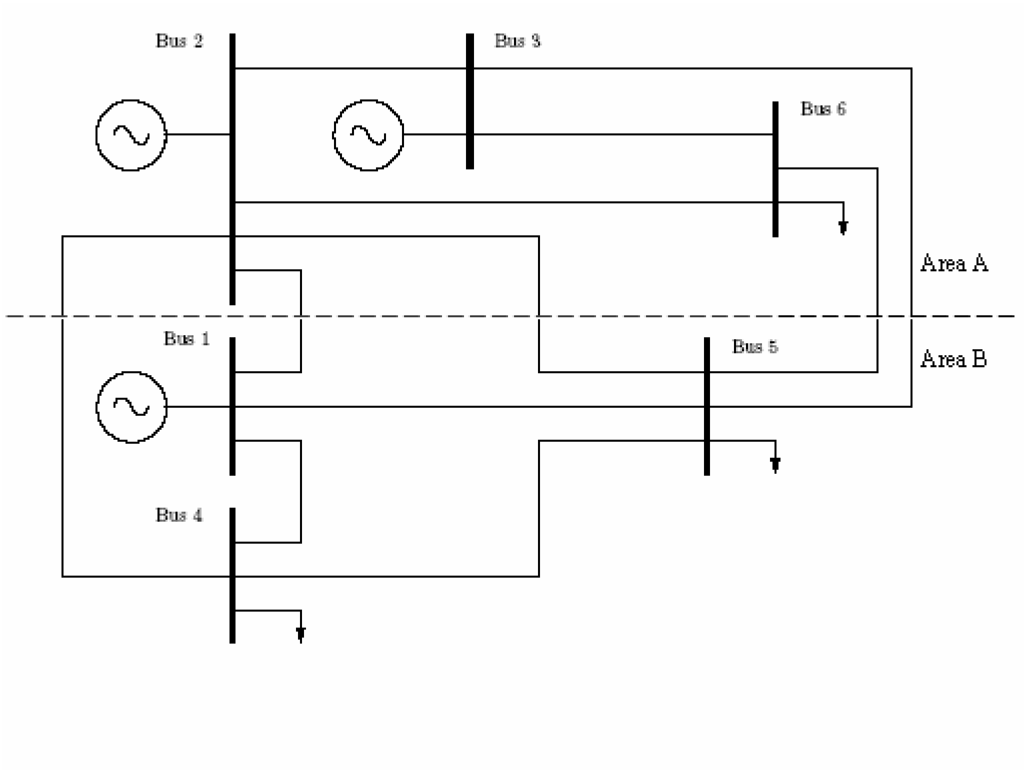

Fig. 4.1 One-line Diagram of 6-bus Test System

The parameters of its operation boundary limits and base case are the same as in section 2.5.1, but with a new limit of $\rho_{c\min} = 0.1$ and $\rho_{c\max} = 0.8$, which are determined by a previous voltage stability investigation.

For different weighting factors $\tau = [0.1,0.2,0.3,0.4,0.5,0.6,0.7,0.8,0.9]$, the multi-objective problem is carried out.

Fig. 4.2 and Fig. 4.3 show the change of active power supply and demand with the increment of weighting factor respectively. They show that when the weighting factor is less than 0.7, the active power generation and demand bids are satisfactory and not affected by the variation of weighting factor; only when the weighting factor exceeds 0.7, they begin to change. This is because when the weighting factor is low, the main concern of the optimal objective is social benefit. In such a simple test system, this objective could be kept at a balance level within a range of security operation constraints. On the other hand, when the weighting factor increases, the system security degree is enhanced to a high emphasis status. Thus both the active power output by generators and demand by loads should be decreased to a lower level so as to ensure that the system can survive more serious disturbance and maintain stability.

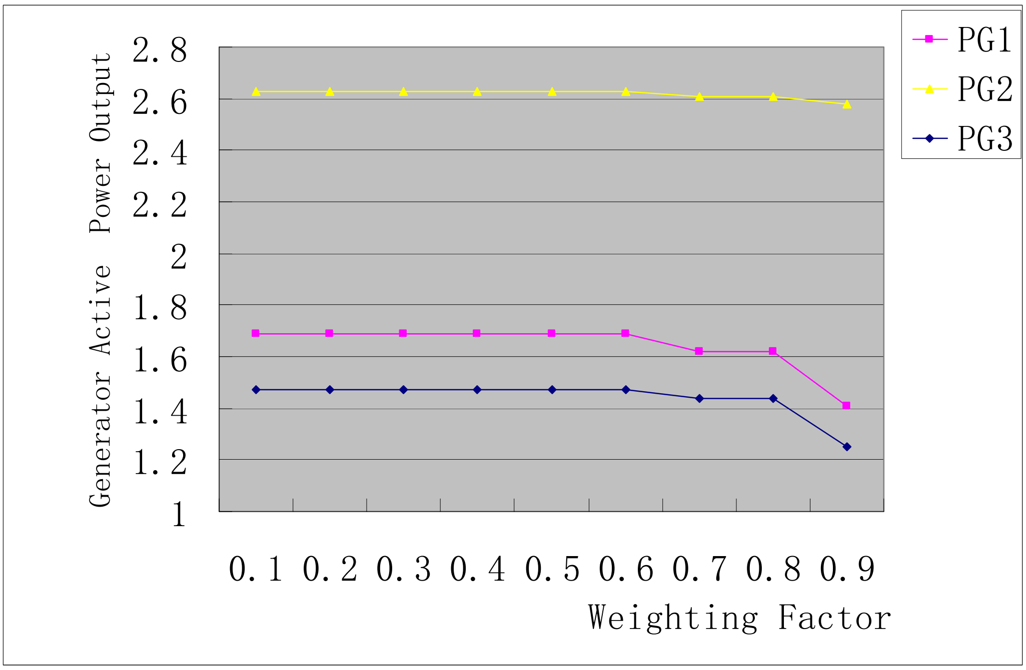

Fig. 4.2 Active Power Supply for the 6-bus Test System

with Change of Weighting Factor

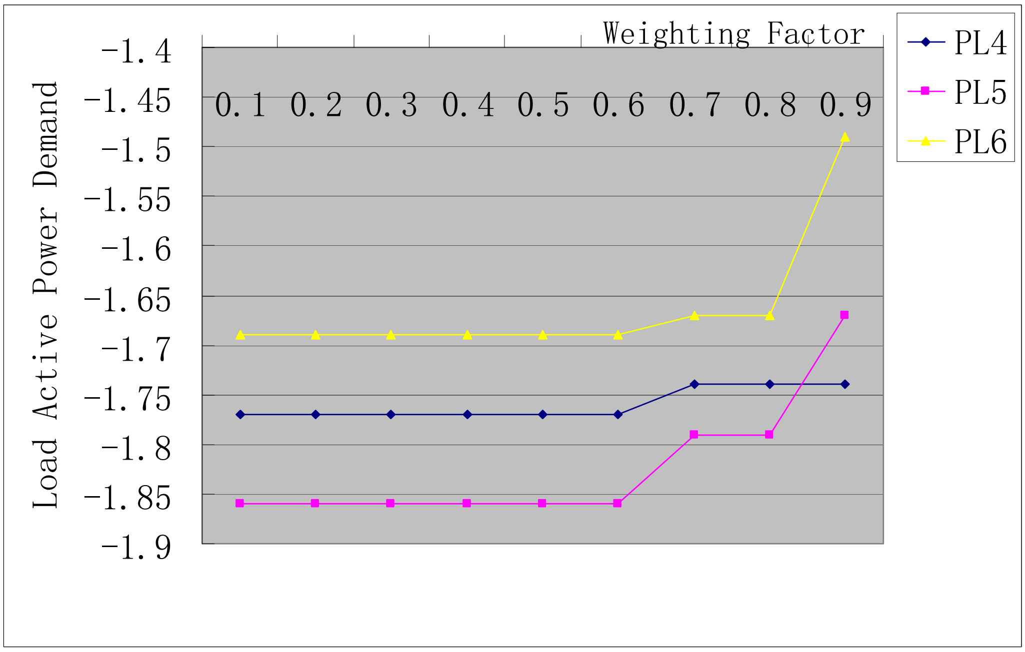

Fig. 4.3 Active Power Demand for the 6-bus Test System

with Change of Weighting Factor

Fig 4.4 and Fig. 4.5 separately show the payment for active power supply and demand with different weighting factors. They show that when security operation is concerned as the main term of optimization, economic factors are considered just on the basis of that stability is ensured enough. Thus the payment level is less than that of the condition when economical benefit is the pivoting interest. With this loss of economical benefit, the load level is kept in a lower level and the potential crisis of congestion can be avoided. At the critical point, the bidding price at each bus is shown in Table 4.1 as follows.

Simulation and data comparison has also been performed on the IEEE 30-bus RTS, the result is similar with this case.

Table 4.1 Power Supply and Demand Bidding of the 6-bus Test System

Bus	1	2	3	4	5	6
B_{Si} [$/h]	8	6	7	——	——	——
B_{Di} [$/h]	——	——	——	9	8	7

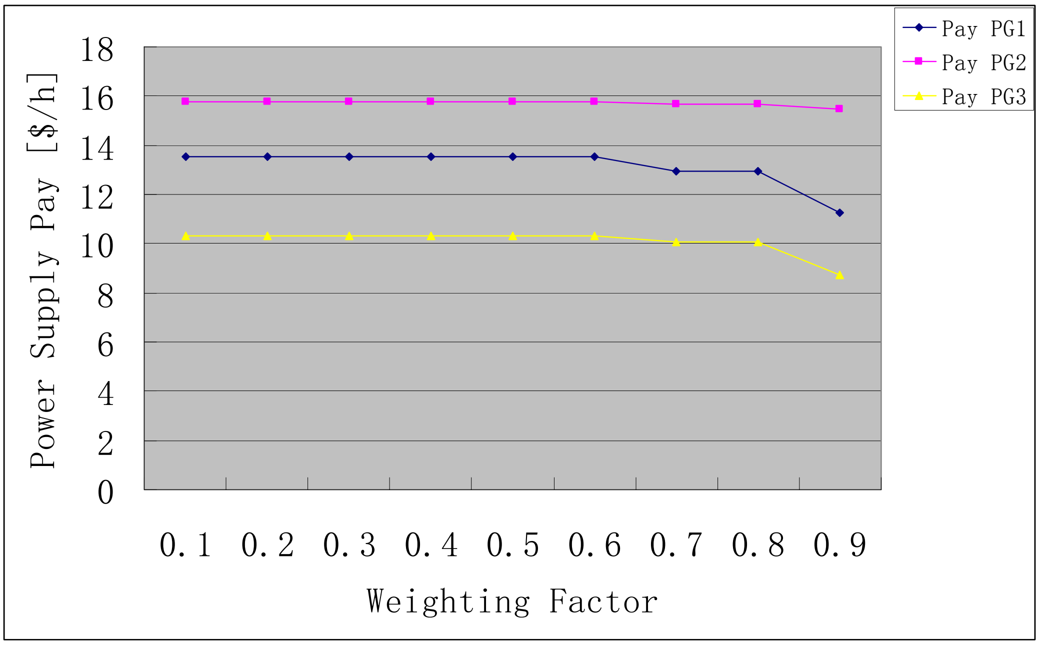

Fig 4.4 Active Power Supply Pay for the 6-Bus Test System

with Change of Weighting Factor

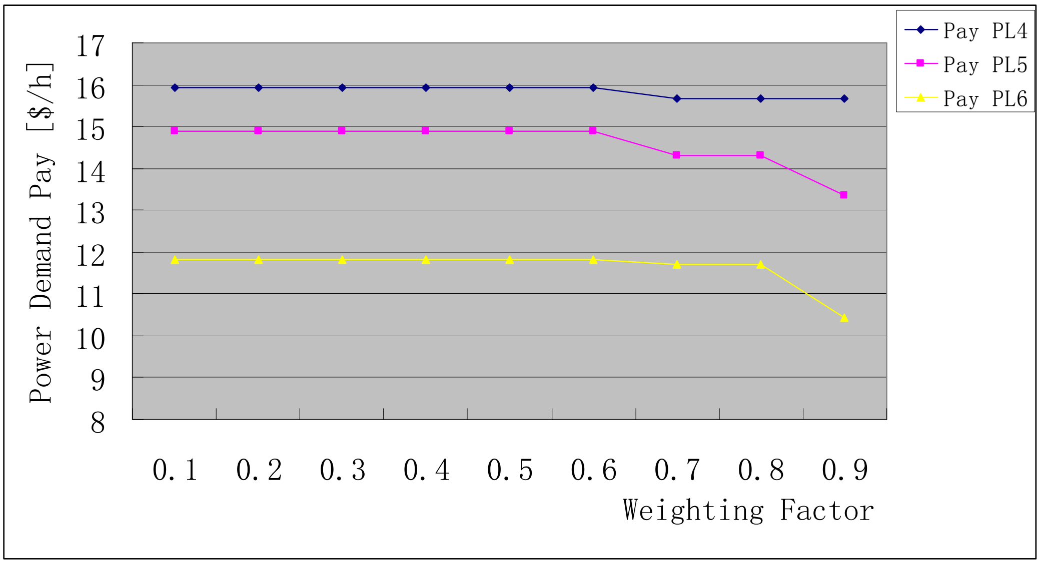

Fig 4.5 Active Power Demand Pay for the 6-Bus Test System

with Change of Weighting Factor

4.5 Summary

In this chapter, a method to combine both the economic and stability considerations in the ATC evaluation is implemented. A multi-objective function of operation constraints is formulated with which both the technical and market implication of ATC can be expressed. A variant PDPCIPM method is employed to solve the OPF problem. Case study on a 6-bus test system is performed to verify the interaction between the economic and stability roles of ATC evaluation.

CHAPTER 5

ATC Evaluation with Transient Stability Constraints by Risk-Based Optimal Method

5.1 Introduction

Evaluation of the cost associated with system security has been a great interest in power systems, especially under the framework of competitive power market. In the last chapter, a consideration of combining the price bidding and system stability together in the determination of ATC is performed. In this chapter, another risk-based optimal method is proposed to include different contingencies and the system transient instability risk cost in the ATC determination.

In the context of security evaluation, the risk is defined as the product of occurrence probability of an unexpected event and its consequences [41]. Through the risk analysis, both probabilities and costs of transient instability events are simultaneously considered. In this way, a bridge is built up between power system economics and security. Meanwhile, due to the adoption of expectation rule for the ATC decision-making process, the definition of risk threshold value is unnecessary, which is essentially different from the previous approaches [2, 40, 69]. With the above ideas, a risk-based optimal ATC compromised between the economics and security of system operations is conveniently determined. Case study on the 39-bus New England test system is given to manifest the validity of the proposed approach.

5.2 Problem Formulation

5.2.1 Model of Transient Instability Risk

5.2.1.1 Transient Instability Probability

Assume that $t_{cl,i}$ is the contingency clearing time decided by the protection apparatus for contingency f_i. Probability of power system transient instability related to contingency f_i is denoted as:

$$\Pr_i(I \mid f_i) = \Pr_i(t_{cl,i} > t_{cr,i}) \quad (i \in S_f) \qquad \text{---- (5.2.1)}$$

where I denotes for transient instability event; $t_{cr,i}$ for critical clearing time (CCT) of contingency f_i; S_f for a set of contingencies considered.

If the randomness of variable $t_{cl,i}$ is ignored, (5.2.1) will be simplified as:

$$\Pr_i(I \mid f_i) = \begin{cases} 0 & t_{cl,i} \le t_{cr,i} \\ 1 & t_{cl,i} > t_{cr,i} \end{cases} \quad (i \in S_f) \qquad \text{---- (5.2.2)}$$

Furthermore, assume that different events are mutually exclusive and exhaustive. According to the theory of conditional probability, probability of transient instability for all the contingencies in set S_f can be estimated by:

$$\Pr_s = \sum_{i \in S_f} [\Pr_i(I \mid f_i) \cdot \Pr(f_i)] \qquad \text{---- (5.2.3)}$$

where $\Pr_s$ is for probability of system transient instability; $\Pr(f_i)$ for occurrence probability of contingency f_i, which is associated with contingency properties, such as contingency location, contingency type and so on.

From (5.2.3), probability of system transient stability $\Pr_s'$ is approximated as:

$$\Pr_s' = 1 - \Pr_s \qquad \text{---- (5.2.4)}$$

5.2.1.2 Transient Instability Impacts

Transient instability impacts could be evaluated by analysis of direct and indirect financial costs incurred due to failures. Indirect cost consequences of transient instability events usually refer to social/political impacts coming from interruption of energy supply, which is usually difficult to measure. For illustrative purpose, only direct impacts of system transient instability are discussed in this research, according to the idea proposed by V. Vittal et al (1999) [69], which can be estimated as following:

$$C_i = C_{i,load} + C_{i,repair} + C_{i,replace} \qquad \text{---- (5.2.5)}$$

where C_i is for costs of system transient instability related to contingency f_i; $C_{i,load}$ for customer interruption costs; $C_{i,repair}$ for repair and start up costs of tripped units; $C_{i,replace}$ for production increase costs caused by replacing lost energy supply with more expensive energy.

For all the contingencies in set S_f, costs of power system transient instability, C_s, is calculated as follows:

$$C_s = \sum_{i \in S_f} (\omega_i \cdot C_i) \qquad \text{---- (5.2.6)}$$

where ω_i is weighted factor for contingency f_i, which is given by:

$$\omega_i = \Pr_i \Big/ \sum_{i \in S_f} \Pr_i \qquad \text{---- (5.2.7)}$$

Obviously, $C_s = 0$ if system keeps stable for all considered contingencies.

5.2.1.3 Transient Instability Risk

With (5.2.3) and (5.2.6), transient instability risk R_s is evaluated by:

$$\begin{aligned} R_s &= \Pr_s \cdot C_s \\ &= \sum_{i \in S_f} [\Pr_i (I \mid f_i) \cdot \Pr(f_i)] \cdot \sum_{i \in S_f} (\omega_i \cdot C_i) \end{aligned} \qquad \text{---- (5.2.8)}$$

5.2.2 Expectation Rule

Let x denote power transferred between areas, then its expectation benefit in concerned operation condition, $E_s(x)$, is calculated by:

$$E_s(x) = (1 - \Pr_s) \cdot B_s(x) - \Pr_s \cdot C_s(x) \qquad \text{---- (5.2.9)}$$

where $B_s(x)$ and $C_s(x)$ are benefit and cost of system operation under power transfer level x, respectively. Note that $C_s(x)$ is calculated by (5.2.6) and $B_s(x)$ by the following:

$$B_s(x) = f(x - x_{base}) \qquad \text{---- (5.2.10)}$$

where x_{base} is for power transferred between areas in base case; f for benefit function of power transfer increase.

In the risk analysis, variable x is usually discrete. That is to say, if the following condition is true,

$$E(x_{opt}) = \max_{i \in S_d} E(x_i) \qquad \text{---- (5.2.11)}$$

According to expectation rule, transfer power x_{opt} is optimal for all possible schemes in set S_d.

If variable x is extended to be continuous, (5.2.11) becomes:

$$E(x_{opt}) = \max E(x) \qquad x \in [\underline{x}, \overline{x}] \qquad \text{---- (5.2.12)}$$

where set $[\underline{x}, \overline{x}]$ is the allowed range of variable x.

5.3 Solution Strategy

ATC is the maximum amount of power that can be transferred from source to sink area without violations of system constraints. In this section, method for analyzing deterministic ATC with constraints for both steady-state and dynamic security of system is firstly presented. Then, model and approach for assessing risk-based optimal ATC with transient stability constraints are discussed. For simplicity, risk-basked optimal ATC constrained by transient stability is called optimal ATC thereafter.

5.3.1 Deterministic Steady-State ATC

For a power corridor Ω, model for analysis of deterministic ATC with steady-state security constraints (named model A) is given by a nonlinear programming problem in (5.3.1)-(5.3.9):

$$\max \sum_{j \in \Omega} P_{lj} \quad \text{---- (5.3.1)}$$

$$s.t. \quad P_m - P_L - P(V,\theta) = 0 \quad \text{---- (5.3.2)}$$

$$Q_m - Q_L - Q(V,\theta) = 0 \quad \text{---- (5.3.3)}$$

$$\sum_{k \in S} P_{m,k} = \sum_{d \in R} P_{L,d} \quad \text{---- (5.3.4)}$$

$$| I(V,\theta) | \leq \bar{I} \quad \text{---- (5.3.5)}$$

$$\underline{V} \leq V \leq \overline{V} \quad \text{---- (5.3.6)}$$

$$\underline{P_m} \leq P_m \leq \overline{P}_m \quad \text{---- (5.3.7)}$$

$$\underline{Q_m} \leq Q_m \leq \overline{Q}_m \quad \text{---- (5.3.8)}$$

$$0 \leq P_L \leq \overline{P}_L \quad \text{---- (5.3.9)}$$

Here, (5.3.1) is for objective function and P_{lj} in it for transfer power of line j in corridor Ω; (5.3.2)-(5.3.4) and (5.3.5)-(5.3.9) for equality and inequality constraints, respectively; notations S and R for generator set on sending side and load set on receiving side of corridor Ω, respectively; $\overline{P}_m$ and $\underline{P_m}$ for upper and lower bounds of generator active power output P_m, respectively; $\overline{Q}_m$ and $\underline{Q_m}$ for upper and lower bounds of generator reactive power output Q_m, respectively; $\overline{P}_L$ for upper bounds of active load P_L; Q_L for reactive load; $P(V,\theta)$ and $Q(V,\theta)$ for real and imaginary network injections, respectively; $\bar{I}$ for thermal limits of line apparent power flows

$I(V,\theta)$; $\overline{V}$ and $\underline{V}$ for upper and lower limits of bus voltage magnitudes V , respectively; θ for bus voltage angles.

In model A, $P_{m,k}\,(k \in S)$ and $P_{L,d}\,(d \in R)$ are all control variables with constant power factors.

5.3.2 Deterministic Dynamic ATC

Transient stability-constrained deterministic ATC model (named model B) is shown in (5.3.10)-(5.3.13). Compared with model A, dynamic security constraints (5.3.12)-(5.3.13) are added.

$$\max \sum_{j \in \Omega} P_{lj} \quad \text{---- (5.3.10)}$$

$$s.t. \quad (5.3.2)\ \text{-}\ (5.3.9) \quad \text{---- (5.3.11)}$$

$$\begin{gathered} |\,\delta_i^l(t) - \delta_j^l(t)\,| \le \overline{\delta} \\ (t \in [0,T];\ \forall l = 1,\ldots,n_c;\ \forall i,\ j = 1,\ldots,n) \end{gathered} \quad \text{---- (5.3.12)}$$

$$\begin{cases} M_i \dfrac{d\tilde{\omega}_i}{dt} = P_{m,i} - P_{e,i} - \dfrac{M_i}{M_T} P_{COI} = f_i(\cdot) \\ \dfrac{d\delta_i}{dt} = \tilde{\omega}_i \qquad\qquad (i = 1,\ldots,n) \end{cases} \quad \text{---- (5.3.13)}$$

where, $\overline{\delta}$ is for an angle threshold; n_c for number of contingencies considered; T for time duration of contingencies; equation (5.3.12) means that all angle differences among generators in T should be less than $\overline{\delta}$ for system (5.3.13) in the frame of center of inertia (COI).

5.3.3 Optimal ATC Assessment

Both models A and B are for deterministic ATC analysis. In this chapter, only transient angle stability is considered as the dynamic constraints of ATC, which is included in Model B. ATC results, however, might be conservative because of omission of probabilistic nature of system events. To overcome this problem, in this research, from the viewpoint of system instability risk, probabilities and costs of different contingencies are also taken into account in evaluating the optimal ATC.

With (5.2.12), the following conclusion is obviously held:

Optimal ATC maximizes expectation benefit of area transfer power with system steady-state security constraints to be satisfied.

Thus, it is deduced that the optimal ATC solution should be satisfied with the following inequality.

$$ATC_B \le ATC_{opt} \le ATC_A \qquad \text{---- (5.3.14)}$$

where TTC_A and TTC_B are for ATC obtained by models A and B, and TTC_{opt} for optimal ATC.

Based on the above analysis, a model for analysis of the optimal ATC, named model C, is built up by (5.3.15)-(5.3.17):

$$\max E_s(\sum_{j\in\Omega} P_{lj}) \qquad \text{---- (5.3.15)}$$

$$s.t. \qquad (5.3.2)\text{ - }(5.3.9) \qquad \text{---- (5.3.16)}$$

$$ATC_B \leq \sum_{j\in\Omega} P_{ij} \leq ATC_A \qquad \text{---- (5.3.17)}$$

It is logical to understand that the optimal ATC determined by model C has made a fair compromise between benefits in the increasing transfer power and the costs for incurrence of system instability. So the optimal balance between power system economics and security is implemented.

Let $x = \sum_{j\in\Omega} P_{lj}$, and hence model C is simply denoted by:

$$\max E_s(x)\,(ATC_B \leq x \leq ATC_A) \qquad \text{---- (5.3.18)}$$

Equation (5.3.18) implies that the solution of the optimal ATC is achieved only through calculating objective function (5.3.15) if constrains (5.3.16)-(5.3.17) are met in advance. Owing to calculation complexity in (5.3.18), a discretization approach is adopted to approximate the optimal solution. In this way, (5.3.18) is modified as follows:

$$E_s(ATC_{opt}) = \max E(x_i) \qquad (i = 1,2,\cdots,n_x) \qquad \text{---- (5.3.19)}$$

where n_x is the number of variable x in range of $[ATC_B, ATC_A]$ used in the discretization analysis.

To improve the precision in ATC_{opt} assessment by (5.3.19), an interpolation method is utilized in the optimal ATC analysis.

If condition (5.3.20) is encountered in ATC analysis,

$$E_s(x_{i-1}) > E_s(x_i) \qquad \text{---- (5.3.20)}$$

the optimal ATC solution can be evaluated by interpolation formula (5.3.20).

$$ATC_{opt} = x_{i-1} + \frac{\Delta E_s(x_{i-1}) \cdot (x_i - x_{i-1})}{\Delta E_s(x_i) - \Delta E_s(x_{i-1})} \qquad \text{---- (5.3.21)}$$

here, $\Delta E_s(x_k)$ $(k = i, i-1)$ is evaluated by:

$$\Delta E_s(x_k) = E_s(x_k) - E_s(x_k - \Delta x) \qquad \text{---- (5.3.22)}$$

on assumption that $E_s(x)$ is continuous and differentiable at x_k, where Δx is a small power increment.

5.3.4 Flow Chart for Optimal ATC Analysis

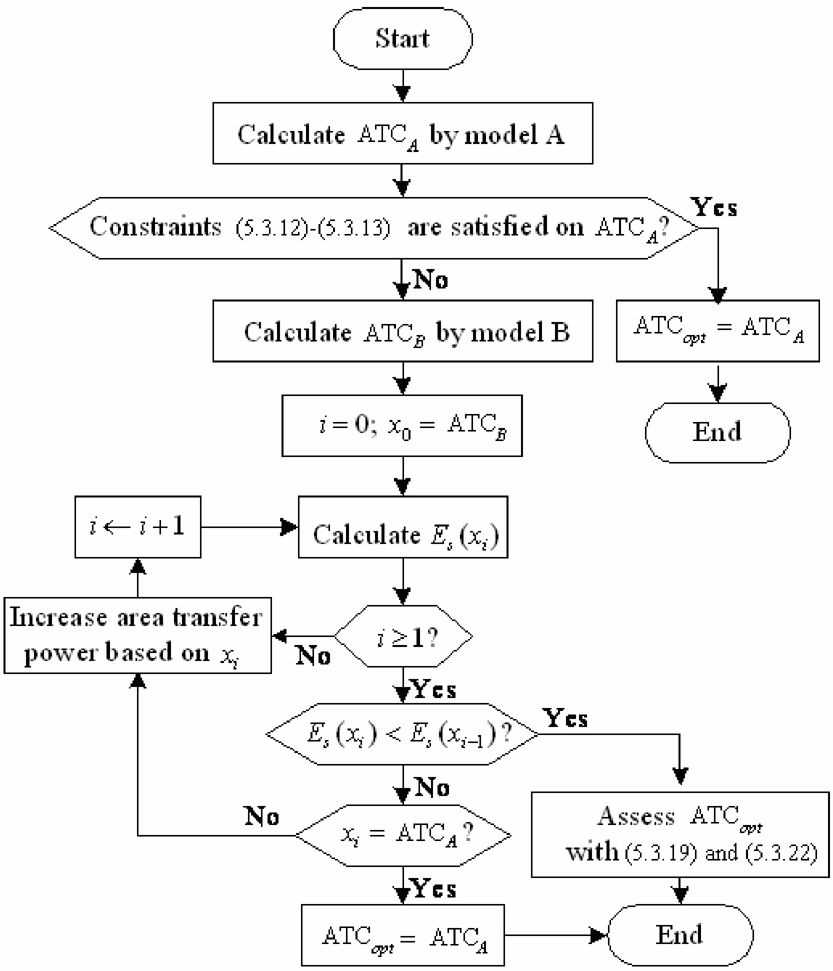

Fig. 5.1 Flow Chart of the Risk-based Optimal ATC Evaluation

The assessment strategy for the optimal ATC analysis is summarized in Fig.5.1, where ATC_A is firstly calculated by model A. Once dynamic security constraints (5.3.12)-(5.3.13) are found not to be satisfied on ATC_A, evaluate the expectation benefits of each transfer power until the optimal ATC solution is detected.

5.4 Case Study and Discussions

To evaluate the effect of the proposed method, a case study was carried out on the 39-bus 10-generator New England test power system. Configuration with three areas named A, B and C is shown in Fig. 5.2. The corridor considered in optimal ATC study is composed of tie lines (16-17) and (16-15), with power transferred from source area A to sink area B. The base-case power outputs of generators and their upper and lower generation limits are listed in Table 5.1.

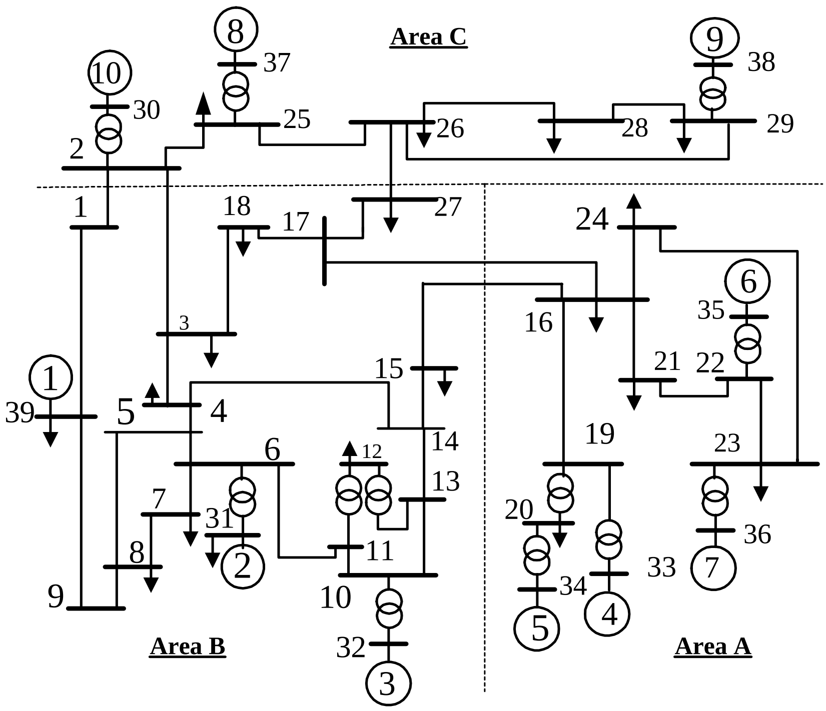

Fig. 5.2 The 39-bus 10-generator New England test power system

Table 5.1 Active Power Generation Limits and Outputs in Base Case of the Generators in 39-bus System

Gen. No.	2	3	4	5	6	7	8	9	10
$P_{\max}$ (MW)	700	800	700	600	800	700	600	900	300
$P_{\min}$ (MW)	490	560	480	420	560	490	420	600	210
P_{base} (MW)	573	650	560	445	585	495	540	650	250

According to the assessment strategy of optimal ATC proposed in section 5.3, model A is calculated at first. In the test, the allowable range of bus voltage is from 0.95p.u. to 1.05p.u. and maximal thermal loading of each line is set as two times of its power flow in base case. With model A, the ATC of the corridor is obtained as $ATC_A = 350.7$ MW. To check the dynamic security of the system on ATC_A, contingency screening is performed. The screening strategy is that only contingencies of 3 phase short circuit at the start and end bus of each line in Areas A and B are considered. In total, 54 contingencies are involved in the screening. Harmful contingencies obtained by the screening are summarized in Table 5.2, where contingency occurrence probability and contingency clearing time are also provided.

Table 5.2 Results of Contingency Screening for Model A

No.	Line /faulted bus	Probability (p.u.)	Contingency clearing time(s)
1	22-21/22	0.01	0.12
2	22-21/21	0.04	0.12

Table 5.2 shows that $ATC_A = 350.7$ MW does not satisfy the requirements of system

dynamic security. With model B and parameter $\overline{\delta} = 180^0$, ATC of the corridor is obtained as $ATC_B = 248.9$ MW. ATC_A and ATC_B are all results of deterministic ATC methods.

In comparison, model C is used for the analysis of optimal ATC of the corridor. According to the function proposed by Audomvongseree K. and Yokoyama A. (2003) [2], let the benefit function of power transfer increase for the corridor be:

$$f(x') = 24 \cdot (1 - (e^{0.001x'} - 1)) \cdot x' \qquad \text{---- (5.4.1)}$$

and $x_{base} = 233.9$ MW, thus:

$$B_s(x) = 24(2 - e^{0.001(x-233.9)})(x - 233.9) \qquad \text{---- (5.4.2)}$$

where x denotes the corridor transfer power.

For evaluation of transient instability costs, based on the ideas proposed by V. Vittal et al (1999) [69], some estimation values used in the analysis are given in Table 5.3.

Table 5.3 Estimation of Transient Instability Impacts

Generation Redispatch	Load lost	Unit startup and repair
32\$/MWh	200\$/MWh	156,999\$/case
（Generation cost: 19\$/MWh）		

If the system can be restored to normal operating state in 10 hours after units are tripped due to occurrence of harmful contingencies in Table 5.2, the ATC results of model C are shown in Table 5.4. Curves in Fig. 5.3 are plotted by the corresponding data in this table.

Table 5.4 Analysis Results of Model C

x [MW]	$\Pr_s$ [p.u.]	R_s [10^4\$]	$(1-\Pr_s)B_s$ [10^4\$]	E_s [10^4\$]
248.9	0	0	0.3595	0.3595
263.7	0.01	0.2828	0.7059	0.4231
278.6	0.01	0.3500	1.0573	0.7074
293.3	0.01	0.4212	1.4029	0.9818
308.0	0.01	0.4976	1.7475	1.2499
312.9	0.01	0.5243	1.8622	1.3378
327.6	0.05	3.0418	2.1162	-0.9255
350.7	0.05	3.7644	2.6318	-1.1327

Fig. 5.3 indicates that with the enhancement of area transfer power, both the benefit and the instability risk of system operation are increased. The maximum expectation benefit of system operation is reached at $ATC = 312.9MW$. According to (5.3.19), the solution of model C is thus approximated by $ATC_{opt} \doteq 312.9\,\text{MW}$.

By comparison of $\left(ATC_{opt} - X_{base}\right)/X_{base} = 33.78\%$ and $\left(ATC_B - X_{base}\right)/X_{base} = 6.41\%$, it is inspiring that the ATC of model C has improved 33.78% relative to corridor transfer power in base case, which is greatly larger than the improvement 6.41% achieved by model B. This is because the ATC by Model C is just the optimal balance between benefits in increasing transfer power and costs in system instability. Another significant advantage in the approach of optimal ATC is that no risk threshold is required during the decision-making process. Therefore, ATC by model C is expected to have more applications in managements of modern power systems.

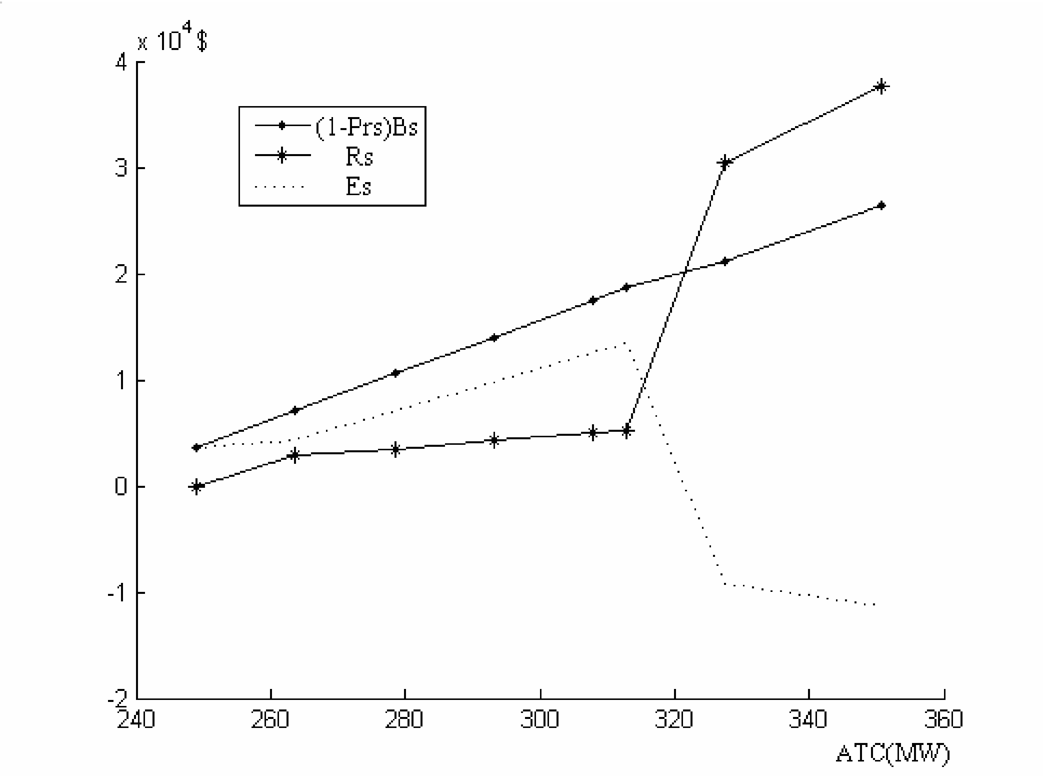

Fig. 5.3 Risk & Benefit of System Operation versus the Area Transfer Power

5.5 Summary

An approach for assessment of risk-based optimal ATC with transient stability constraints is developed in this chapter. Both probabilities and costs of transient instability events are considered. Due to the application of expectation rule, the optimal risk ATC between economics and security is conveniently achieved, which is essential to improve the operation level in system resource usage. Simulation on the 39-bus 10-generator New England test power system validates the effectiveness of the proposed approach.

CHAPTER 6

Application of FACTS Devices for ATC Enhancement

6.1 Introduction

With increased interconnections among power grids, more electrical power is transferred from one region with affluent generation capacity to another where the power supply is far from satisfying the local demand. In addition to being a significant technical index that all participants in the power markets need to know with the aim of stable and secure operation, the value of ATC acts also as a market signal that inducts the power supplier and consumer to perform their transaction for better economical benefit. Among the issues associated with ATC, participants are mainly concerned with two issues. One is how to evaluate ATC with different constraints as fast as possible with sufficient accuracy. The other is how to increase the ATC between areas so that participants may have more power exchange transaction under satisfactory security so that the total social benefit is improved. In the previous chapters, investigations on ATC evaluation with a variety of dynamic and static constraints via different solution methodologies are discussed. In this chapter, the issue of how to enhance the ATC value between interconnected areas by Flexible AC Transmission Systems (FACTS) devices is studied.

Since the early 1980's, advances in Flexible AC Transmission Systems (FACTS) controllers in power systems have led to their application in improving stability of power networks. Because the power-electronics-based FACTS controllers are designed to directly control the AC transmission lines, their applications for various purposes are developed under the electricity market. Several studies analyzing the application of FACTS controllers for voltage and transient angle stability have been reported by former researchers. In such research, the effect of FACTS controller on the economic operation and voltage stability of the network is the principle motivation behind incorporating FACTS into various OPF formulations. The main idea behind FACTS is to use network parameters as controls to direct flow, thus eliminating problems caused by unwanted loop or parallel flows, etc., providing dynamic reactive power support and voltage control, influencing real and reactive power flow, which hence improving the system performance.

Since FACTS controllers can provide reactive-power compensation and benefit to increase the active power transfer between areas, it is important to study the effect of FACTS devices on ATC. In 2003, Xiao et al [79] proposed a methodology for improving ATC by UPFC via stochastic approach.

In this research, an algorithm of enhancing ATC by FACTS devices via a variant Primal-Dual Predictor-Corrector Interior Point Method (PDPCIPM) is proposed, followed by a case study on the IEEE 30-bus Reliability Test System (RTS).

6.2 Problem Formulation

6.2.1 Objective Function

For the sake of explanation, in this chapter, the parameter ρ_c introduced in Chapter 4 is employed in the objective function to express the maximum value of ATC. As that in Chapter 4, ρ_c is a parameter to represent the power supply and demand condition at critical point. This critical point is the operation condition which is limited by any concerned constraints, such as transient angle stability limit, dynamic voltage stability limit, bus voltage limit, generator active or reactive power output limit, system singularity, thermal limit, etc. At the critical point, the active power of generator and load is as follows:

$$P_{Gc} = (1 + \rho_c + \lambda_{Loss})P_{G0} \qquad \text{---- (6.2.1)}$$

$$P_{Lc} = (1 + \rho_c)P_{L0} \qquad \text{---- (6.2.2)}$$

where, λ_{Loss} is the coefficient that represents the system active power loss;

P_{G0} and P_{L0} is respectively the power supply and demand at base case.

The upper and lower limits of ρ_c are obtained by previous studies with special concerned constraints. When ATC reaches the optimal value with constraints, it means the critical point is found, and ρ_c is obtained.

Thus the objective function can be formulated as:

$$Min(-\rho_c) \qquad \text{---- (6.2.3)}$$

6.2.2 Power Flow Equation Constraints

Two groups of power flow equation constraints should be satisfied as below, where (6.2.4) and (6.2.5) are for normal operation points, while (6.2.6) and (6.2.7) are for the critical point.

$$P_{Gi} - P_{Li} - \sum_{j=1}^{n} |U_i||U_j|(G_{ij} \cos\theta_{ij} + B_{ij} \sin\theta_{ij}) = 0 \quad \text{---- (6.2.4)}$$

$$Q_{Gi} - Q_{Li} - \sum_{j=1}^{n} |U_i||U_j|(G_{ij} \sin\theta_{ij} - B_{ij} \cos\theta_{ij}) = 0 \quad \text{---- (6.2.5)}$$

$$P_{Gic} - P_{Lic} - \sum_{j=1}^{n} |U_{ic}||U_{jc}|(G_{ij} \cos\theta_{ijc} + B_{ij} \sin\theta_{ijc}) = 0 \quad \text{---- (6.2.6)}$$

$$Q_{Gic} - Q_{Lic} - \sum_{j=1}^{n} |U_{ic}||U_{jc}|(G_{ij} \sin\theta_{ijc} - B_{ij} \cos\theta_{ijc}) = 0 \quad \text{---- (6.2.7)}$$

6.2.3 Inequality Constraints for Operation Limits and Critical Point Parameter ρ_c

Operation limits, such as the bus voltage limits, generator active and reactive power output upper and lower limits, load active and reactive power limits, thermal limits, tap ratio limit of ULTC, etc. and upper and lower limits of ρ_c are listed as follow. Here, $\rho_{c\min}$ and $\rho_{c\max}$ are obtained by previous studies with special concerned constraints.

$$\rho_{c\min} \le \rho_c \le \rho_{c\max} \quad \text{---- (6.2.8)}$$

$$U_{i\min} \le |U_i| \le U_{i\max} \quad \text{---- (6.2.9)}$$

$$P_{Gi\min} \le |P_{Gi}| \le P_{Gi\max} \quad \text{---- (6.2.10)}$$

$$Q_{Gi\min} \le \left|Q_{Gi}\right| \le Q_{Gi\max} \quad \text{---- (6.2.11)}$$

$$\left|I_{ij}\right| \le I_{ij\max} \quad \text{---- (6.2.12)}$$

$$0 \le \left|P_{Li}\right| \le P_{Li\max} \quad \text{---- (6.2.13)}$$

$$0 \le \left|Q_{Li}\right| \le Q_{Li\max} \quad \text{---- (6.2.14)}$$

$$r_{\min} \le r \le r_{\max} \quad \text{---- (6.2.15)}$$

6.2.4 Constraints Imposed by FACTS Devices

With the introduction of FACTS devices, some new parameters appear and thus new constraints emerge [23].

To clarify the physical meaning of these parameters and constraints, a brief description of three main FACTS devices is illustrated in the following.

6.2.4.1 Thyristor Controlled Phase Shifter (TCPS)

By serially connecting thyristor controlled boosting transformer into transmission line, the output voltage is different from the input, there are phase shift and magnitude change between the two voltages. The structure of TCPS is shown in Fig. 6.1, and its operating characteristic is illustrated in Fig. 6.2. Its turn ratio equation is given by:

$$\frac{U'}{U} = \frac{e^{j\phi}}{K} \quad \text{---- (6.2.16)}$$

where K and ϕ are the control parameters of TCPS.

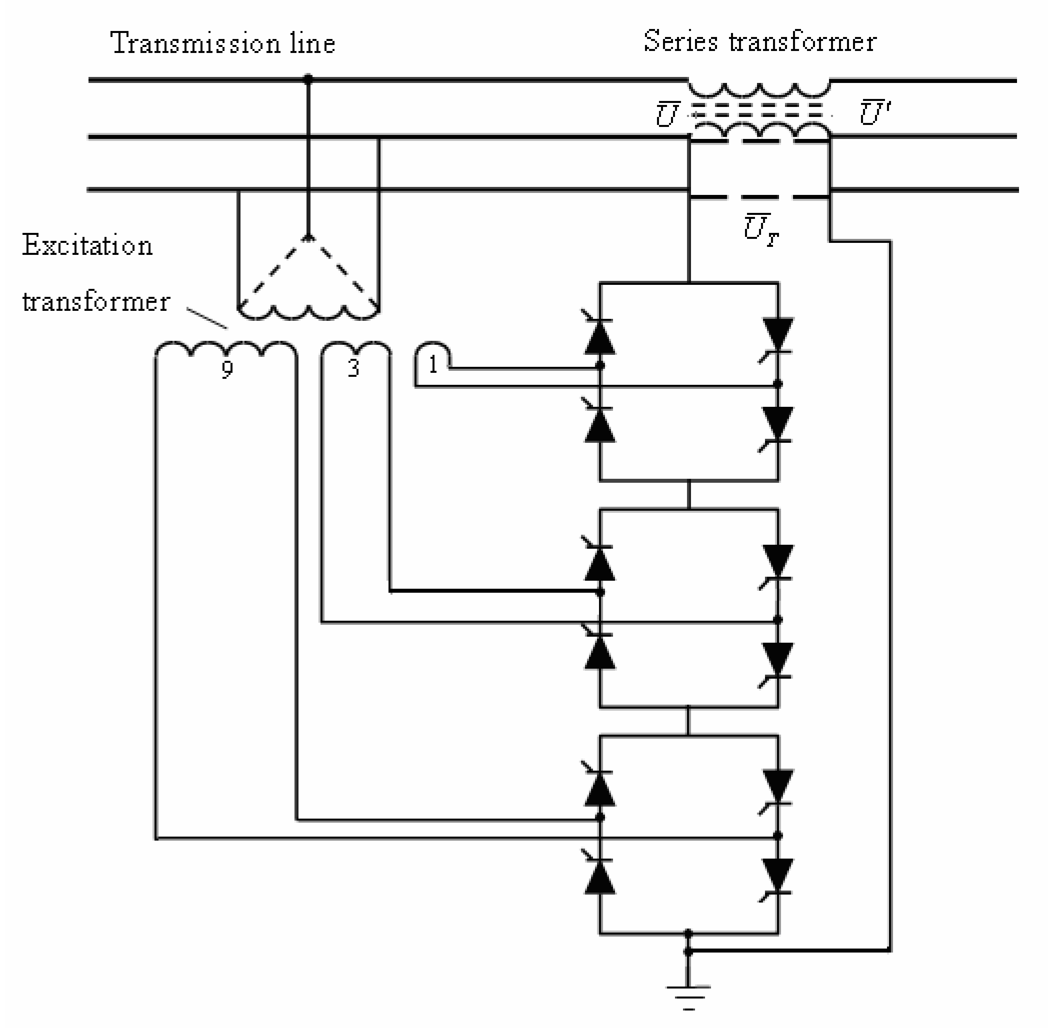

Fig. 6.1 Structure of Thyristor Controlled Phase Shifter

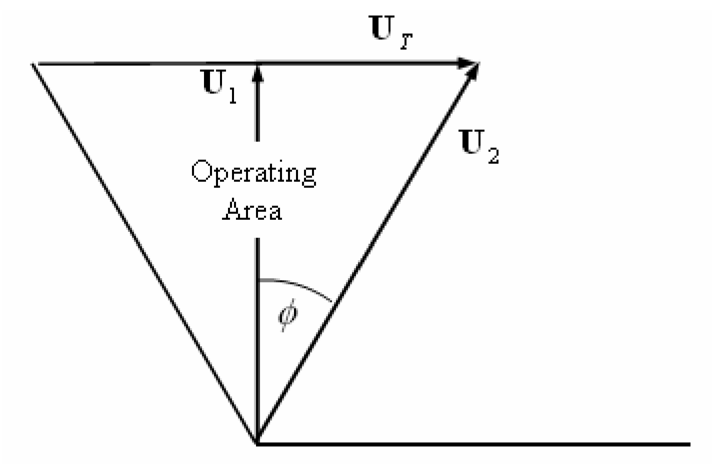

Fig. 6.2 TCPS Operating Characteristic

Its equivalent circuit is shown in Fig. 6.3. From which, the active and reactive power flow equations of TCPS line can be deduced as follows:

$$P_{ij} = U_i^{\,2} g_{ij} / K^2 - U_i U_j (g_{ij} \cos(\delta_{ij} + \phi) + b_{ij} \sin(\delta_{ij} + \phi)) / K \quad \text{---- (6.2.17)}$$

$$Q_{ij} = -U_i^{\,2} (b_{ij} / K^2 + B/2) - U_i U_j (g_{ij} \sin(\delta_{ij} + \phi) - b_{ij} \cos(\delta_{ij} + \phi)) / K \quad \text{---- (6.2.18)}$$

$$P_{ji} = U_i^{\,2} g_{ij} - U_i U_j (g_{ij} \cos(\delta_{ij} + \phi) - b_{ij} \sin(\delta_{ij} + \phi)) / K \quad \text{---- (6.2.19)}$$

$$Q_{ji} = -U_j^{\,2} (b_{ij} + B/2) + U_i U_j (g_{ij} \sin(\delta_{ij} + \phi) + b_{ij} \cos(\delta_{ij} + \phi)) / K \quad \text{---- (6.2.20)}$$

where

$$g_{ij} = \frac{r_{ij}}{r_{ij}^2 + x_{ij}^{\,2}}, \quad b_{ij} = -\frac{x_{ij}}{r_{ij}^2 + x_{ij}^{\,2}} \quad \text{---- (6.2.21)}$$

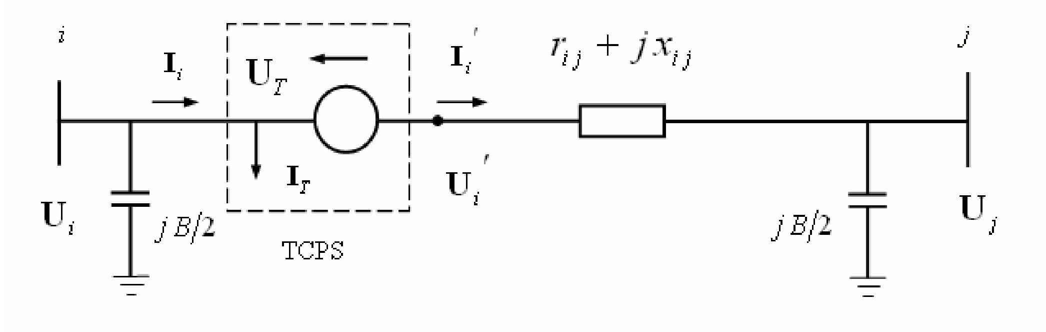

Fig 6.3 Equivalent Circuit of TCPS

6.2.4.2 Thyristor Controlled Series Compensation (TCSC)

The series impedance of a high voltage transmission line is usually inductive, with only 5-10 percent resistance. This provides convenient conditions to control the steady-state impedance of a transmission line by adding both a thyristor controlled series capacitor and a thyristor controlled series reactor. Since the capacitor presents negative impedance and the reactor gives positive impedance, the introduction of a controllable series capacitor or reactor means that variable negative or positive impedance is added in series with the transmission line's natural positive impedance. Thus thyristor controlled series compensation (TCSC) can vary the impedance continuously to levels below and up to the transmission line's natural impedance.

A general structure of TCSC is shown in Fig. 6.4, and its equivalent circuit is shown in Fig. 6.5. From which, the power flow equations of TCSC line can be derived as following:

$$P_{ij} = U_i^2 g_{ij} - U_i U_j (g_{ij} \cos\delta_{ij} + b_{ij} \sin\delta_{ij}) \quad \text{---- (6.2.22)}$$

$$Q_{ij} = -U_i^2 (b_{ij} + B/2) - U_i U_j (g_{ij} \sin\delta_{ij} - b_{ij} \cos\delta_{ij}) \quad \text{---- (6.2.23)}$$

$$P_{ji} = U_j^2 g_{ij} - U_i U_j (g_{ij} \cos\delta_{ij} - b_{ij} \sin\delta_{ij}) \quad \text{---- (6.2.24)}$$

$$Q_{ji} = -U_j^2 (b_{ij} + B/2) + U_i U_j (g_{ij} \sin\delta_{ij} + b_{ij} \cos\delta_{ij}) \quad \text{---- (6.2.25)}$$

where

$$g_{ij} = \frac{r_{ij}}{r_{ij}^2 + (x_{ij} - x_c)^2}, \quad b_{ij} = -\frac{x_{ij} - x_c}{r_{ij}^2 + (x_{ij} - x_c)^2} \quad \text{---- (6.2.26)}$$

Here, the only difference between normal line power flow equations and the TCSC line power flow equations is the controllable reactance x_c.

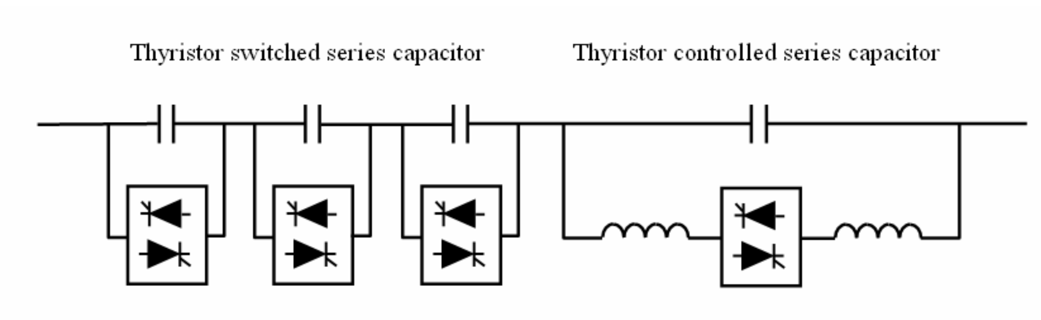

Fig. 6.4 Structure of Thyristor Controlled Series Compensation

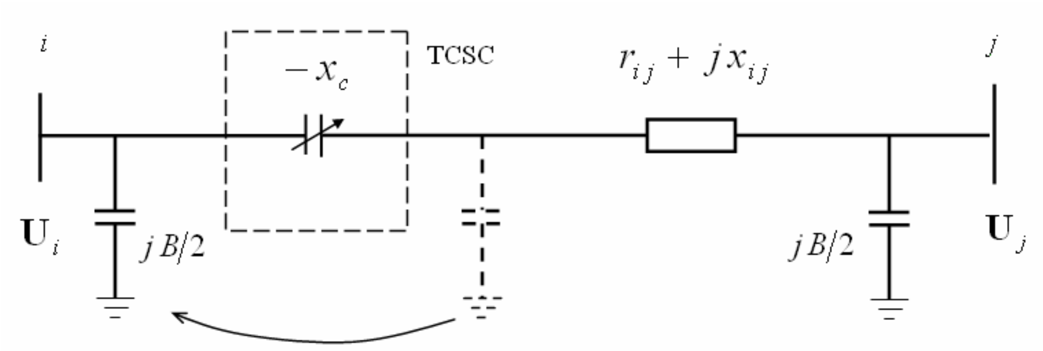

Fig 6.5 Equivalent Circuit of TCSC

6.2.4.3 Unified Power Flow Controller (UPFC)

UPFC is a kind of powerful and versatile FACTS device that combines the feature of TCSC, TCPS and SVC (Static Var Compensator), and has the ability to simultaneously control all three parameters of power flow – voltage, line impedance and phase angle. It consists of shunt and series transformers, which are connected by GTO converters and a DC link, its typical structure is shown in Fig. 6.6. UPFC has three controllable parameters, namely the magnitude and the angle of inserted voltage ($\mathbf{U}_T$ and ϕ_T) and the magnitude of the current ($\mathbf{I}_q$). The effect of UPFC on network can be modelled by a series inserted voltage source $\mathbf{U}_T$ and two tapped currents $\mathbf{I}_T$ and $\mathbf{I}_q$. The equivalent circuit of UPFC is shown in Fig. 6.7.

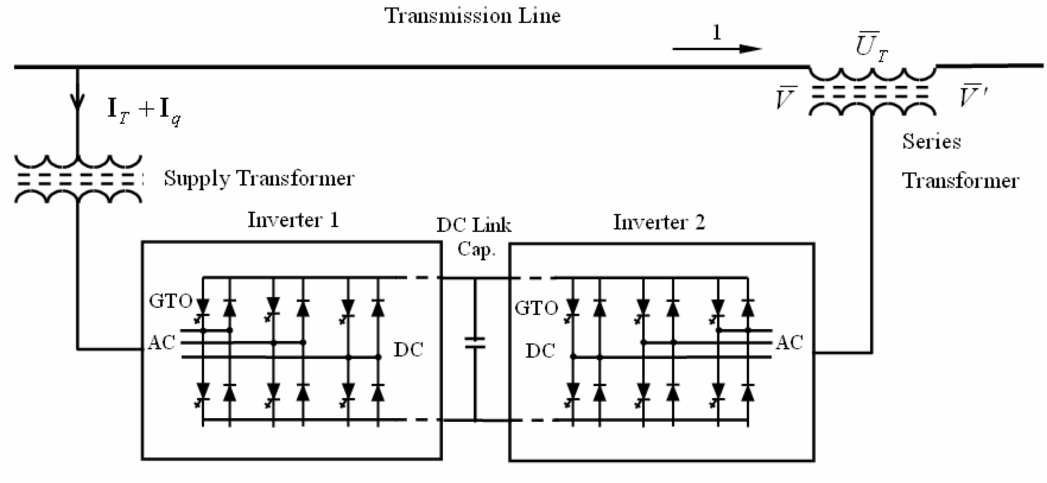

Fig. 6.6 Structure of Unified Power Flow Controller

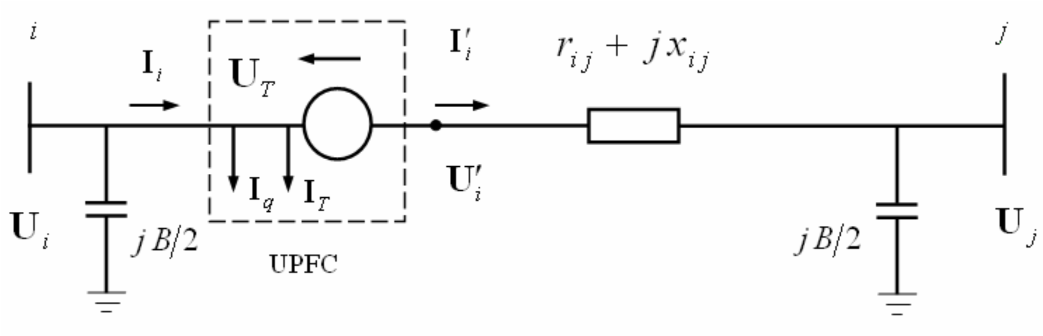

Fig 6.7 Equivalent Circuit of UPFC

The active and reactive power flow equations of UPFC line are derived as follows:

$$P_{ij} = (U_i^2 + U_T^2)g_{ij} + 2U_iU_Tg_{ij}\cos(\varphi_T - \delta_{ij}) - U_jU_T(g_{ij}\cos\varphi_T + b_{ij}\sin\varphi_T) \\ - U_iU_j(g_{ij}\cos\delta_{ij} + b_{ij}\sin\delta_{ij})$$

---- (6.2.27)

$$Q_{ij} = -U_iI_q - U_i^2(b_{ij} + B/2) - U_iU_T[g_{ij}\sin(\varphi_T - \delta_{ij}) + b_{ij}\cos(\varphi_T - \delta_{ij})] \\ - U_iU_j(g_{ij}\sin\delta_{ij} - b_{ij}\cos\delta_{ij})$$

---- (6.2.28)

$$P_{ji} = U_j^{\,2} g_{ij} - U_j U_T (g_{ij} \cos\varphi_T - b_{ij} \sin\varphi_T) - U_i U_j (g_{ij} \cos\delta_{ij} - b_{ij} \sin\delta_{ij})$$

---- (6.2.29)

$$Q_{ji} = -U_j^{\,2} (b_{ij} + B/2) - U_j U_T (g_{ij} \sin\varphi_T - b_{ij} \cos\varphi_T) + U_i U_j (g_{ij} \sin\delta_{ij} + b_{ij} \cos\delta_{ij})$$

---- (6.2.30)

6.2.4.4 Constraints for FACTS Devices

New inequality constraints for the FACTS devices control parameters are listed as follows:

$K_{i\min} \le K_i \le K_{i\max}$, $i \in S_{TCPS}$ ---- (6.2.31)

$\phi_{i\min} \le \phi_i \le \phi_{i\max}$, $i \in S_{TCPS}$ ---- (6.2.32)

$X_{Ci\min} \le X_{Ci} \le X_{Ci\max}$, $i \in S_{TCSC}$ ---- (6.2.33)

$0 \le U_{Ti} \le U_{Ti\max}$, $i \in S_{UPFC}$ ---- (6.2.34)

$-\pi \le \phi_{Ti} \le \pi$, $i \in S_{UPFC}$ ---- (6.2.35)

$I_{q_i\min} \le I_{qi} \le I_{q_i\max}$, $i \in S_{UPFC}$ ---- (6.2.36)

where, S_{TCPS}, S_{TCSC}, S_{UPFC} is respectively the set of buses with TCPS, TCSC and UPFC.

In addition to the above inequality constraints, active and reactive power injection should also be added to the power flow equations for those buses installed with FACTS devices.

6.3 Solution Strategy

For the OPF problem as formulated in section 6.2, the variant Primal-Dual Predictor-Corrector Interior Point Method (PDPCIPM) proposed in section 2.4.2 is employed to be the solution method with the aim of both robustness and reliability. Details about this method can be found in section 2.4.2 and is not repeated in this chapter.

6.4 Case Study and Discussions

To validate the ATC enhancement by installation of FACTS devices with variant PDPCIPM method, simulation tests are performed on the IEEE 30-bus Reliability Test System (RTS) as below.

Different from the partition structure in chapter 2, in this investigation, the whole system is divided into two areas as shown in Fig. 6.8. Buses 1-13 belong to the source area A, and buses 14-30 are in sink area B. With this split, all the generators are in area A.

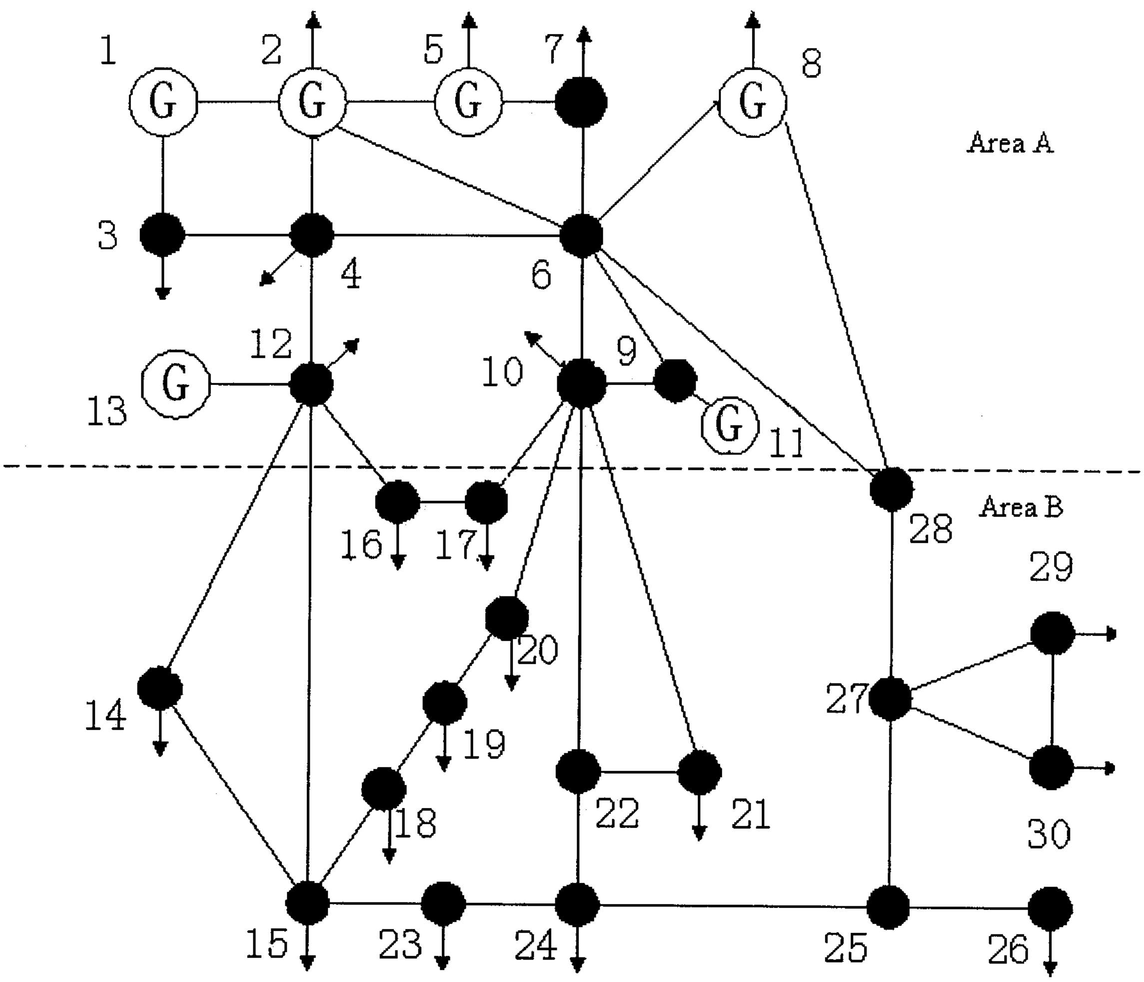

Fig. 6.8 One-line Diagram of IEEE 30-bus RTS

In this study, from the base case, the active power on each load bus increases uniformly according to their power factors at base case, and the active generator output is distributed among generators 2,5,8,11,13 as the rate of 1:1:2:3:2 while the network losses are supplied by the slack bus.

When there is no FACTS installed, ρ_c=1.66. To test the effect of FACTS devices, a TCPS is installed at bus 3, a TCSC is added to bus 18, and a UPFC is settled at bus 28. ρ_c=2.23 is obtained with the FACTS control parameters as shown in Table 6.1. It is obvious that FACTS devices enhance the ATC between two areas considerably.

Table 6.1 Control Parameters of FACTS Devices for the Enhanced ATC

K_3	ϕ_3	X_{C18}	U_{T28}	ϕ_{T28}	I_{q28}
1.077	-10^o	-0.041	0.3947	-88.19^o	0.5

6.5 Summary

In this chapter, how to enhance the ATC value by FACTS devices is investigated. An OPF mathematical model is established, where by representing three main FACTS devices, namely TCPS, TCSC and UPFC, in equivalent circuit, new constraints of their control parameters and injected power are added to the model. A variant PDPCIPM that is proposed in the previous chapter 2 is employed as the solution method. Tests are implemented on IEEE 30-bus RTS to find the effect of FACTS on ATC, by comparing the result of with and without FACTS devices on the system. The results show that the FACTS devices can help improve the ATC value distinctly.

CHAPTER 7

Conclusions

7.1 Summary

This thesis investigates the Available Transfer Capability (ATC) evaluation methods with both dynamic and static constraints, its role as a market signal in addition to being a technical index in the power market and the interaction between the two roles, as well as ATC enhancement by FACTS devices.

Following the background introduction and an overview of former research related to this topic, the model of considering transient angle stability constraints in ATC determination is established in Chapter 2 with a variant Primal-Dual Predictor-Corrector Interior Point Method (PDPCIPM) as the solution method. In Chapter 3, another type of dynamic limit, dynamic voltage constraints is included in the mathematical model and solved by a Quasi-Steady-State method. Under the new power market environment, economic factors should be considered on the condition of stability operation. Hence, in Chapter 4, the mathematical model of calculating ATC with consideration on both stability and price bidding is established followed by an analysis of their interactions. In Chapter 5, a risk-based optimal method is proposed to include different contingences and the system transient instability risk in the ATC determination. After the studies on ATC evaluation with a variety of dynamic and static constraints, as well as the consideration of both technical and economic factors as the optimal objective via different solution methodologies, the application of FACTS devices for ATC enhancement is investigated in Chapter 6. The main conclusions and findings of this thesis are as follow.

1. An optimization operation point of power system obtained with traditional static system operation constraints is possibly either transiently unstable or voltage unstable under certain credible contingencies. Mathematically, either angle transient or dynamic voltage stability assessment will include some differential constraints which describe the transient or dynamic behavior in the process. Thus the key point lies in how to treat them with multi-dimensional Differential-Algebraic-Equations (DAEs) to obtain a satisfactory result with appropriate calculation effort. In this research, a variant PDPCIPM and a QSS method are proposed respectively for two kinds of dynamic constrained ATC evaluation.

2. Different power system structures will have different operation identity. Some are vulnerable to disturbance on angle stability while some others are more prone to voltage instability. The two dynamic problems of transient angle stability and dynamic voltage stability are conceptually different and usually occur under different system operation conditions by distinct contingencies. In addition, their acting duration following disturbances and influences are different from one another. Hence in this research, ATC calculation with transient angle and dynamic voltage stability constraints are investigated separately.

3. The most common contingency which introduces transient angle stability potential is a three-phase short circuit on certain bus. By a variant PDPCIPM method, ATC with transient angle stability constraints can be evaluated in a few iterations with reasonable accuracy and its characteristic of fast convergence is insensitive to the system scale and number of control variables.

4. The most common contingency which affects voltage stability is the outage of certain transmission line, especially in a heavily loaded system. In this research, ATC calculation with dynamic voltage stability constraints is solved by QSS method. As a multi-time-scale problem, by QSS approximation, the voltage dynamics are decomposed into two terms, whose short-term part is passed over while the long-term evolution is reproduced to be solved in a fast process. By this method, ATC with dynamic voltage stability constraints can be evaluated with acceptable accuracy while the calculation speed is accelerated considerably.

5. Study results show that a system with heavy loads and large power transmission through long distance may have more likelihood to suffer from voltage instability than transient angle instability. In modern bulk systems, with wide and deep interconnections among areas, substantive power exchange via long transmission tie-lines is rather common all around the world. In recent years, voltage stability violations or even voltage collapses emerge in many countries. These devastating phenomena warrant the study results in this thesis.

6. Under the power market environment, economic factors should also be a substantial concern on the precondition of stability operation. In this research, a

multi-objective OPF problem of calculating ATC with consideration on both stability and economics is established and their interactions are analyzed. When security operation is concerned as the main criterion of optimization, economic factors are considered just on the basis that stability is ensured enough. Thus the economical benefit is less than that of the criterion where it is the pivoting interest. With this loss of economical benefit, the system is kept within an abundant stable scope, and the potential crisis of congestion can be avoided. On the other hand, when economic factors are dominating, the system may operate at a more stressed condition which is much near to the stability boundary.

7. Through a risk-based optimal method suggested in this thesis, ATC determination with different contingences associated with the system transient instability risk is developed. In this context, both probabilities and costs of transient instability events are simultaneously considered. Due to the application of expectation rule, the optimal ATC compromised between economics and security is successfully achieved. This is considered to be a substantial improvement in the operation level of system resource usage.

8. Besides the studies on algorithms of ATC evaluation with a variety of dynamic and static constraints as well as both technical and economic factors as the objective, the participants of power market also pay attention to how to increase the ATC between areas. This ensures that more power exchange transaction under satisfactory security application can be performed. In this research, FACTS devices are applied to meet this requirement, investigations show that the installment of appropriate FACTS equipment can help improve the ATC value distinctly.

7.2 Future Work

1. Although the two types of dynamic stability problems usually emerge following different contingencies, with more complicated load characteristics and operation conditions more close to the stability boundary, a system may suffer from another dynamic instability after surviving one harassment. For example, in a system disturbed by a three-phase short circuit, the common measure is to trip one crucial line connected to this bus, and the system will enter a transient angle stability following this perturbation. If the contingency occurs near a transmission line with heavy load and there is not enough reactive power support nearby, although the system can survive this transient angle stability, it may suffer dynamic voltage instability soon following. In this case, the condition is even worse than pure dynamic voltage stability problem with a stable operation originally because the former dynamic process of transient angle stability has devastatingly changed the system structure and parameters. So ATC calculation which includes both types of dynamic constraints should be investigated for more complicated system conditions. The dynamic mechanism of such an integrated dynamic process will also be instructive for other optimal problems under power market environment.

2. In an on-line environment, ATC must be calculated for many point-to-point or area-to-area transfer cases among interconnected bulk systems with consideration of credible contingencies. In this thesis, methods to determine dynamic ATC with technical and economic objective have been proposed and implemented on some typical test cases. For a practical system, there are much more buses, loads and transmission lines, as well more credible simultaneous contingencies, and the

problem dimension is much more than these cases. To satisfy the real-time security operation, in which system condition should be assessed as soon as possible and counter-measures should be given out appropriately and timely, parallel computation could be performed. In this context, the method in this thesis could be executed on several computers simultaneously. Thus the result will be gained in a satisfactorily short period as the overall outcome of all the parallel computations.

3. With the development of power market, many countries are aware that timely publishing ATC value on OASIS as a significant technical index and market signal influences the transaction and power transfer to a great extent. They are also concerned about how to improve the ATC along tie-lines between interconnected areas. With the methods proposed in this thesis, further research can be carried out on a practical system. Based on the structure characteristics of the particular system, installation of appropriate FACTS devices can be suggested to enhance the ATC level.

4. In the interconnected systems, higher operation stability will be gained with larger ATC value between them. However, this is not always the only expectation of a power system operation authority. The costs of improving ATC should also be considered at the same time. To improve the ATC value by FACTS devices or other measurements, there may be several possible choices. Costs and benefits comparison for different scheme of applying FACTS should also be performed so that the most appropriate one with satisfactory costs and improved ATC level is selected to the individual system.

5. In this thesis, all of the researches are executed on AC power systems. It is observed that in recent years, HVDC has been used in many bulk interconnected power systems for power transfer via long distance and has shown substantial advantages over the AC systems. ATC calculation and improvement issues related with HVDC will be an interesting future research direction. Investigations on this aspect, together with the work preformed on AC power systems, are of great practical significance, and will bring more strong and comprehensive support in the evolving of wider and wider power system interconnections.

APPENDICES

Appendix A. 6-bus Test System

The 6-bus test system is shown in Fig. A.1.

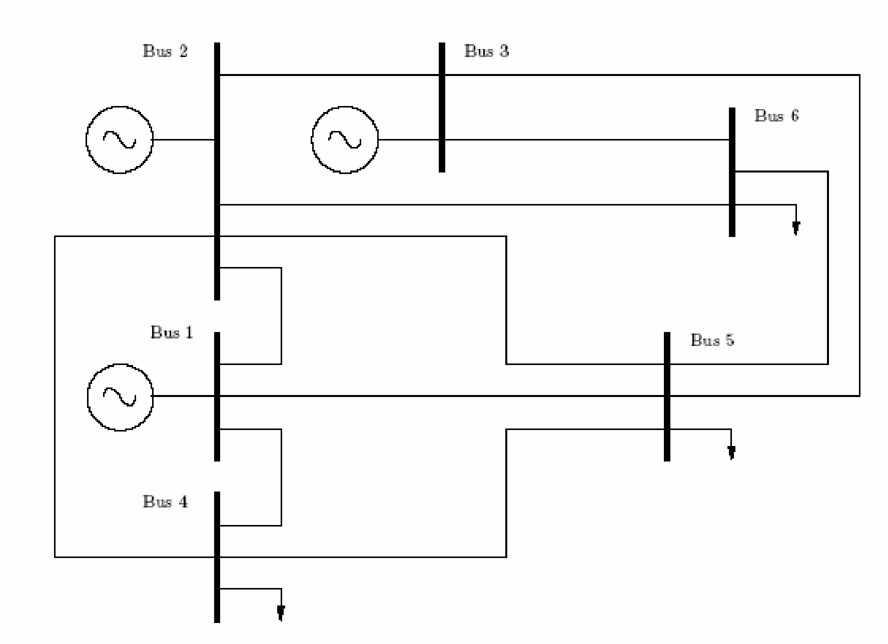

Fig. A.1 6-bus test system

Its generation and load data at base case and other necessary data are listed in Table A.1 and Table A.2 respectively.

Table A.1 Base Case Generation and Load Data of 6-bus Test System

Bus	1	2	3	4	5	6
P (p.u.)	0.9	1.396	0.6	-0.9	-1	-0.9
Q (p.u.)	0.315	0.651	0.733	-0.51	-0.66	-0.51

Table A.2 6-Bus System Line Data

Branch No.	Bus No's	R p.u.	X p.u.	B/2 p.u.	Rating p.u.
1	2-3	0.05	0.25	0.030	0.3082
2	3-6	0.02	0.10	0.010	1.3973
3	4-5	0.20	0.40	0.040	0.1796
4	3-5	0.12	0.26	0.025	0.6585
5	5-6	0.10	0.30	0.030	0.2000
6	2-4	0.05	0.10	0.010	1.3740
7	1-2	0.10	0.20	0.020	0.2591
8	1-4	0.05	0.20	0.020	0.9193
9	1-5	0.08	0.30	0.030	0.8478
10	2-6	0.07	0.20	0.025	0.9147
11	2-5	0.10	0.30	0.020	0.7114

Appendix B. IEEE 30-bus Reliability Test System

The IEEE 30-bus system is shown in Fig. A.2.

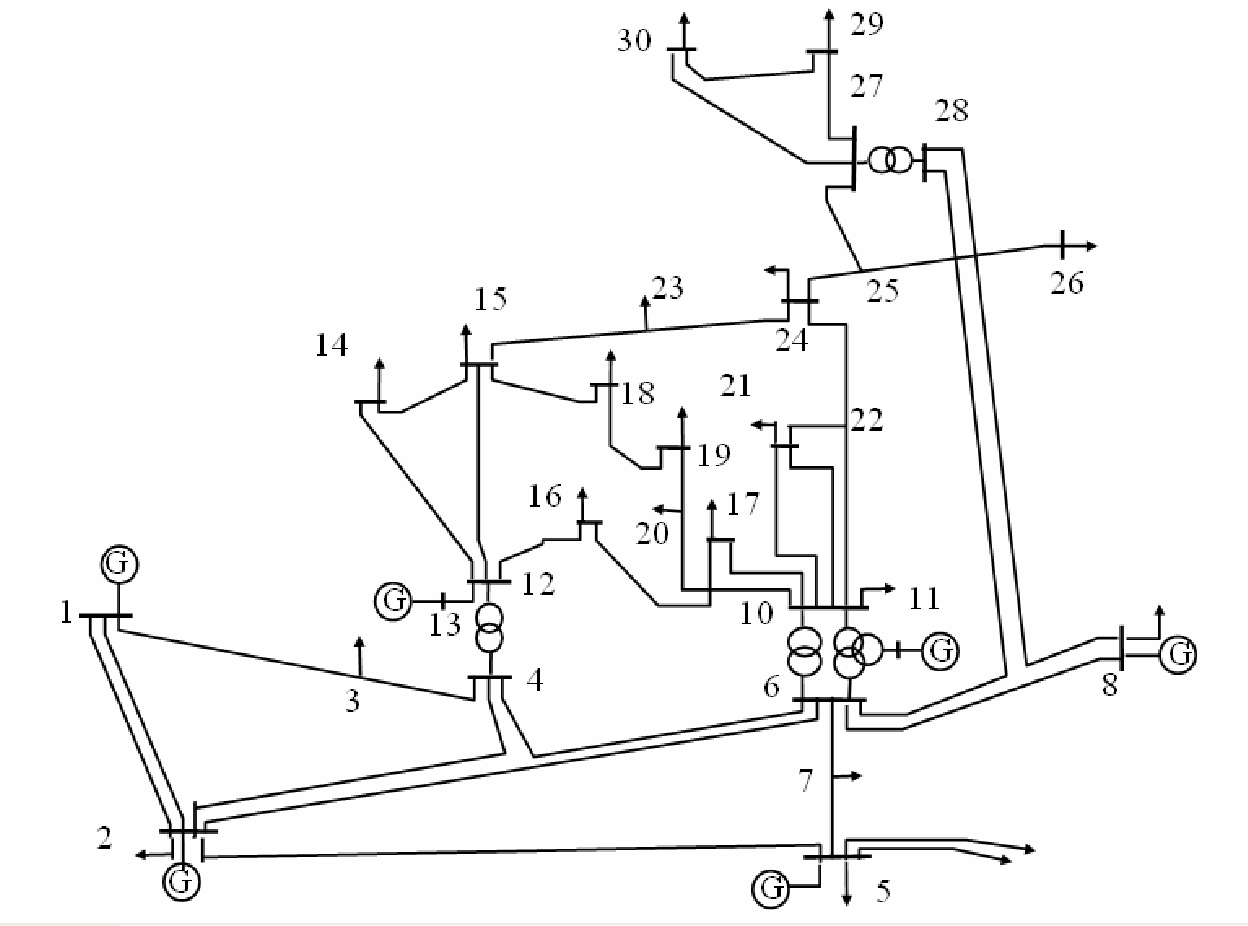

Fig. A.2 IEEE 30-bus test system

The generation data, branch data, load data and other necessary data are listed in Table A.3 to Table A.8 respectively.

Table A.3 IEEE 30-bus System Generation Data

Bus No.	P_G^{min} (MW)	P_G^{max} (MW)
1	50	200
2	20	80
5	15	50
8	10	35
11	10	30
13	12	40

Table A.4 IEEE 30-bus System Load Data

Bus No.	Load MW	Load MVAR	Bus No.	Load MW	Load MVAR
1	0.00	0.00	16	1.8	1.80
2	21.70	12.70	17	5.8	5.80
3	2.40	1.20	18	0.9	0.90
4	7.60	1.60	19	3.4	3.40
5	94.20	19.00	20	0.7	0.70
6	0.00	0.00	21	11.2	11.20
7	22.80	10.90	22	0.0	0.00
8	30.00	30.00	23	1.6	1.60
9	0.00	0.00	24	6.7	6.70
10	5.80	2.00	25	0.0	0.00
11	0.00	0.00	26	2.3	2.30
12	11.20	7.50	27	0.0	0.00
13	0.00	0.00	28	0.0	0.00
14	6.20	1.60	29	0.9	0.90
15	8.20	2.50	30	1.9	1.90

Table A.5 IEEE 30-bus System Line Data

Branch No.	Bus No's	R p.u.	X p.u.	B/2 p.u.	Rating p.u.
1	1-2	0.0192	0.0575	0.0264	1.30
2	1-3	0.0452	0.1852	0.0204	1.30
3	2-4	0.0570	0.1737	0.0184	0.65
4	3-4	0.0132	0.0379	0.0042	1.30
5	2-5	0.0472	0.1983	0.0209	1.30
6	2-6	0.0581	0.1763	0.0187	0.65
7	4-6	0.0119	0.0414	0.0045	0.90
8	5-7	0.0460	0.1160	0.0102	0.70
9	6-7	0.0267	0.0820	0.0085	1.30
10	6-8	0.0120	0.0420	0.0045	0.32
11	6-9	0.0000	0.2080	0.0000	0.65
12	6-10	0.0000	0.5560	0.0000	0.32
13	9-11	0.0000	0.2080	0.0000	0.65
14	9-10	0.0000	0.1100	0.0000	0.65
15	4-12	0.0000	0.2560	0.0000	0.65
16	12-13	0.0000	0.1400	0.0000	0.65
17	12-14	0.1231	0.2559	0.0000	0.32
18	12-15	0.0662	0.1304	0.0000	0.32
19	12-16	0.0945	0.1987	0.0000	0.32
20	14-15	0.2210	0.1997	0.0000	0.16
21	16-17	0.0824	0.1932	0.0000	0.16
22	15-18	0.1070	0.2185	0.0000	0.16
23	18-19	0.0639	0.1292	0.0000	0.16
24	19-20	0.0340	0.0680	0.0000	0.32
25	10-20	0.0936	0.2090	0.0000	0.32
26	10-17	0.0324	0.0845	0.0000	0.32
27	10-21	0.0348	0.0749	0.0000	0.32
28	10-22	0.0727	0.1499	0.0000	0.32
29	21-22	0.0116	0.0236	0.0000	0.32
30	15-23	0.1000	0.2020	0.0000	0.16
31	22-24	0.1150	0.1790	0.0000	0.16
32	23-24	0.1320	0.2700	0.0000	0.16
33	24-25	0.1885	0.3292	0.0000	0.16
34	25-26	0.2544	0.3800	0.0000	0.16
35	25-27	0.1093	0.2087	0.0000	0.16
36	28-27	0.0000	0.3960	0.0000	0.65
37	27-29	0.2198	0.4153	0.0000	0.16
38	27-30	0.3202	0.6027	0.0000	0.16
39	29-30	0.2399	0.4533	0.0000	16
40	8-28	0.0636	0.2000	0.0000	32
41	6-28	0.0169	0.0599	0.0000	32

Table A.6 Regulated Bus Data

Bus No.	Voltage magnitude p.u.	Minimum MVAR capability	Maximum MVAR capability
2	1.045	-40.0	50.0
5	1.010	-40.0	40.0
8	1.010	-10.0	40.0
11	1.082	-6.0	24.0
13	1.071	-6.0	24.0

Table A.7 Transformer Data

Transformer destination	Tap setting
4----12	0.932
6----9	0.978
6----10	0.969
28----27	0.968

Table A.8 Static Capacitor Data

Bus No.	Susceptance (p.u.)
10	0.190
24	0.043

REFERENCES

[1] Anderson P.M., Fouad A.A., Power System Control and Stability-2nd, IEEE Press, Wiley-Interscience, 2003

[2] Audomvongseree K., Yokoyama A., "A Risk Based TTC Evaluation by Probabilistic Method," Proc. of IEEE Power Tech Conference, vol. 2, pp. 179 - 184, 2003

[3] Benjamin J., Interior-point Techniques in Optimization, Kluwer,1997

[4] California Energy Commission (CEC), "Flexible AC Transmission Systems Benefits Study," San Diego Gas and Electric, San Diego, CA, Oct. 1999

[5] Canizares C.A., "Calculating Optimal System Parameters to Maximize the Distance to Saddle-node Bifurcations," IEEE Trans. Circuits Syst. I, vol. 45, pp. 225 - 237, 1998

[6] Cañizares C.A., Faur Z.T., "Analysis of SVC and TCSC Controllers in Voltage Collapse," IEEE Trans. Power Syst., vol. 14, No. 1, pp. 158 – 165, Feb. 1999

[7] Chen L., Taka Y., Okamoto H., Tanabe R., Ono A., "Optimal Operation Solutions of Power Systems with Transient Stability Constraints," IEEE Trans. Circuits Syst., vol. 48, pp. 327 - 339, Mar. 2001

[8] Chowdhury B.H., Taylor C.W., "Voltage Stability Analysis: V-Q Power Flow Simulation Versus Dynamic Simulation," IEEE Trans. Power Syst., vol. 15, No. 4, pp. 1354 - 1359, 2000

[9] Chung C.Y., Wang Lei, Howell F., Kundur P., "Generation Rescheduling Methods to Improve Power Transfer Capability Constrained by Small-Signal Stability," IEEE Trans. Power Syst., vol. 19, pp. 524 - 530, Feb. 2004

[10] Clements K.A., Davis P.W., Frey K.D., "An Interior Point Algorithm for Weighted Least Absolute Value Power System State Estimation," IEEE/PES Winter Meeting, 1991

[11] Contaxis G.C., Delkis C., Korres G., "Decoupled Optimal Load Flow Using Linear or Quadratic Programming," IEEE Trans. Power Syst., vol. PWRS-1, No. 1, pp. 1 - 7, 1986

[12] Dai Y.J., McCalley J.D., Vittal V., "Simplification, Expansion and Enhancement of Direct Interior Point Algorithm for Power System Maximum Loadability," IEEE Trans. Power Syst., vol. 15, No. 3, pp. 1014 - 1021, 2000

[13] David A.K., "Dispatch Methodologies for Open Access Transmission Systems," IEEE Trans. Power Syst., vol. 13, No. 1, pp. 46 - 53, February 1998

[14] De Tuglie E., Dicorato M., La Scala M., Scarpellini P., “A Static Optimization Approach to Assess Dynamic Available Transfer Capability,” IEEE Trans. Power Syst., vol. 15, No. 3, pp. 1069 - 1076, Aug. 2000

[15] Diao Q.H., Shaaban M., Ni Y.X., “Inter-area Total Transfer Capability Calculation Using Sequential Quadratic Programming Method in Power Market", Automation of Electric Power Systems, vol. 24, pp. 5 - 8, Dec. 2000

[16] Dobson I., Lu L., “Computing an Optimum Direction in Control Space to Avoid Saddle Node Bifurcations,” IEEE Trans. Automat. Contr., vol. 37, pp. 1616 - 1620, Oct.1998

[17] Ejebe G.C., Tong J., Waight J.G., Frame J.G., Wang X., Tinney W.F., “Available Transfer Capability Calculations,” IEEE Trans. Power Syst., vol. 13, pp. 1521 - 1527, 1998

[18] Ejebe G.C., Waight J.G., Sanots-Nieto M., Tinney W.F, “Fast Calculation of Linear Available Transfer Capability,” IEEE Trans. Power Syst., vol. 15, No. 3, pp. 1112 - 1116, 2000

[19] European Transmission System Operators (ETSO), “Definitions of Transfer Capabilities in Liberalized Electricity Markets,” http://www.etso-net.org/, April 2001

[20] Feng Z., Ajjarapu V., Maratukulam D.J., “A Comprehensive Approach for Preventive and Corrective Control to Mitigate Voltage Collapse,” IEEE Trans. Power. Syst., vol. 15, pp. 791 - 797, May 2000

[21] Flueck A.J., Chiang H.D., Shah K.S., “Investigating the Installed Real Power Transfer Capability of a Large Scale Power System Under a Proposed Multiarea Interchange Schedule Using CPFLOW,” IEEE Trans. Power. Syst., vol. 11, No. 2, pp. 883 - 889, 1996

[22] Gan D., Thomas R.J., Zimmerman R.D., “Stability-constrained Optimal Power Flow,” IEEE Trans. Power Syst., vol. 15, pp. 535 - 540, May 2000

[23] Ge S.Y., Chung T.S., “Optimal Active Power Flow Incorporating Power Flow Control Needs in Flexible AC Transmission Systems,” IEEE Trans. Power Syst., vol. 14, No. 2, pp. 738 – 744, May 1999

[24] Granville S., “Optimal Reactive Dispatch through Interior Point Methods,” IEEE Trans. Power Syst., vol. 9, No. 1, pp. 136 - 146, 1994

[25] Gravener M.H., Nwankpa C., “Available Transfer Capability and First Order Sensitivity,” IEEE Trans. Power Syst., vol. 14, No. 2, pp. 512 - 518, 1999

[26] Greene S., Dobson I., Alvarado F.L., “Sensitivity of transfer capability margins with a fast formula,” IEEE Trans. Power Syst., vol. 17, No. 1, pp. 34 - 40, 2002

[27] Grijalva S., Sauer P.W., Weber J.D., "Enhancement of Linear ATC Calculations by the Incorporation of Reactive Power Flows," IEEE Trans. Power Syst., vol. 18, No. 2, pp. 619 - 624, 2003

[28] Hamoud G., "Assessment of Available Transfer Capability of Transmission Systems," IEEE Trans. Power Syst., vol. 15, pp. 27 - 32, 2000

[29] Hingorani N.G., "Flexible AC Transmission Systems," IEEE Spectrum, pp. 40 – 45, Apr. 1993

[30] Hiskens I.A., Pai M.A., Sauer P.W., "An Iterative Approach to Calculating Dynamic ATC," Proc. of Bulk Power System Dynamics and Control IV—Restructuring, Santorini, Greece, pp. 585 – 590, Aug. 1998

[31] Housos E., Irisarri G., "Real and Reactive Power System Security Dispatch Using a Variable Weights Optimization Method," IEEE Transaction on Power Apparatus and Systems, vol. PAS-102, pp. 1260 - 1268, 1983

[32] Huneault M., Galiana F.D., "A Survey of the Optimal Power Flow Literature," IEEE Trans. Power Syst., vol. 6, No. 2, pp. 762 – 770, 1991

[33] Irisarri G., Kimball L.M., Clements K.A., Bagchi A., Davis P.W., "Economic Dispatch with Network and Ramping Constraints via Interior Point Methods," IEEE Trans. Power Syst., vol. 13, No. 1, pp. 236 - 242, 1998

[34] Irisarri G.D., Wang X., Tong J., Mokhtari S., "Maximum Loadability of Power Systems Using Interior Point Nonlinear Optimization Method," IEEE Trans. Power Syst., vol. 12, No. 1, pp. 162 - 172, 1997

[35] Irving M.R., Sterling M.J.H., "Economic Dispatch of Active Power with Constraints Relaxation," Proceedings of the IEEE, vol. 130, Pt. C, NO. 4, pp. 172 - 177, July, 1983

[36] Kundur P., Power System Stability and Control, New York: McGraw-Hill Inc., 1994

[37] Landgren G.L., Terhune H.L., Angel R.K., "Transmission Interchange Capability Analysis by Computer," IEEE Trans. on Power Apparatus and Systems, vol. PAS-91, No. 6, pp. 2405 - 2414, 1972

[38] Luo X., Patton A.D., Singh C., "Real Power Transfer Capability Calculations Using Multi-Layer Feed-Forward Neural Networks," IEEE Trans. Power Syst., vol. 15, No. 2, pp. 903 – 908, 2000

[39] Machowski J., Bialek J.W., James R., Power System Dynamics and Stability, Chichester, Englandd : John Wiley, 1997

[40] McCalley J.D., Fouad A.A., Vittal V., Irizarry-Rivera A.A., Agrawal B.L., Farmer R.G., "A Risk-Based Security Index for Determining Operating Limits in

Stability-Limited Electric Power Systems," IEEE Trans. Power Syst., vol. 12, pp. 1210 - 1219, Aug. 1997

[41] McCalley J.D., Vittal V., Abi-Samra N., "An Overview of Risk Based Security Assessment," Proc. of IEEE Power Engineering Society Summer Meeting, vol. 1, pp. 8 - 22, 1999

[42] Medina J., Quintana V.H., Conejo A.J., Thoden F.P., "A Comparison of Interior-Point Codes for Medium-Term Hydro-Thermal Coordination," IEEE Trans. Power Syst., vol. 13, No. 3, pp. 836 - 843, Aug. 1998

[43] Mehrotra S., "On the Implementation of a Primal-dual Interior Point Method," SIAM J. Optim., vol. 2, pp. 575 – 601, 1992

[44] Mello J.C.O., Melo A.C.G., Granville S., "Simultaneous Transfer Capability Assessment by Combining Interior Point Methods and Monte-Carlo Simulation," IEEE Trans. Power Syst., vol. 12, No. 2, pp. 736 - 742, 1997

[45] Momoh J.A., Guo S.X., Ogbuobiri E.C., Adapa R., "The Quadratic Interior Point Method for Solving Power System Optimization Problems," IEEE Trans. Power Syst., vol. 9, No. 3, pp. 1327 - 1336, 1994

[46] Momoh J.A., Koessler R.J., Bond M.S., Stott B., Sun D., Papalexopoulos, A., Ristanovic, P., "Challenges to Optimal Power Flow," IEEE Trans. Power Syst., vol. 12, No. 1, pp. 444 – 455, Feb. 1997

[47] Mota-Palomino R., Quintana V.H., "A Penalty Function-Linear Programming Method for Solving Power System Constrained Economic Operation Problems," IEEE Transaction on Power Apparatus and Systems, vol. PAS-103, pp. 1414 - 1442, June 1984

[48] Mota-Palomino R., Quintana V.H., "Sparse Reactive Power Scheduling by a Penalty-Function-Linear Programming," IEEE Trans. Power Syst., vol. PWRS-1, pp. 31 - 39, 1986

[49] Nabona N., Ferris L.L., "Optimization of Economic Dispatch Through Quadratic and Linear Programming," Proceedings of the IEE, vol. 120, No. 5, pp. 574 - 580, May 1973

[50] North American Electric Reliability Council, "Available Transfer Capability Definition and Determination," http://www.nerc.com/, June 1996

[51] Ou Y., Singh C., "Assessment of Available Transfer Capability and Margins," IEEE Trans. Power Syst., vol. 17, No. 2, pp. 463 - 468, 2002

[52] Ponnambalam K., Quintana V.H., Vannelli A., "A Fast Algorithm for Power System Optimization Problems Using an Interior Point Method," IEEE Trans. Power Syst., vol. 7, No. 2, pp. 892 - 899, 1992

[53] Quintana V.H., Torres G.L., Medina-Palomo J., "Interior-Point Methods and Their Applications to Power Systems: A Classification of Publications and Software Codes," IEEE Trans. Power Syst., vol. 15, No. 1, pp. 170 - 176, Feb. 2000

[54] Rosales R.A., Ruiz-Vega D., Ernst D., Pavella M., Giri J., "On-line Transient Stability Constrained ATC Calculations," IEEE 2000 Power Engineering Society Summer Meeting, vol. 2, pp. 1291 -1296, 2000

[55] Rosehart W., Canizares C.A., Quintana V. H., "Optimal Power Flow Incorporating Voltage Collapse Constraints," Proc. of IEEE /PES Summer Meeting, pp. 820 - 825, 1999

[56] Santos-Neito M., Quintana V.H., "Linear Reactive Power Studies for Longitudinal Power Systems," Proc. of 9th PSCC Conference, pp. 783 - 787, 1987

[57] Sauer P.W., Pai M.A., Power System Dynamics And Stability, Upper Saddle River, N.J.: Prentice Hall, 1998

[58] Sauer P.W., Reinhard K.E., Overbye T.J., "Extended Factors for Linear Contingency Analysis," Proc. of the 34th Annual Hawaii International Conference on System Sciences, pp. 697 – 703, 2001

[59] Shaaban M., Li W., Liu H., Yan Z., Ni Y.X., Wu F., "ATC Calculation with Steady-State Security Constraints Using Benders Decomposition," IEEE Proc. Gen. Tran. & Dis., vol. 150, No. 5, pp. 611 – 615, Sept. 2003

[60] Shen C.M., Laughton M.A., "Power System Load Scheduling with Security Constraints Using Dual Linear Programming," Proceedings of the IEEE, vol. 117, No. 1, pp. 2117 - 2127, 1970

[61] Song Y.H., Johns Allan T., Eds., Flexible AC Transmission Systems (FACTS), Inst. Elect. Eng. Power and Energy Series 30, IEE, 1999

[62] Stadlin W.O., Fletcher D.L., "Voltage Versus Reactive Current Model for Dispatch and Control," IEEE Transaction on Power Apparatus and Systems, vol. PAS-101, No. 10, pp. 3751 - 3758, Oct. 1982

[63] Stott B., Hobson E., "Power System Security Control Calculation Using Linear Programming," IEEE Trans. Power Syst., vol. PAS-97, pp. 1713 - 1731, 1978

[64] Taylor C.W., Power System Voltage Stability, McGraw-Hill Inc., 1994

[65] Tsai C.Y., Lu C.N., "Bootstrap Application in ATC Estimation," IEEE Power Engineering Review, vol. 21, No. 2, pp. 40 - 42, 2001

[66] Vaahedi E., Mansour Y., Fuchs C., Granville S., Latore M.D.L., Hamadanizadeh, H., "Dynamic Security Constrained Optimal Power Flow/VAR Planning," IEEE Trans. Power. Syst., vol. 16, pp. 38 - 43, Feb. 2001

[67] Van Cutsem T., "Voltage Instability: Phenomena, Countermeasures, and Analysis Methods," Proceedings of the IEEE, vol. 88, pp. 208 - 227, 2000

[68] Van Cutsem T., Vournas C., Voltage Stability of Electric Power Systems, Kluwer Academic Publishers, 1998

[69] Vittal V., McCalley J.D., Van Acker V., Fu W., Abi-Samra N., "Transient Instability Risk Assessment," Proc. of IEEE Power Engineering Society Summer Meeting, vol. 1, pp. 206 - 211, 1999

[70] Wang R., Lasseter R. H., "Re-dispatching Generation to Increase Power System Security Margin and Support Low Voltage Bus," IEEE Trans. Power. Syst., vol. 15, pp. 496 - 501, May 2000

[71] Wang X., Ejebe G.C., Tong J., Waight J.G., "Preventive/Corrective Control for Voltage Stability Using Direct Interior Point Method," IEEE Trans. Power. Syst., vol. 13, pp. 878 - 883, Aug. 1998

[72] Wei H., Sasaki H., Kubokawa J., Yokoyama R., "An Interior Point Nonlinear Programming for Optimal Power Flow Problems with a Novel Data Structure," IEEE Trans. Power Syst., vol. 13, No. 3, pp. 870 - 877, 1998

[73] Wells D.W., "Method for Economic Secure Loading of a Power System," Proceedings of the IEEE, vol. 115, No. 8, pp. 606 - 614, 1968

[74] Wood A.J., Wollenberg B.F., Power Generation, Operation, and Control, New York: Wiley, 1996

[75] Wu Y.C., Debs A.S., Marsten R.E., "A Direct Nonlinear Predictor-Corrector Primal-Dual Interior Point Algorithm for Optimal Power Flows," IEEE Trans. Power Syst., vol. 9, No. 2, pp. 876 - 883, May 1994

[76] Xia F., Meliopoulos A.P.S., "A Methodology for Probabilistic Simultaneous Transfer Capability Analysis," IEEE Trans. Power Syst., vol. 11, No. 3, pp. 1269 - 1278, 1996

[77] Xia Y., Chan K.W., Liu M.B., Wu J., "Calculation of Available Transfer Capability with Transient Stability Constraints," Proc. of IEEE DRPT Conference, Hong Kong, vol. 1, pp. 128 – 132, Apr. 2004

[78] Xiao Y., Song Y.H., Sun Y.Z., "A Hybrid Stochastic Approach to Available Transfer Capability Evaluation," IEE Proc. Gen. Tran. & Dis., vol. 148, No. 5, pp. 420 – 426, Sept. 2001

[79] Xiao Y., Song Y.H., Sun Y.Z., "A Novel Power-Flow Control Approach to Power Systems With Embedded FACTS Devices," IEEE Trans. Power Syst., vol. 18, No. 1, pp. 305 – 312, Feb. 2003

[80] Xie K., Song Y.H., Stonham J., Yu E.K., Liu G.Y., "Decomposition Model and Interior Point Methods for Optimal Spot Pricing of Electricity in Deregulation Environments," IEEE Trans. Power Syst., vol. 15, No. 1, pp. 39 - 50, Feb. 2000

[81] Yan X., Quintana V.H., "An Efficient Predictor-Corrector Interior Point Algorithm for Security-Constrained Economic Dispatch," IEEE Trans. Power Syst., vol. 12, No. 2, pp. 803 - 810, 1997

[82] Yuan Y., Kubokawa J., Sasaki H., "A Solution of Optimal Power Flow with Multicontingency Transient Stability Constraints," IEEE Trans. Power Syst., vol. 18, No. 3, pp. 1094 – 1102, 2003

[83] Zhang X.M., Song Y.H., Lu Q., Mei S.W., "Dynamic Available Transfer Capability (ATC) Evaluation by Dynamic Constrained Optimization," IEEE Trans. Power Syst., vol. 19, No.2, pp. 1240 - 1242, 2004

Useful URL:

1. http://www.ferc.gov/
2. http://www.nerc.com/
3. http://www.ieee.org/
4. http://www.iee.org/
5. http://www.transmission.bpa.gov/
6. http://www.serc.gov.cn/
7. http://www.etso-net.org/
8. http://www.ee.washington.edu/research/pstca/